

V. PHYSICS AT A HIGGS FACTORY

A. Skrinsky, Chair



V. PHYSICS AT A HIGGS FACTORY, A. Skrinsky (INP, Novosibirsk), Chair

Overview of the Higgs Factory $\mu^+ \mu^-$ Collider Concept - *D. Cline* (UCLA)

Higgs Boson Mass/Physics - *G. Kane* (U Mich)

Progress Report Detector Backgrounds - *I. Stumer* (BNL)

Beam Halo vs Beam Decays in $\mu^+ \mu^-$ Colliders: Effect on Detector and Machine Designs -
N. Mokhov (FNAL)

Determining the Energy Scale of the 50-GeV First Muon Collider Using $g-2$ Precession -
R. Raja/A. Tollestrup (FNAL)

Tracking Concepts of High-Luminosity Muon Colliders - *M. Atac* (FNAL/UCLA)

OVERVIEW OF THE HIGGS FACTORY
 $\mu^+\mu^-$ COLLIDER CONCEPT

David B. Cline

UCLA

Center for Advanced Accelerators

1. The Scientific Case for The Higgs Boson
2. Higgs Factory (HF) $\mu^+\mu^-$ Collider Concept
3. Mass Range of Interest for HF and SUSY Higgs Bosons
4. Precision Electro Weak Parameters – LHC-CMS Prospects
5. When might we know M_H Range for Planning H.F.
6. Study of Exotic Physics with Higgs Boson – NFC/FCNC

THEMIS

SUMMARY

TO GET A NEW FACILITY IN THE US IT WILL BE ESSENTIAL TO DEMONSTRATE ITS PHYSICS NEED

WHY SHOULD THERE BE
A FUNDAMENTAL SCALAR
PARTICLE OR INTERACTION

A LITTLE HISTORY

~ 1932 FERMI INVENTS THEORY OF WEAK INTERACTION



4 Fermion Point like (Spm⁴)

~ 1937 HEISENBERG AND OTHERS SHOW THEORY DIVERGENT $\sigma_{\nu e} \sim E^2$

$\sigma_{\nu e} \rightarrow \infty$ as $E \rightarrow \infty$ and Violates Unitarity at $\sim 300 \text{ GeV}$ in CM

~ 1938-48 Concept of W (Weakon) (Spm¹)

o Klein \rightarrow Local \rightarrow Unitary

$\sigma_{\nu e} \rightarrow \ln E$, $E \gg M_W$

But theory still Divergent since $m_W \rightarrow 0$
 $W+W \rightarrow W+W$ $\sigma_{WW} \rightarrow \infty$

~ 1966-68 Ward, Salam, Glashow, Weinberg etc like particular

show how divergences can be cured (using Higgs Mechanism)

P. Higgs

Relate M_H to m_W

- i) Invent Neutral ~~Vector~~ Vector Z^0 to cure divergence $W_L + W_L \rightarrow W_L + W_L$
 - { WWC 73 } Z^0 disc 83
 - { at CERN }

- ii) Need Neutral Scalar to cure divergence in $W_L + W_L \rightarrow W_L + W_L$ H^0 ??
- Most likely $M_H < 1 \text{ TeV}$ - But could be cut out pole?

Natural conservation laws for neutral currents* \Rightarrow NFC

Sheldon L. Glashow and Steven Weinberg

Lyman Laboratory of Physics, Harvard University, Cambridge, Massachusetts 02138

(Received 20 August 1976)

We explore the consequences of the assumption that the direct and induced weak neutral currents in an $SU(2) \otimes U(1)$ gauge theory conserve all quark flavors naturally, i.e., for all values of the parameters of the theory. This requires that all quarks of a given charge and helicity must have the same values of weak T_3 and T_1 . If all quarks have charge $+2/3$ or $-1/3$ the only acceptable theories are the "standard" and "prevector" models, or their generalizations to six or more quarks. In addition, there are severe constraints on the couplings of Higgs bosons, which apparently cannot be satisfied in pure vector models. We also consider the possibility that nonrenormalizable counterterms cancel all the currents. A natural supersymmetric model of this sort is described. The experimental consequences of charm nonconservation in direct or induced neutral currents are found to be quite dramatic.

NC 1973
1972
1983

NO
FCNC
SO FAR

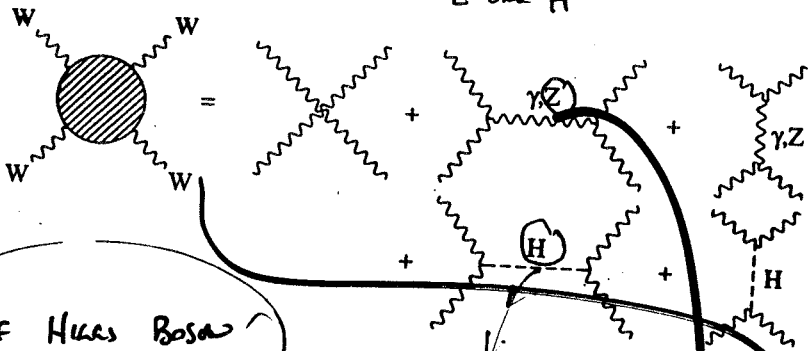
Natural Flavor Conservation **NFC**

- 1) 1 Higgs Boson $(\begin{smallmatrix} +2/3 \\ 0 \\ -1/3 \end{smallmatrix}) = (2)(\chi)(\psi)$
- 2) All quark $\Rightarrow (\begin{smallmatrix} +2/3 \\ 0 \\ -1/3 \end{smallmatrix}) = (2)(\chi)(\psi)$

Has Now only been tested directly -
IS KEY COMPONENT OF STANDARD MODEL!

S. Willenbuch
JTP only
Fall 86

CURE FOR DIVERGENCES
WITH Z and H



Discard

Problem with a Single SU model Higgs

SELF COUPLING

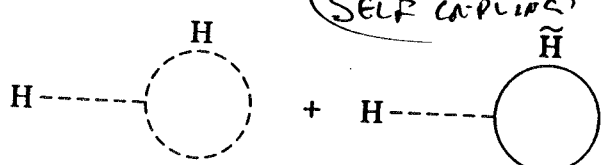


Figure 5: (a) Quadratically-divergent one-loop correction to the Higgs vacuum-expectation value from a Higgs loop; (b) the quadratic divergence is cancelled by a Higgsino loop in a supersymmetric theory.

WHAT COTS UP
THIS DIVERGENCE??

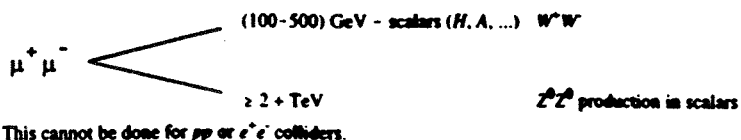
THE HIGGS BOSON
COULD BE THE
LAST PARTICLE TO
BE DISCOVERED

FROM VIEWPOINT OF EXPERIMENT!

Table 4. The scalar sector.

With a high-mass t quark, precision LEP/SLD data and the theorists' dreams of a SUSY world, the scalar (pseudo-scalar sector) is possibly very complex and may require several types of colliders.⁷ Consider:

- If the low-mass Higgs has $m > 130$ GeV, MSSM is not allowed.
- If $m > 200$ GeV, there are constraints from the requirement that perturbation theory be useful up to very high energy and from the stability of the vacuum.
- If $m < 130$ GeV, MSSM is possibly ok, but we may expect other particles (H, A), and the width of the low mass Higgs may change.
- The scalar sector may be extremely complex, requiring pp (LHC) and $\mu^+\mu^-$ colliders (and possibly NLC and $\gamma\gamma$ colliders).
- In high energy collisions, vector states are allowed unless a special method is used. Consider $\mu^+\mu^-$ colliders with polarized μ^\pm :



- A $\mu^+\mu^-$ collider is complimentary to the LHC/CMS detector.

- NFC still untested for many processes -

Std Model Higgs

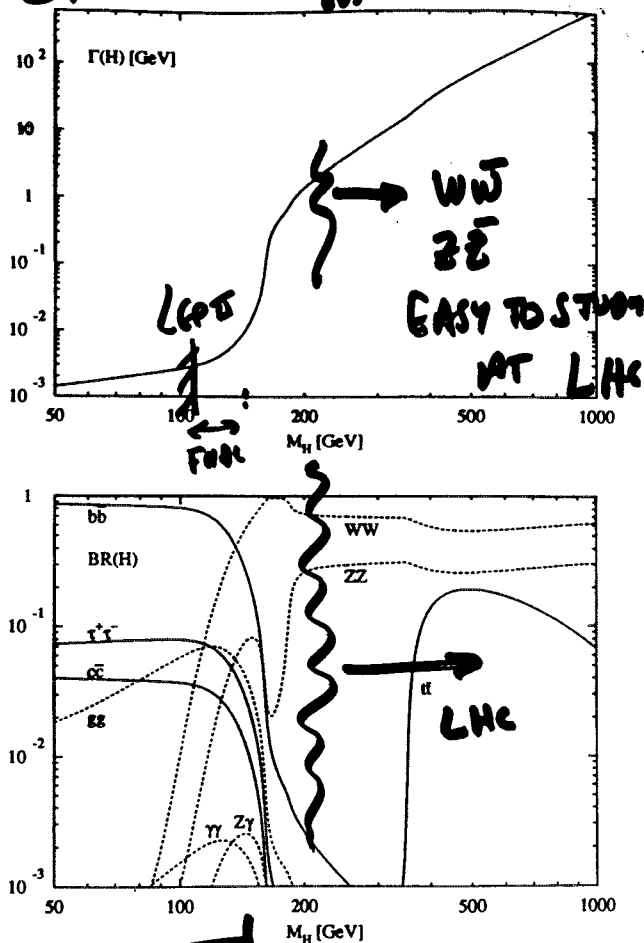


Figure 2: Total decay width $\Gamma(H)$ in GeV and the main branching ratios $BR(H)$ of the Standard Model Higgs decay channels, using the inputs of Tab. 2.

1/2 (92)

CONCEPT OF A HIGGS FACTORY (I)

(~ 1992 Napa $\mu^+\mu^-$ Collider meeting)
 was first to conceive of this (1st specific use to measure the properties of the Scalar Sector) ^{Meeting} _{then} ⁱⁿ _{Series}

In the Standard model the H^0 couples mainly to WW and ZZ

If $M_H < M_{2W}, M_{ZZ}$ the ~~coupling~~ ^{coupling} is very weak - hence $\Gamma_{H^0} \sim \text{MeV} - 50 \text{ MeV}$
 If $M_H \gg M_{2W}$ $\Gamma_{H^0} \sim \text{GeV} \rightarrow 10 \text{ GeV}$

There a low mass Higgs is hard to discover and difficult to study

In contrast for $H^0 > M_{ZZ}$ it is easy to produce - ie $p+p \rightarrow H^0$

The Compact Muon Solenoid $\rightarrow Z+Z$
 Detector (1989) was mounted $\rightarrow \mu\mu$
 to study this mode

So a Higgs Factory is mainly interesting for $M_H < M_{2W}$ or $M_{ZZ} < 180 \text{ GeV}$

EARLY CONCEPT OF HIGGS FACTORY ¹⁹⁹²
 Collider NAPA

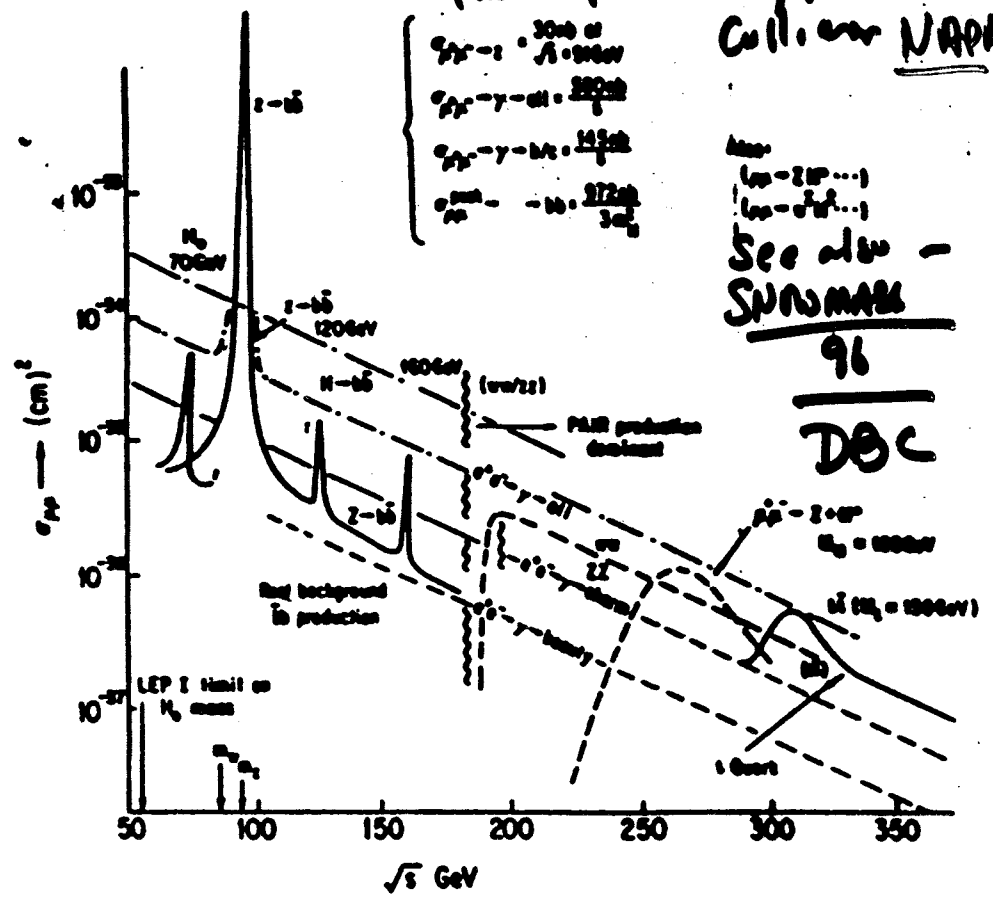


Fig. 1. The first concept of a Higgs factory $\mu^+\mu^-$ collider from the Napa Workshop.

SCAN FOR HIGGS

1994
Savitsky pp
mtg
DBE
SNOW MASS
96

Table 6. Examples of the scan for the Higgs at different mass.

(A) $m_H = 60 \text{ GeV}$ - $H \rightarrow b\bar{b}$ - Background from $Z \rightarrow b\bar{b}$ reduced.

$\sigma_{H \rightarrow b\bar{b}} = 8 \times 10^{-36} \text{ cm}^2$

$\delta p/p = 0.01\%$

Procedure

$\sigma_{Z \rightarrow b\bar{b}} = 4 \times 10^{-36} \text{ cm}^2$

$\Sigma \sigma_Z + \sigma_H = 12 \times 10^{-36} \text{ cm}^2$ at resonance

Known position within 1 GeV. For each scan point, a 5 σ is to be observed.

[Assume $\mathcal{L} = 10^{32}$; $\Delta t = 5 \times 10^4 \text{ s}$ for 100 scan points]

(B) $m_H = 100 \text{ GeV}$

$\sigma_{H \rightarrow b\bar{b}} = 9 \times 10^{-36} \text{ cm}^2$

$\frac{\delta p}{p} = 0.01\%$

Same scan method.

$\geq 3\sigma$ effect

Conclude that $\mathcal{L} = 10^{32} \text{ cm}^2 \text{ sec}^{-1}$ and that $\delta p/p = 0.01\%$ is adequate to find the Higgs.

Also Bayes / Bayes
Two, Non etc

WHY THE STUDY OF HIGGS

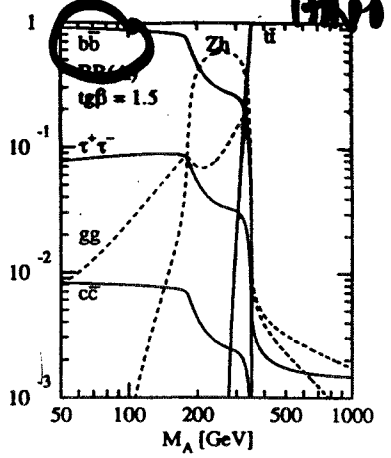
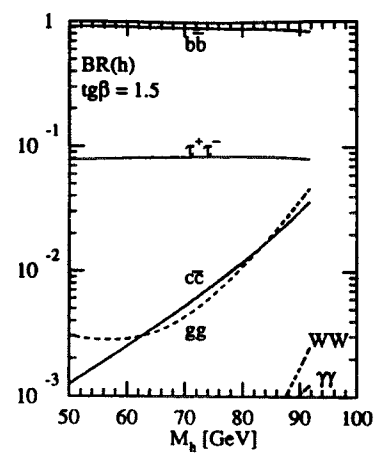
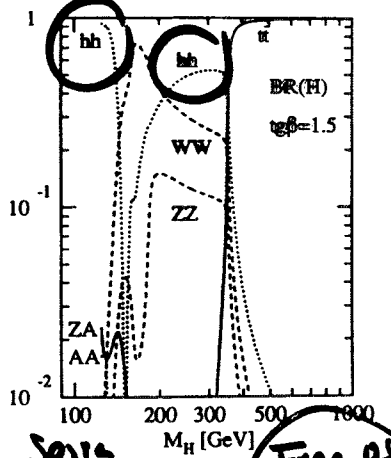
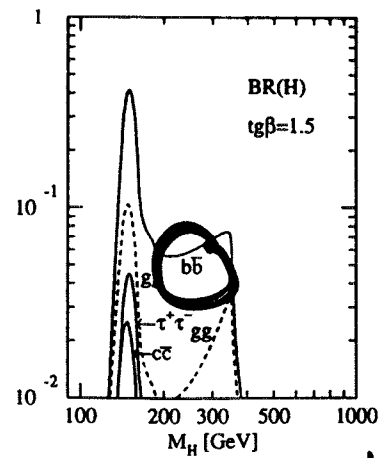


Fig. 3a



Djouani, Ka... spira

Figure 3: Branching ratios of the MSSM Higgs bosons h, A(a), H(b), H[±](c) and their total decay widths Γ(Φ)(c), using the inputs of Tab. 2.

Free as from Theora

HDECAY - Program with stu/ MSSM
Higgs Decays DESY 97-074

CURRENT
LIMITS ON Higgs Masses

Updated Limits

- H_{SM}^0 $m > 77.1 \text{ GeV}$ 95% CL (LEP WG) $e^+e^- \rightarrow ZH$
 EW fit: $m = 145^{+116}_{-66} \text{ GeV}$
 $m < 420 \text{ GeV}$ 95% CL
 NAJ $\approx 28 \text{ GeV}$
- SUSY h, A $m_h > 64.5 \text{ GeV}$ (ALEPH) $e^+e^- \rightarrow hZ$
 $m_A > 64.5 \text{ GeV}$ $\tan\beta > 1$ $e^+e^- \rightarrow hA$
 - may exist fine-tuned escapes from limits
- H^\pm $m > 54.5 \text{ GeV}$ $e^+e^- \rightarrow H^+H^-$
 $p\bar{p} \rightarrow t\bar{t} \rightarrow H^\pm X$ CDF & D0 limits
- New LEP limits on parameter space for
 charginos neutrinos $m_{\chi^\pm} \geq 91 \text{ GeV}$
 sleptons $\tilde{e}, \tilde{\mu}$ $m_{\tilde{e}} > 80, m_{\tilde{\mu}} > 73$ for small m_0
 stop sbottom

We heard more on Wed -

THERE ARE
BOUNDS OF Higgs MASS

WHAT CUTS OFF THE DIVERGENCE

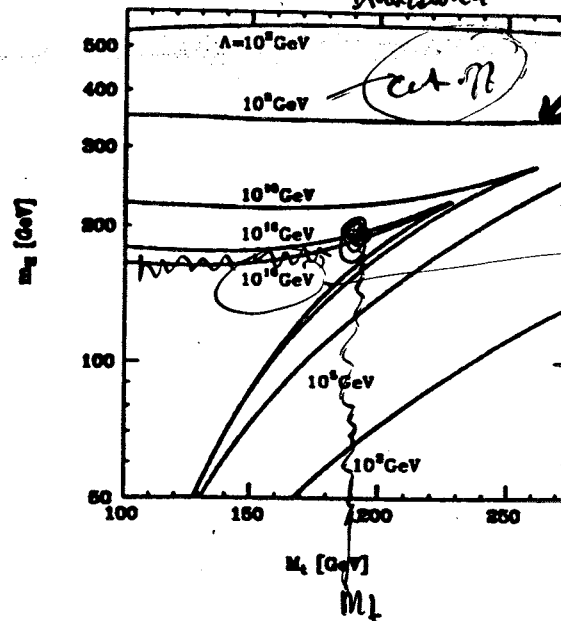


Figure 1: Bounds on the Higgs mass as a function of the top quark mass for different values of the scale Λ , at which new physics is expected to appear.

OTHER "EVIDENCE" FOR LOW MASS Higgs

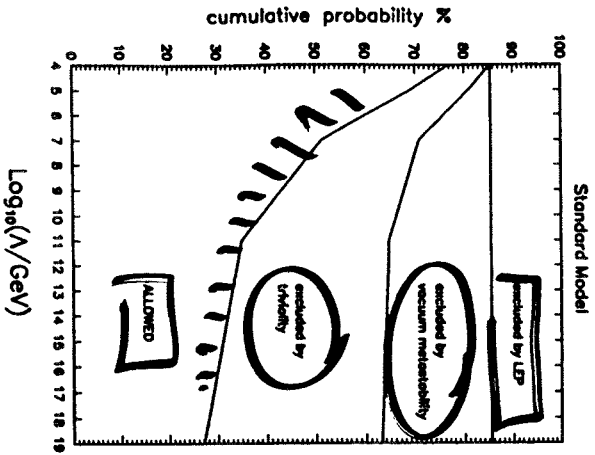
- USING PRECISION ELECTROWEAK DATA
(Z^0 parameter, M_{W^+} , M_t , $\sin^2 \theta_w$ etc)
etc

Current data suggest $M_H < 300$ GeV

After LEP 2 provides precision MW this bound could improve

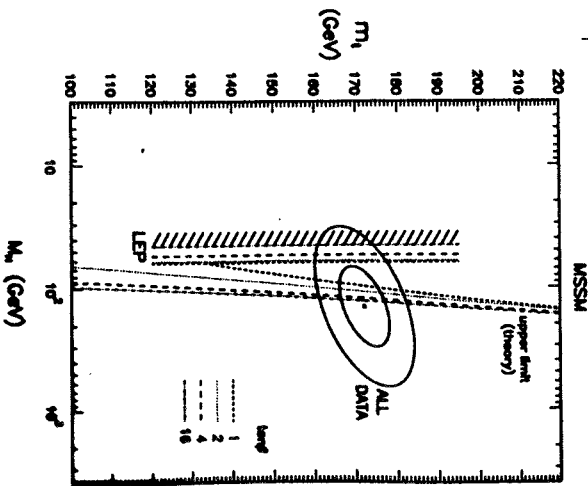
- By ~ 200 we may have a limit with an error of ± 10 GeV that is believable (or so?)

{ All in All it is a good bet that if the Higgs exists AT LEAST ONE WILL BE AT LOW MASS }



Limits on Higgs mass

Mass not set by theory



LAST YEAR

7614

3d

2. Cumulative (integrated) probabilities in the various ranges excluded or allowed in the Minimal Supersymmetric Standard Model. No value of A can be excluded.

FIG. 3. Indirect bounds on M_h and one-sided experimental and theoretical limits in the Minimal Supersymmetric Standard Model. Apart from the Higgs sector, the MSSM spectrum is assumed to be decoupled. Solid ellipses represent the 1- σ and 2- σ contours as in Fig. 1. The vertical lines are the LEP lower bounds on M_h from which derived elliptical contours. The values

EW Data

EW Data

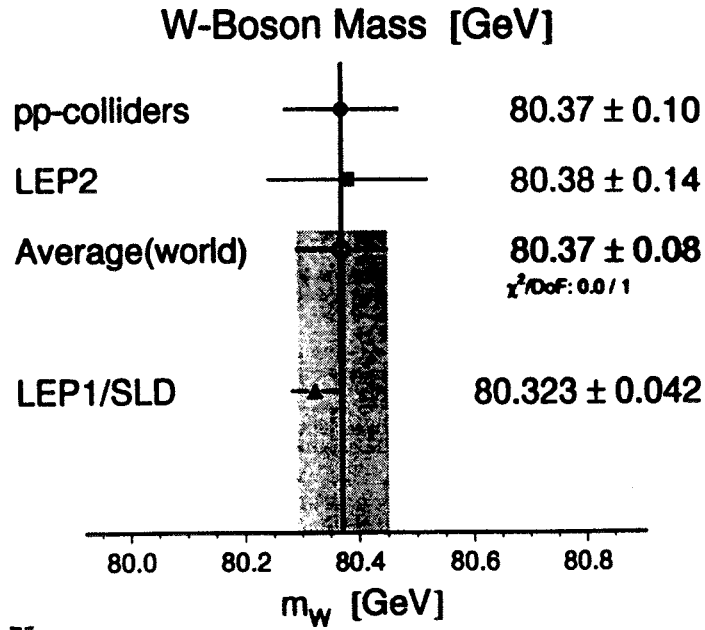
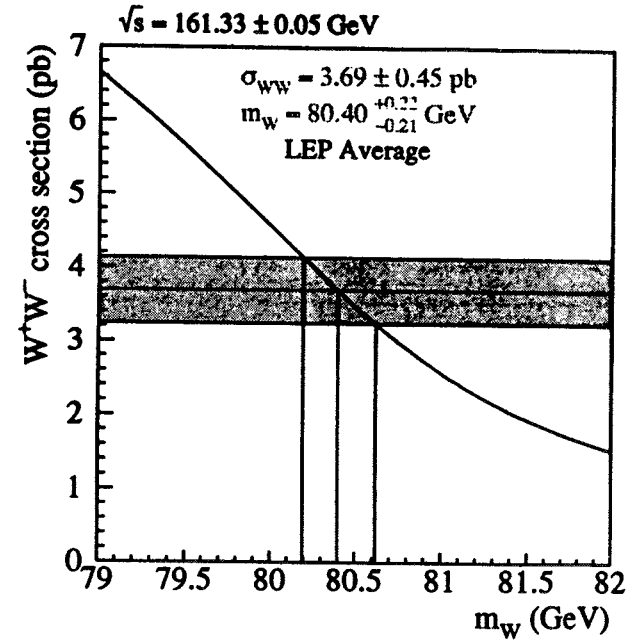


Figure 5: Comparison of the direct W mass measurements at the Tevatron and LEP2 and the indirect determination using LEP1 and SLD data.

m_W from σ_{WW} at 161 GeV



Final LEP 161 GeV W mass
LEP EW Working Group

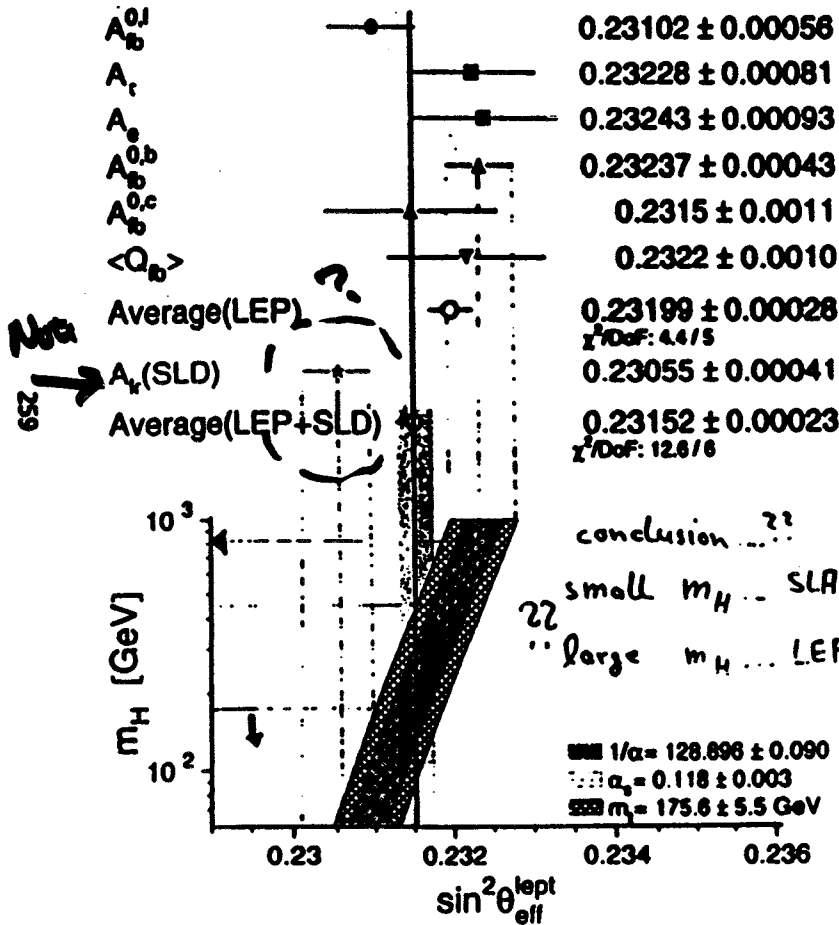
9

Figure 3: WW cross section at $\sqrt{s} = 161.3 \text{ GeV}$ as a function of W mass. The band represents the experimental measurement.

Summary of $\sin^2 \theta_{\text{eff}}^{\text{lept}}$

Effective Electroweak Mixing Angle

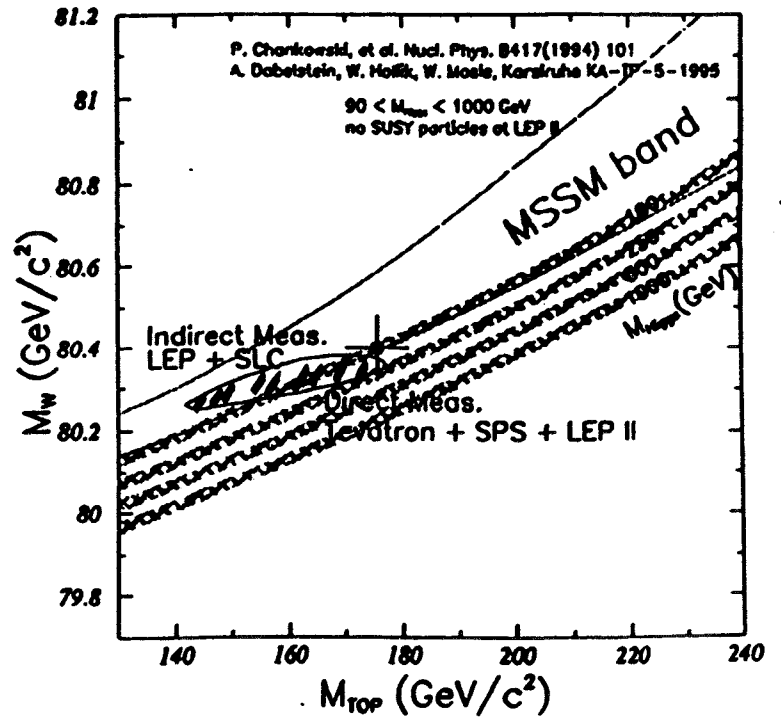
$$\sin^2 \theta_{\text{eff}}^{\text{lept}} = 1/4 (1 - (\bar{g}_V^2 / \bar{g}_A^2))$$



all precision data ...

$$m_H = 115 \pm \frac{116}{66} < 420 \text{ GeV (95\% c.l.)}$$

attention: (1987) $m_{\text{top}} < 180 \text{ GeV}$ U. Amaldi et al.
 (1988) $m_{\text{top}} < 169 \text{ GeV}$ G. Costa et al. (90% c.l.)
 (1991) $m_t = 132 \pm \frac{27}{31} \pm \frac{13}{19}$ LEP coll.



MORE RECENT FITS TO EW
PARAMETER SUCCESSES

— LOW MASS HIGGS —

Davies & Hoche
97

$$M_h = 129^{+103}_{-92} \text{ GeV}$$

Erlen & Longaker
97

$$M_h = 122^{+137}_{-77} \text{ GeV}$$

EW Fit Chan
97

$$M_h = 115^{+116}_{-66} \text{ GeV}$$

$M_h < 420 \text{ GeV } 95\% \text{ C.L.}$

NEW
LEP II limit $\rightarrow M_h > 88 \text{ GeV}$

WE MAY BE TEMPTED TO
ASSUME M_h IS SMALL! \Rightarrow Higgs
Factory!

October 7, 1997

LBL-40877
hep-ph/9710308

Combining real and virtual Higgs boson
mass constraints¹

Michael S. Chanowitz²

Theoretical Physics Group
Lawrence Berkeley National Laboratory
University of California
Berkeley, California 94720

Abstract:

Within the framework of the standard model we observe that there is a significant discrepancy between the most precise Z boson decay asymmetry measurement and the limit from direct searches for Higgs boson production. Using methods inspired by the Particle Data Group we explore the possible effect on fits of the Higgs boson mass. In each case the central value and the 95% confidence level upper limit increase significantly relative to the conventional fit. The results suggest caution in drawing conclusions about the Higgs boson mass from the existing data.

- RECENT YEARS ALSO $Z \rightarrow b\bar{b}$ Problem
 → biased the Fits
 UNTIL EW PARAMETERS ARE
 CONSISTENT WE CAN'T ~~TRUST~~
 M_h ESTIMATE !

Tables

Table 1. Values for $\sin^2\theta_{eff}^{lepton}$ from asymmetry measurements[1] with 1 σ experimental errors. The corresponding Higgs boson masses, the 95% CL upper and lower limits, and the confidence level for $m_H < 77$ GeV are given for each measurement.

	$\sin^2\theta_{eff}^{lepton} (1\sigma)$	m_H (GeV)	$m_{95}^>, m_{95}^<$	$P(< 77\text{GeV})$
A_{LR}	0.23055 (41)	16	3, 80	0.95
A_{FB}^b	0.23236 (43)	520	100, 2700	0.03
A_{FB}^c	0.23102 (56)	40	5, 290	0.71
A_τ	0.23228 (81)	440	30, 6700	0.14
A_e	0.23243 (93)	590	28, 13000	0.14
Q_{FB}	0.23220 (100)	380	14, 10000	0.21
A_{FB}^{τ}	0.23140 (111)	83	2, 3000	0.48

↑
 Is there
 a conflict

8

WHY IS MASS OF h
 IMPORTANT FOR HIGGS FACTORY

LOGIC OF HIGGS

STUDY ON FUTURE

Why a Higgs Factory

Table 3. Logic of detailed study of the Higgs sector.

If particles in the scalar sector are ever discovered, it will be essential to determine their properties, which will give direct information about the nature of the particle and the underlying theory. Three simple examples can be cited:

1. Suppose a Higgs-like particle is discovered with mass 110 GeV. This could either be the Standard Model (SM) Higgs or an MSSM Higgs. A measurement of the width of the state would presumably tell the difference. However, the SM width is 5 MeV - a formidable measurement!
2. Suppose a Higgs-like particle is discovered with a mass of 150 GeV. This is presumably beyond the MSSM bound, but it could be an NMSSM or an SM Higgs. A measurement of the width could presumably resolve the issue.
3. Suppose a Higgs-like particle of mass 165 GeV is discovered. This is presumably even beyond the NMSSM limits. If this is an SM Higgs, can we learn more by the study of the rare decay modes?

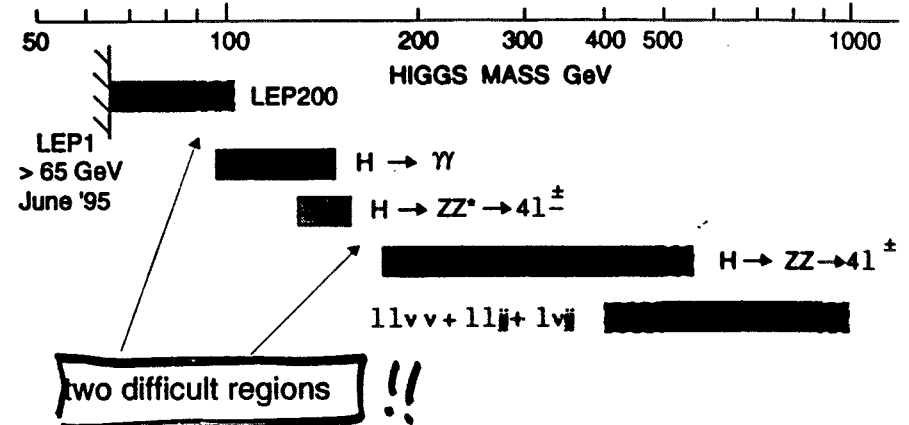
1) $m_h > 150$ GeV - sort out

2) $m_h > 2M_w$ - LHC may do all important physics

SM Higgs search at LHC

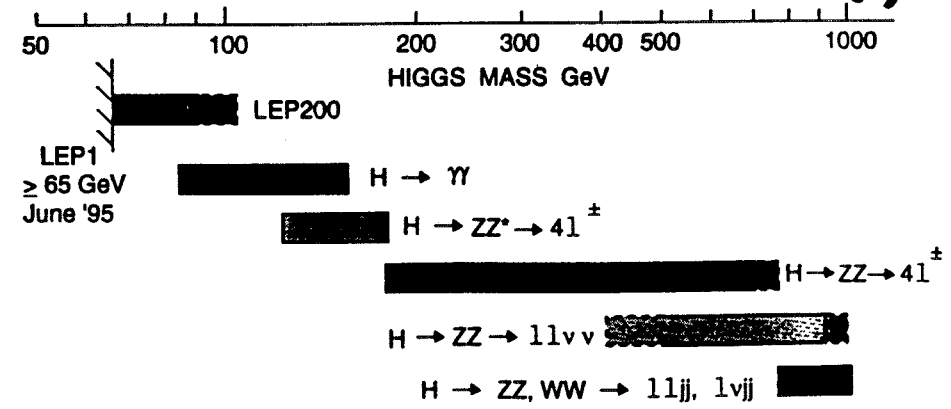
i) mass range explorable at $\sqrt{s} = 14$ TeV
with $3 \cdot 10^4 \text{ pb}^{-1}$ taken at $10^{33} \text{ cm}^{-2}\text{s}^{-1}$

CMS



ii) explorable mass range with 10^5 pb^{-1}
taken at $10^{34} \text{ cm}^{-2}\text{s}^{-1}$

(Hyl d ~ 200 GeV)



Total Weight : 14,500 t
Overall diameter : 14.60 m
Overall length : 21.60 m
Magnetic field : 4 Tesla

Compare **MSL** Solenoid - Mainly p (4p...) Detector

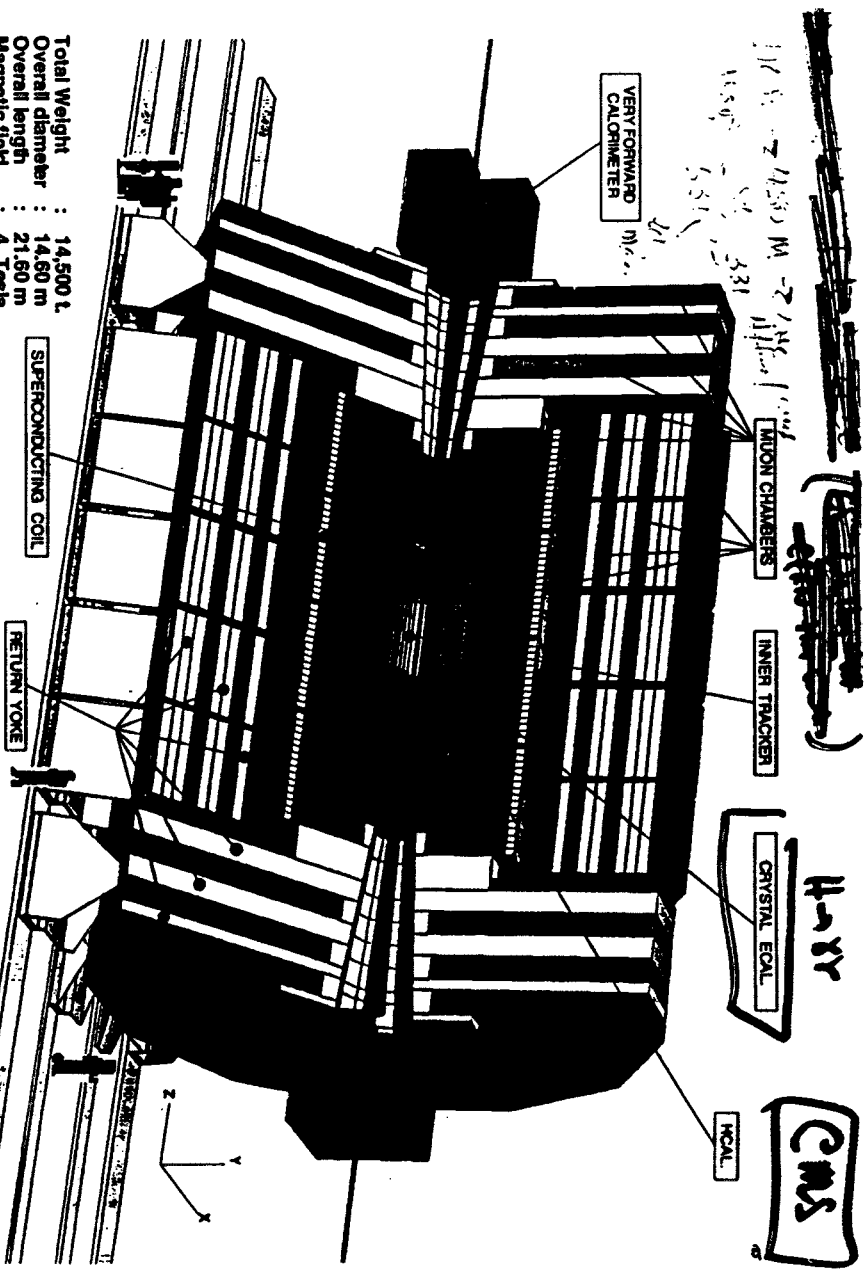


Table 12.4a

Signal significance for $H \rightarrow 4$ charged leptons for $m_H = 130, 150, 170$ GeV at 10^5 pb^{-1} without lepton isolation.

	$m_H = 130$ GeV	$m_H = 150$ GeV	$m_H = 170$ GeV	$t\bar{t}$	$Z b\bar{b}$	ZZ^*
Events in $m_H \pm 2\sigma_H$	41.7	108.3	29.3	4.8/GeV	0.97/GeV	1.8/GeV
Significance	6.1	12.1	4.1			

Table 12.4b

Signal significance for $H \rightarrow 4$ muons for $m_H = 130, 150, 170$ GeV at $2 \times 10^5 \text{ pb}^{-1}$ with muon isolation.

	$m_H = 130$ GeV	$m_H = 150$ GeV	$m_H = 170$ GeV	$t\bar{t}$	$Z b\bar{b}$	ZZ^*
Events in $m_H \pm 2\sigma_H$	31.3	74.1	20.3	0.9/GeV	0.3/GeV	1.3/GeV
Significance	7.4	15.2	5.0			

12.1.6 $H \rightarrow ZZ \rightarrow 4$ Charged Leptons

The $H \rightarrow ZZ \rightarrow 4 \ell^{\pm}$ channel is sensitive, even with only 10^4 pb^{-1} , over a wide mass range, from $2m_Z$ up to about 400 GeV [19]. The main background is non-resonant ZZ production. For $m_H \leq 300$ GeV, the natural width of the Higgs is small (e.g. $\Gamma_H = 1.5$ GeV for $m_H = 200$ GeV), and a good four-lepton mass resolution will facilitate an early observation.

For the ZZ continuum background, the $q\bar{q} \rightarrow ZZ$ subprocess was simulated. The $gg \rightarrow ZZ$ contribution was accounted for by multiplying the $q\bar{q} \rightarrow ZZ$ cross-section by a factor of 1.33 [20]. No k -factors were included for the signal or background.

Internal bremsstrahlung was included using PHOTOS. The fraction of Z s falling outside the $(m_Z \pm 6)$ GeV window, due to the internal bremsstrahlung alone, is 12% for $Z \rightarrow e^+e^-$ and 7% for $Z \rightarrow \mu^+\mu^-$. To account for external bremsstrahlung, a full GEANT simulation of the response to electrons was performed [17] and electron energies were measured in the calorimeter, as discussed in Sect. 11.4. The muon momenta were smeared according to parametrized resolutions obtained from a full GEANT simulation [18]. With $m_H = 300$ GeV, the Z mass resolution in the Gaussian peak region for $Z \rightarrow e^+e^-$ events is 2.2 GeV, and for $Z \rightarrow \mu^+\mu^-$ events, 2.1 GeV. In calculating the expected number of events, a reconstruction efficiency of 95% per lepton was included. No lepton isolation cuts were applied as the $t\bar{t}$ background is negligible.

The p_T and η selection cuts are the same as for the ZZ^* channel. At $m_H = 300$ GeV, the overall (η and p_T) 4-lepton acceptance in the electron channel is 55%, and in the muon channel, 59%. For $m_H = 600$ GeV, the acceptances are 77% and 79%, respectively. Two e^+e^- or $\mu^+\mu^-$ pairs with an invariant mass consistent with a Z were required. The Z mass window is large, $(m_Z \pm 6)$ GeV, since there are no backgrounds which are critically affected by the two-lepton mass cut. Due to bremsstrahlung and momentum resolution, $\approx 40\%$ of the events are lost due to this cut (see Sect. 11.4). A more sophisticated method, using the fine granularity of the ECAL, could allow the recovery of a fraction of the radiative losses in the future.

Figure 12.11 shows the expected 4-lepton mass spectrum for $m_H = 300, 500$ and 600 GeV, with the ZZ background. The event rates shown are for $2 \times 10^4 \text{ pb}^{-1}$ and 10^5 pb^{-1} .

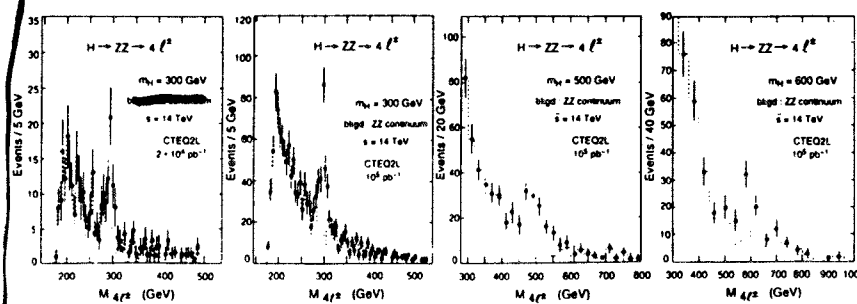


Fig. 12.11. The four-lepton mass distributions for $H \rightarrow ZZ \rightarrow 4 \ell^{\pm}$ superimposed on the ZZ continuum background for $m_H = 300$ and $2 \times 10^4 \text{ pb}^{-1}$ and for $m_H = 300, 500$ and 600 GeV with 10^5 pb^{-1} .

The crystal calorimeter was assumed to have an energy resolution given by $\Delta E/E = 2\%/\sqrt{E} \oplus 0.5\% \oplus 0.200/E$ in the barrel and $\Delta E/E = 5\%/\sqrt{E} \oplus 0.5\% \oplus 0.200/E$ in the endcap, where there is a preshower detector. At high luminosity, a barrel pre-shower detector covers $|\eta| < 1.1$, resulting in a resolution of $\Delta E/E = 5\%/\sqrt{E} \oplus 0.5\% \oplus 0.200/E$ and an ability to measure the photon direction with resolution $\Delta\alpha = 40 \text{ mrad}/\sqrt{E}$ in this region. For more details concerning both the \sqrt{s} configurations and the breakdown of the mass resolution, see Sect. 4.1.



The background to the $H \rightarrow \gamma\gamma$ signal may be divided into three categories:

- prompt diphoton production from quark annihilation and gluon fusion diagrams, which gives an irreducible background,
- prompt diphoton production from significant higher-order diagrams - primarily bremsstrahlung from the outgoing quark line in the QCD Compton diagram,
- background from jets, where an electromagnetic energy deposit originates from the decay of neutral hadrons in a jet or from 1 jet + 1 prompt photon.

The prompt diphoton background was generated using CTEQ2L structure functions in PYTHIA. For the bremsstrahlung background, a previous PYTHIA calculation for $\sqrt{s} = 16$ TeV, $m_{\text{top}} = 150$ GeV, and HMRSB structure functions, was rescaled to take account of the new parameters. The resulting cross-sections are given in Table 12.1. It is assumed that the jet background is reduced to an insignificant level ($< 10\%$) by the combination of isolation and π^0 rejection cuts.

Figure 12.3 shows a background-subtracted two-photon effective mass plot for a simulated single experiment, for an integrated luminosity of 10^5 pb^{-1} (taken at high luminosity) with signals at $m_H = 90, 110, 130$ and 150 GeV. Figure 12.4 shows a similar plot, for an integrated luminosity of $3 \times 10^4 \text{ pb}^{-1}$ taken at low luminosity.

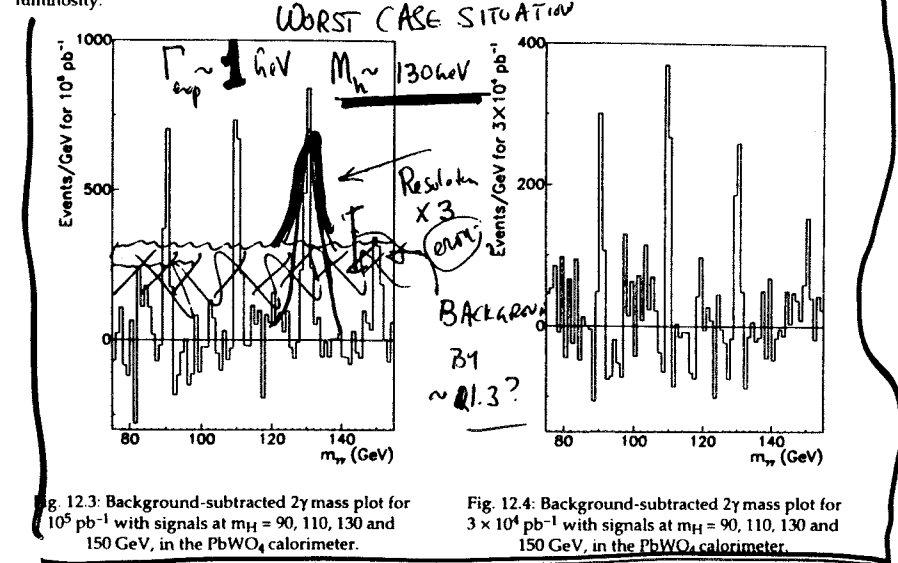


Fig. 12.3. Background-subtracted 2γ mass plot for 10^5 pb^{-1} with signals at $m_H = 90, 110, 130$ and 150 GeV, in the PbWO_4 calorimeter.

Fig. 12.4. Background-subtracted 2γ mass plot for $3 \times 10^4 \text{ pb}^{-1}$ with signals at $m_H = 90, 110, 130$ and 150 GeV, in the PbWO_4 calorimeter.

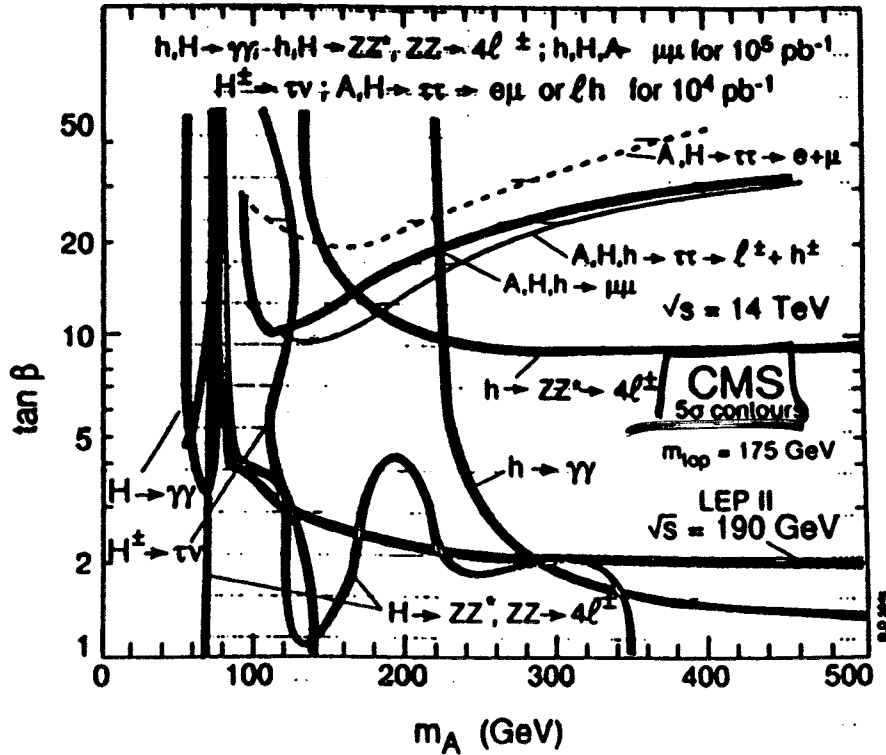
Figures 12.5 and 12.6 show contours giving the cross-section times branching ratio required to give specified signal significances ($N_S / \sqrt{N_B}$), as a function of mass. The significances were calculated by counting events within a mass window of optimum width, corresponding to the width containing about 75% of the signal. After a single year of running at $10^{34} \text{ cm}^{-2}\text{s}^{-1}$ (10^5 pb^{-1} , Fig. 12.5), an SM Higgs could be discovered across the full range 85 to 150 GeV. After only $3 \times 10^4 \text{ pb}^{-1}$ (Fig. 12.6), taken at low luminosity, an SM Higgs could be discovered between 95 and 150 GeV.

LHC OBSERVED BUT CAN'T REALLY STUDY LIGHT HIGGS

Significance contours for MSSM Higgs bosons

WHAT ABOUT "TOTAL SUSY"
AT LHC

Regions of the MSSM parameter space ($m_A, \tan\beta$)
explorable through various SUSY Higgs channels



THESE ARE FOR LIMITS BUT
IF THERE IS A SUSY THRESHOLD...

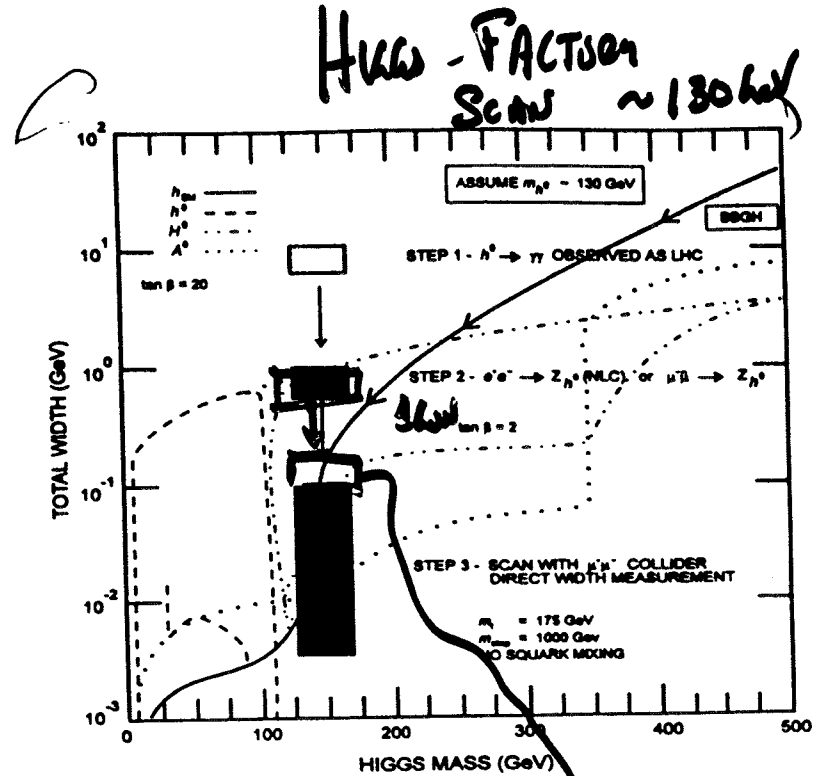
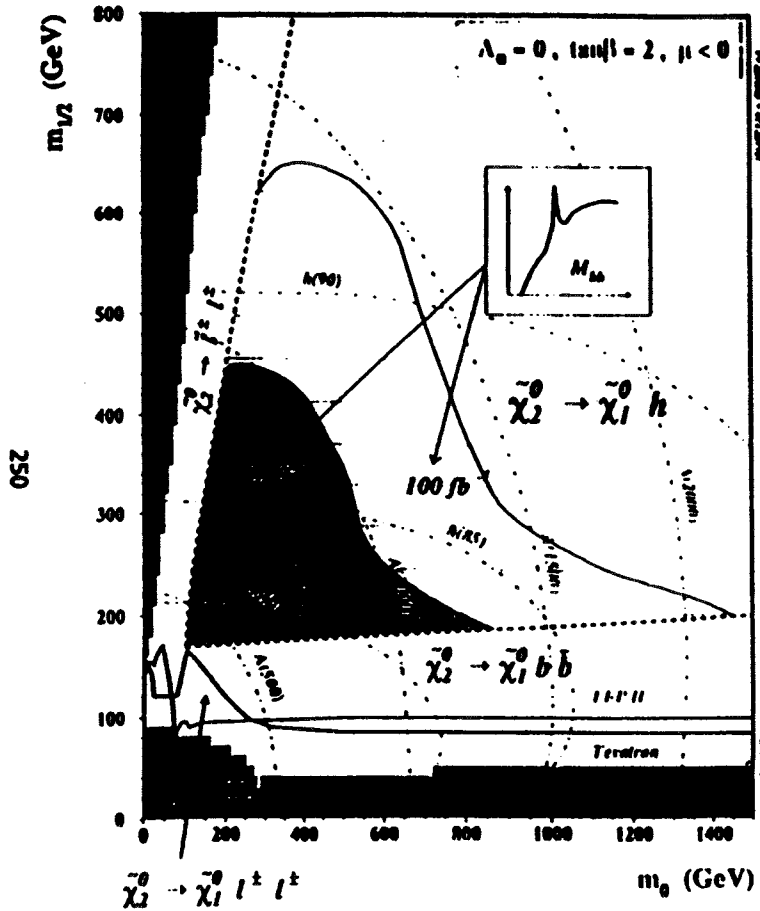


Fig. 2. Higgs-factory $\mu^+\mu^-$ collider concept. The Higgs is discovered at the LHC (CMS) and the width further reduced at the NLC or at a $\mu^+\mu^-$ collider. The final stage is to scan for the Higgs at the $\mu^+\mu^-$ collider. Existing models can be distinguished by their widths. (Adapted from Ref. 12 (BGGH = Barger, Berger, Gunion, Han) and Ref. 14.)

Comments from
Neal Tully

**IN THIS CASE A HIGGS FACTORY
MAY NOT BE NECESSARY !!**

Domains of $h \rightarrow b\bar{b}$ peak visibility
in the framework of mSUGRA model



WHEN MAY WE KNOW THAT
A HIGGS FACTORY IS ESSENTIAL

- 1) EW Measurements in Sit
 ~ 2001 — LEP II
 ~ 2001 — TEV 2 + Main
 may "prime" $m_h < 180 \text{ GeV}$ Japan
 OR LEP II $\rightarrow m_h \leq 105 \text{ GeV}$
- 2) FNAL MAY DISCOVER $m_h < 180 \text{ GeV}$
 $\sim 2003 ?$
- 3) LHC Discover Higgs but not
total SUSY
 $\sim 2007 ?$
 2001 - early
 2003 - reach
 2007 - later

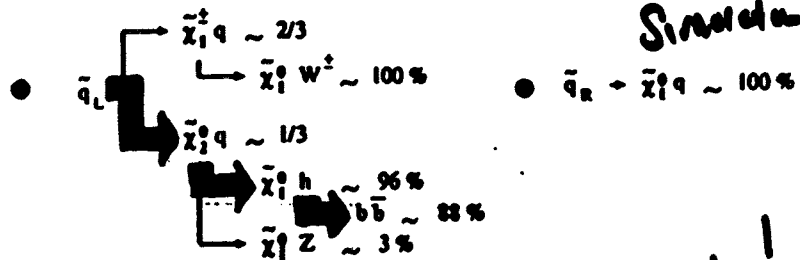
Example of masses and branching ratios at one point
 in $m_0, m_{1/2}$ space :

● $m_0 = 500$ GeV, $m_{1/2} = 500$ GeV, $A_0 = 0$, $\tan\beta = 2$, $\mu < 0$

$m_{\tilde{g}} = 1224$ GeV $m_{\tilde{q}} \leq m_{\tilde{g}}$ $m_{\tilde{t}_1} = 852$ GeV
 $m_{\tilde{t}_2} = 217$ GeV
 $m_{\tilde{b}_1} = 427$ GeV $m_{\tilde{b}_2} = 611$ GeV $m_h = 89.7$ GeV

dominant decays :

● $\tilde{g} \rightarrow \tilde{q}\tilde{q}$ ($\tilde{t}_1, \tilde{t}_1 - 49\%$, $\tilde{b}_1, \tilde{b}_1 - 17\%$)



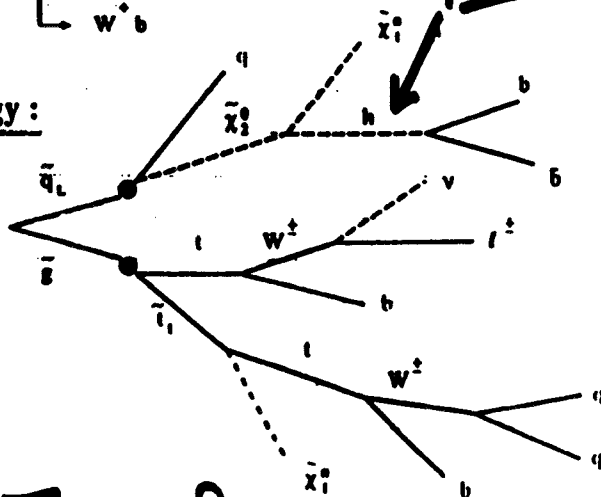
● $\tilde{t}_1 \rightarrow \tilde{X}_1^0 t \sim 94\%$
 $\tilde{t}_1 \rightarrow W^+ b$

Recall
 CMS
 Simulation

Note!

event topology :

- ▶ 4 b-jets
- + 3 non-b jets
- + \cancel{E}



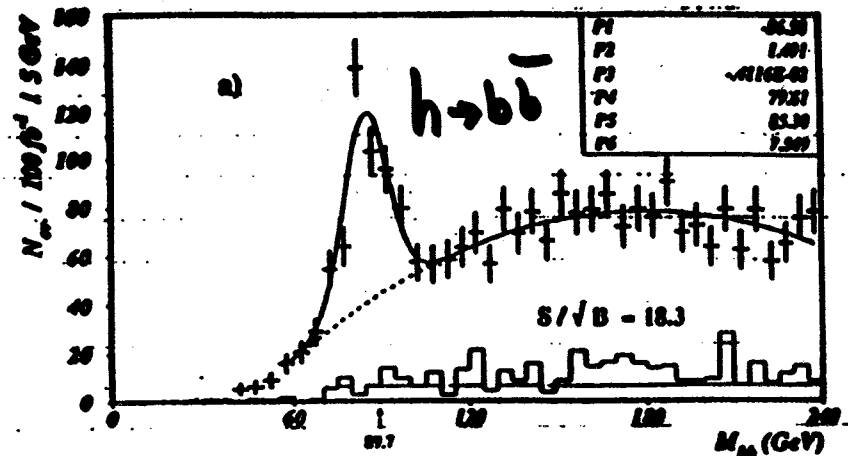
S. Abdullin
 D. Denegri

— TOTAL SUSY AT LHC —

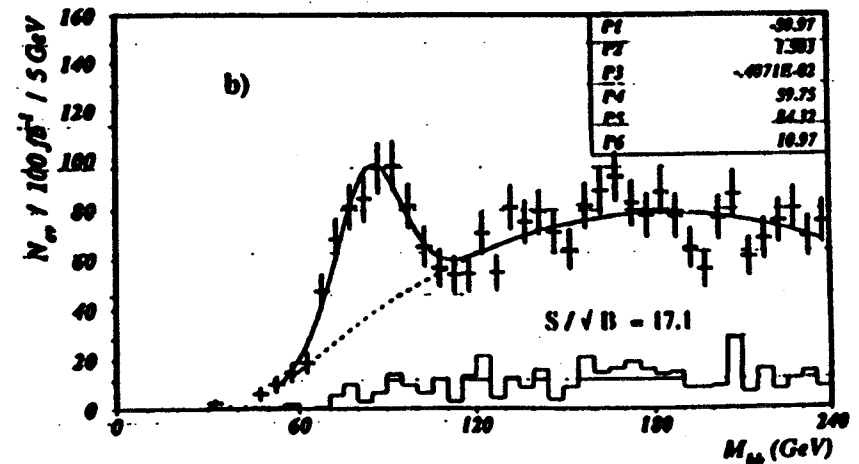
$h \rightarrow b\bar{b}$ in $mSUGRA$

E_T Cuts

nominal CMS performance

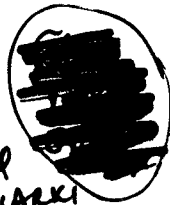


HCAL : $\sigma/E = 120\% / \sqrt{E} \oplus 10\%$



Here OBSERVED in $b\bar{b}$
 OR Manual BR STATE!!

SEARCH FOR FCNC HIGGS DECAY AT A HIGGS FACTORY



- THE ABSENCE OF FCNC IN QUARKS
TRANSITIONS COMES FROM QCD
MECHANISM - THERE IS NO
KNOWN REASON FOR THE SUPPRESSION
IN THE SCALAR SECTOR
(EXCEPT FOR THE GLASHOW-WEINBERG
ASSUMPTION IN 79)

- $K \rightarrow \pi^+ \nu \bar{\nu}$... ARE INSENSITIVE TO
THE HIGGS SECTOR
SINCE $H \rightarrow \nu \bar{\nu}$
 $\rightarrow e \bar{e}$ (if ν is small)

- IN ADDITION MODELS OF A COMPOSITE
HIGGS THAT $t\bar{t}$ COULD HAVE FCNC - (Almost
+ Sand)

- AT A HIGGS FACTORY ONE CAN SEARCH FOR
FOR $H \rightarrow q_i \bar{q}_i$ $\rightarrow s\bar{s}$ $\rightarrow c\bar{c}$ } Low
NEEDS
HIGGS

$\rightarrow t\bar{t}$ or $t\bar{u}$
for $M_H > M_t$

Probably to the level of $\sim 10^{-4} - 10^{-5}$

TESTING NFC at a $\mu^+ \mu^-$ Higgs Factory (if $M_H > 150$ GeV)

Fig. 6. Possible probe of new physics in a rare Higgs decay mode.

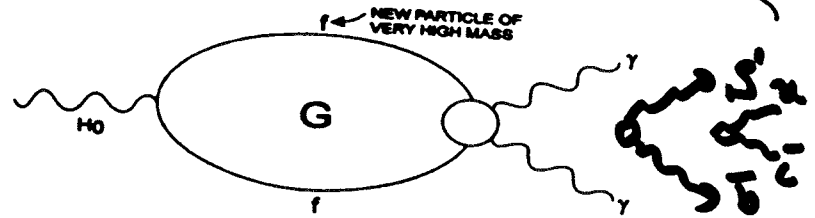


Fig. 6. Possible probe of new physics in a rare Higgs decay mode.

This same new Physics
may cut off the divergence
in the Higgs Section

Summary

- 1) All of our current success in Weak Interactions Phys. has come from ~~avoiding~~ AVOIDING DIVERGENCES → (Feynman, 't Hooft) 1950s } 1983 CERN PP GP } "GP".
 (WGC) 80s
- 2) The Higgs sector has a serious "sickness" - self energy corrections
 - a) Susy corrects → $M_h < 150$ GeV
divergence → $M_A \dots$
 - b) Some unknown phys. would diverge (study NFE ...)
 at NP
- 3) A Higgs Factory is to study the Higgs sector BUT
 - If $M_h > 200$ GeV the LHC (CMS/ATLAS) will do a very good job!
 - $160 \text{ GeV} < M_h < 200$ GeV - Susy Higgs not NP
 - $M_h < 150$ GeV - Higgs Factory essential → NP
- 4) If the LHC crosses a threshold so that Susy is dominant - Higgs study is likely done by SUSY → decays - Not Necessary

WHEN A HIGGS FACTORY IS NEEDED AND WHY

<u>M_{Higgs}</u>	<u>Standard model or Susy</u>	<u>pp Colliders if needed</u>	<u>Comments</u>
$\sim 88 \rightarrow 130$ GeV ↓ LEET Limit ↓ NMSB Limit	Susy Higgs mass Range - Higgs very small	yes(?)	However if M_h is low LHC may be <u>blinded</u> with $h \rightarrow b\bar{b}$ (CMS Study)
$\sim 150 \sim 200$ GeV	Outside η Susy Higgs - but self coupling stability still to be explored	yes!!	In <u>background mass range</u> to study at LHC
$200 - 300$ GeV	Outside Susy Range - but can be observed at LHC	No? for h^0	If low mass Susy observed and seen if LHC played with h^0 H, A difficult to study at LHC
> 300 GeV	For SM Model Higgs For $A, H \dots$ Susy Higgs	No for h^0 → yes for A, H	

Higgs Factory "Crown Jewel" of pp Colliders
BUT MUST BE JUSTIFIED!

HIGGS BOSON MASS/PHYSICS

DISCUSS :

- HOW LIKELY IS A HIGGS BOSON TO EXIST?
- HOW LIKELY IS IT TO HAVE A PARTICULAR MASS?
- SEVERAL HIGGS BOSONS? MASSES?
- PRODUCTION? DECAYS?
- WHEN IS h LIKELY TO BE DETECTED DIRECTLY?
- WHAT WILL BE KNOWN ABOUT h BEFORE μC ?

G. KANE, $\mu C 92$

• HIGGS PHYSICS -- TECHNICALLY OK,
CONCEPTUAL MYSTERY

- VERY DIFFICULT TO CONSTRUCT ALTERNATIVES TO HIGGS MECHANISM, IN ORDER TO GIVE MASSES TO GAUGE BOSONS AND FERMIONS AND HAVE RENORMALIZABLE THEORY
- HIGGS PHYSICS ORIGIN CENTRAL PROBLEM OF STANDARD MODEL
- HIGGS PHYSICS POINTS WAY TO HOW TO EXTEND SM, SINCE SM ALONE IS NOT STABLE TO RADIATIVE CORRECTIONS, NOR CAN THE EW SYMMETRY BE BROKEN INTERNALLY
- CURRENTLY STILL (BARELY) CONCEIVABLE THAT NO HIGGS BOSON EXISTS

HOW LIKELY IS h^0 ?

- THERE IS GOOD EVIDENCE THAT BREAKING OF EW SYMMETRY IS PERTURBATIVE, AND GOOD EVIDENCE THAT NATURE IS SUPERSYMMETRIC

- predicted by SUSY*
- UNIFICATION OF GAUGE COUPLINGS -- THEY CHANGE AS GO TO SMALLER DISTANCES BECAUSE OF SUPER PARTNERS IN LOOPS
 - AGREEMENT OF PRECISION MEASUREMENTS WITH SM -- SUSY ONLY ENTERS THROUGH LOOPS SO EFFECTS SMALL
 - PERTURBATIVE DERIVATION OF HIGGS MECHANISM -- $M_{H_{top}}^2 < 0$ BECAUSE OF TOP LOOP IF m_{top} LARGE

predicted by SUSY

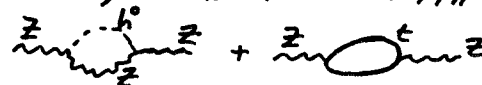
- IF SUSY, THEN h^0 EXISTS

• ANALYSIS OF LEP DATA

$m_{h^0}^{SUSY} \leq m_{h^0}^{SM}$

$$\Rightarrow m_{h^0} = 100_{-50}^{+100} \text{ GeV}$$

ALL PARTICLES ARE SOMETIMES COMBINATIONS OF ALL OTHERS -- PROPERTIES OF VIRTUAL PARTICLES AFFECT BEHAVIOR OF OBSERVED ONES -- LAMB SHIFT ~1947, TOP QUARK AT LEP 1991



$$\Rightarrow \delta(\text{OBSERVABLES}) \sim () G_F m_t^2 + () g_2^2 \ln(m_h/m_Z)$$

\Rightarrow VERY LIKELY h^0 EXISTS

-- MAYBE DON'T BET YOUR HOUSE ON IT BUT SURELY DON'T BET AGAINST IT WHEN PLANNING

WE KNOW h^0 EXISTS, CAN CONSTRAIN MASS

m_{h^0} ?

ASSUMES SM --
MUST $\lesssim m_h$

• EXPERIMENTAL CONSTRAINT

$$m_{h^0} \approx 100^{+100}_{-50} \text{ GeV}$$

-- WILL IMPROVE A LITTLE -- COUPLE OF THEORETICAL CORRECTIONS, THEN ALL WILL BE INCLUDED THAT COULD HAVE AN EFFECT \sim EXPERIMENTAL SENSITIVITY
-- SOME REVISION OF PRECISION MEASUREMENTS IN PROGRESS -- BETTER m_t ACCURACY -- BETTER UNDERSTANDING OF α_s

• THEORETICAL CONSTRAINTS -- DEPEND ON:

▲ WHICH THEORY -- SM, MSSM, GENERAL SUSY, X

-- SM OFTEN USED AS TOY MODEL, TO CALIBRATE DETECTORS, BUT UNLIKELY TO DESCRIBE NATURE BECAUSE OF HIERARCHY PROBLEM -- SOME EXTENSION OF SM NEEDED, USUALLY AFFECTS HIGGS SECTOR

▲ WHETHER THEORY IS PERTURBATIVE UP TO \sim UNIF SCALE, OR INSTEAD NEW STRONGLY INTERACTING PHYSICS APPEARS AT LOWER SCALES -- EVIDENCE FOR PERTURBATIVITY, DON'T BET AGAINST IT IN PLANNING

▲ IN SM, STABILITY OF VACUUM

CONSIDER SM

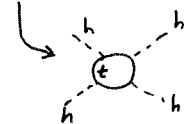
$$V = \mu^2 \phi^2 + \lambda \phi^4, \lambda \sim m_h^2$$

-- ASSUME PERTURBATIVE TO $\approx 10^{16}$ GeV

$$\Rightarrow 130 \lesssim m_h \lesssim 190 \text{ GeV}$$

• UPPER LIMIT -- IF m_h TOO LARGE THEN λ LARGER AT SCALE $\sim m_h$ -- THEN AS EXTRAPOLATE λ TO HIGH SCALE IT BLOWS UP

• LOWER LIMIT -- λ HAS TOP LOOP -- CAN GO NEGATIVE



SO WORLD DOES NOT STAY IN STABLE MINIMUM -- IF m_h TOO SMALL THEN λ STARTS SMALL -- $\lambda \sim 0$ AS GOES NEGATIVE SO PERTURBATIVE, CALCULABLE -- BUT POTENTIAL ONLY GAUGE INVARIANT AT EXTREMA, SO INTRINSIC UNCERTAINTY

NOTE -- IN SM, m_h NOT CALCULABLE -- DEPENDS ON λ -- λ NOT MEASURABLE OUTSIDE OF HIGGS SECTOR

MSSM -- h^0 EXISTS

$$30 \lesssim m_{h^0} \lesssim 130 \text{ GeV}$$

EXPT
NOW
 $75 \lesssim m_{h^0}$

$$m_h^2 \leq \underbrace{m_{\frac{Z}{2}}^2 \cos^2 2\beta}_{\text{TREE LEVEL}} + \underbrace{\frac{3}{4\pi} v_s \frac{m_t^4}{m_W^2} \ln \left(\frac{m_{\frac{Z}{2}}^2 m_{\frac{Z}{2}}^2}{m_{\frac{Z}{2}}^2} \right)}_{\text{LOOP CORRECTIONS}} + \dots$$

- NOTE --- IF $\tan\beta \rightarrow 1$ THEN $\cos 2\beta \rightarrow 0$ --- IF $m_{\frac{Z}{2}}^2 \rightarrow m_{\frac{Z}{2}}^2$ THEN $\ln(\dots) \rightarrow 0$
 --- NO VACUUM STABILITY LOWER BOUND ---
 RUNNING OF λ GETS CONTRIBUTIONS FROM
 TOP AND STOPS --- THEY APPROXIMATELY
 CANCEL --- POTENTIAL ALWAYS STABLE

[MSSM = THEORY WITH SM PARTICLES AND
 THEIR SUPERPARTNERS, SM $SU(3) \times SU(2) \times$
 $U(1)$ SYMMETRY, 2 HIGGS DOUBLETS ---
 GENERAL SOFT SUSY BREAKING]

NOTE --- IN SUSY, m_h CALCULABLE IN TERMS OF
 PARAMETERS THAT CAN BE MEASURED OUTSIDE
 THE HIGGS SECTOR ($\tan\beta, m_{\frac{Z}{2}}, m_{\frac{Z}{2}}^2$ ---)

GENERAL SUSY

-- ANY HIGGS SECTOR, ANY SUSY
 BREAKING, NO ASSUMPTIONS BUT
 PERTURBATIVITY

$$\Rightarrow m_{h^0} \lesssim 150 \text{ GeV}$$

PRESENTLY $\pm \sim 10\%$

e.g.

$$m_{h^0}^2 \leq m_{\frac{Z}{2}}^2 \left(\cos^2 2\beta + \frac{2\lambda^2}{g_s^2} \cos^2 \theta_w \sin^2 2\beta \right) + (\dots) m_{\frac{Z}{2}}^4 \ln m_{\frac{Z}{2}}^2 / m_t^2$$

EXTRA TERM BOUNDED IF ALL COUPLINGS
 PERTURBATIVE --- BOUND CALCULABLE

X

- IF NO SUSY, MAYBE NO h^0 -- NO MODEL OR UNDERSTANDING OF WHAT TO EXPECT -- MAYBE GAUGE BOSONS INTERACT STRONGLY, IF SO MAY OR MAY NOT BE OBSERVABLE -- MAYBE TOP INTERACTS STRONGLY -- IF WW INTERACT STRONGLY, COULD BE ABOVE ~ 8 TeV
- INTERESTING APPROACH -- JIM WELLS -- MAYBE TOP GETS PART OF MASS FROM NORMAL HIGGS MECHANISM, PART FROM CONDENSATE DUE TO (NEW) STRONG INTERACTION -- ALSO GET SCALAR ($t\bar{t}$ BOUND STATE) -- SCALAR MAY OR MAY NOT MIX WITH h^0 -- PROPERTIES OF " h^0 " CAN BE VERY DIFFERENT -- CAN HAVE REDUCED COUPLING TO Z, W -- COUPLINGS TO $b\bar{b}$ CAN BE SMALLER -- VERY DIFFERENT PRODUCTION CROSS SECTIONS
(COUPLING TO $\mu^+\mu^-$ CAN BE MUCH SMALLER)

SO

\Rightarrow UNLESS BEING MISLEAD BY BOTH DATA AND THEORY, AND GAUGE COUPLING UNIFICATION JUST UNLUCKY ACCIDENT,

$$m_{h^0} \lesssim 150 (\pm 10\%) \text{ GeV}$$

AND

$$\text{PROBABLY } m_{h^0} < 130 \text{ GeV}$$

- ALSO -- THERE ARE SOME HINTS THAT $\tan\beta \lesssim 2$, $m_{\tilde{t}} \lesssim m_t$
 $\Rightarrow m_{h^0} < 100 \text{ GeV}$

ONCE h^0 FOUND -- WOULD LIKE TO CONFIRM CONSISTENT WITH SUSY

- SM -- ONE DOUBLET OF COMPLEX FIELDS (ϕ^\pm) \rightarrow 4 REAL STATES, 3 BECOME $W_{LONG}^\pm, Z_{LONG} \Rightarrow$ 1 PHYSICAL BOSON
- SUSY -- TWO COMPLEX DOUBLETS \rightarrow 8 REAL STATES -- STILL 3 BECOME $W_{LONG}^\pm, Z_{LONG} \Rightarrow$ 5 PHYSICAL BOSONS h^0, A^0, H^0, H^\pm
- POSSIBLY ADDITIONAL STATES
- ONLY ONE COMBINATION GIVES MASS TO W, Z -- MASS EIGENSTATES LINEAR COMBINATIONS -- SO ALL "MIGGS BOSONS"

• ONLY SURE WAY TO TELL IS TO DETECT ADDITIONAL STATES A^0, H^0, H^\pm

• POSSIBLY CAN SHOW Γ_{TOT}^h OR $g(U\bar{U}h)/g(D\bar{D}h)$ DIFFERENT FROM SM

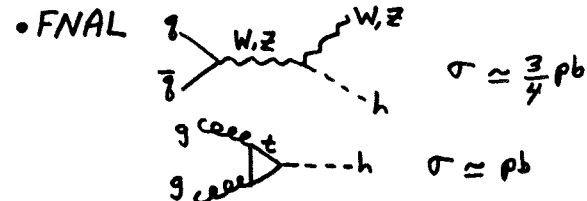
• PROBABLY $m_{h^0} <$ SM LOWER LIMIT

• PROBABLY PRECISE MEASUREMENT OF m_{h^0} NOT DEFINITIVE SINCE CALCULATION OF m_{h^0} HAS SCALE, SCHEME DEPENDENCE (~ 1 G.V.?)

WHEN WILL h^0 PROBABLY BE DETECTED? WHAT WILL BE MEASURED?



- SEARCH FOR $m_{h^0}^{SM} \leq 100$ GeV BY ~ 2000
- MEASURE $g(ZZh)g(hb\bar{b})$
- OBSERVE DECAY TO $b\bar{b}$ ONLY
- SOME PRODUCTION, DECAY DISTRIBUTIONS



-- USE W, Z TRIGGER, OR τ 'S

- $W(\rightarrow l^+\nu) h(\rightarrow b\bar{b})$
- $W(\rightarrow jj) h(\rightarrow \tau\tau)$
- $Z(\rightarrow \nu\bar{\nu}, l^+l^-) h(\rightarrow b\bar{b})$
- $Z(\rightarrow jj) h(\rightarrow \tau\tau)$

GUNION, HAN, MARCIANO, STANGE, WILLENDORF, ARENDA, GK

\Rightarrow OBSERVE h_{SM}^0 IF $m_{h^0} \leq 120$ [$W(\rightarrow l^+\nu)h$]
 $m_{h^0} \leq 135$ [ALL MODES]

(STILL SOMEWHAT CONTROVERSIAL)

-- SUSY SITUATION UNDER STUDY -- COULD BE SAME
 -- COUPLINGS CHANGE -- IF σ REDUCED THEN M_A NOT TOO LARGE, SEE $h^0 + A \rightarrow b\bar{b} b\bar{b}, b\bar{b} \tau\tau$

NOTE --- AT FNAL, BY 2006 EXPECT

$$\geq 50 \text{ fb}^{-1} \quad (2 \text{ DETECTORS})$$

$$\Rightarrow N_{\text{EVENTS OF } h^0 \text{ PRODUCED}} \approx 1.75 \text{ pb} \times 50 \text{ fb}^{-1} \approx 85,000$$

\Rightarrow ONCE MASS MEASURED, CAN
DETECT $BR(\tau\bar{\tau}), BR(\gamma\gamma) \sim 10^{-3}$,
 $BR(\mu^+\mu^-) \sim \frac{1}{3} 10^{-3}$

• CAN TRY FOR $g(\tau\bar{\tau}h), g(c\bar{c}h)$

$$-- \sigma(h^0 + X) \sim g(\tau\bar{\tau}h) \rightarrow \dots$$

$$-- BR(h^0 \rightarrow \text{hadrons}) \approx \underbrace{BR(c\bar{c}) + BR(gg) + BR(bb)}_{\sim g(W\bar{W}h^0)}$$

$$-- \sigma(h^0 + \gamma) \sim g(\tau\bar{\tau}h^0) \quad \text{DICUS, REPKO ET AL}$$

WHAT MIGHT PREVENT DETECTION AT LEP, FNAL!

• $\sin^2(\beta - \alpha) \ll 1$ SO ZZh, WW_h SMALL
-- PROBABLY $h^0 + A^0$ OK AT FNAL,
CERTAINLY OK AT NLC (400)

• MIX SINGLET INTO h^0

$$W, Z \text{ MASS FROM } D_\mu h = (\partial_\mu - ig_2 \vec{W} \cdot \vec{T}) h$$

$$\left(\begin{array}{c} \cdot \\ \cdot \\ \cdot \end{array} \right) \left(\begin{array}{c} \cdot \\ \cdot \\ \cdot \end{array} \right)$$

$$\text{FERMION MASS FROM}$$

$$\bar{L} H e_R$$

$$\left(\cdot \cdot \right) \left(\cdot \right)$$

SO SINGLET UNCOUPLED FROM Z, W ,
FERMIONS -- BUT CAN MIX IN WAVE
FUNCTIONS OF MASS EIGENSTATES
(LIKE STERILE ν)

-- BUT OK IN PRINCIPLE -- MUST GET

$M_{W, Z, \text{FERMION}}$ -- IF " h^0 " MAINLY
SINGLET, THEN NEXT STATE SATISFIES
BOUND $M \lesssim 150 \text{ GeV}$, AND IT CAN
BE PRODUCED -- NOT AT LEP OR
FNAL, OK AT NLC (400) --
PRESUMABLY OK AT HEAC

OKADA ET AL
ELLWANGER,
SAYO ET AL
SUNION, HÄGER
ET AL

• WELLS SCENARIO

CONCLUDE

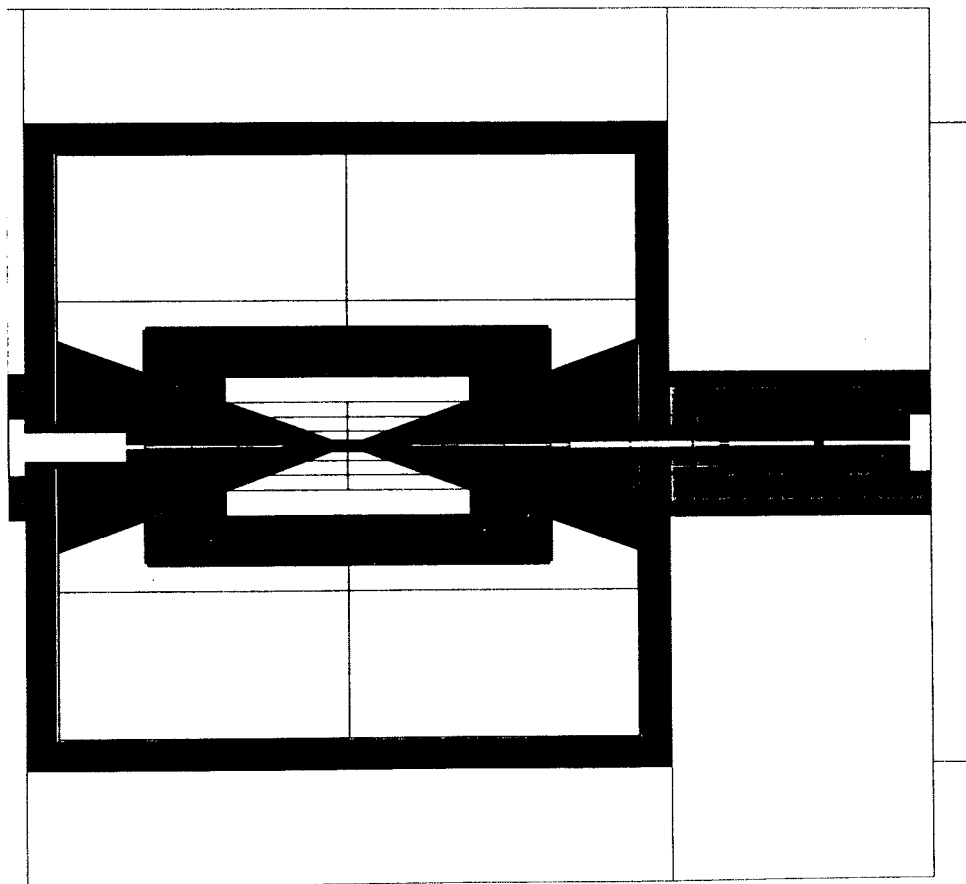
- PROBABLY h^0 EXISTS
- $m_{h^0} \lesssim 150$ GeV
- PROBABLY $m_{h^0} < 130$ GeV
- SOME INDICATION $m_{h^0} < 100$ GeV
- PROBABLY $\geq 75,000$ h^0 PRODUCED
AT FNAL, BR (XX, MM) DETECTED
- HEAVY HIGGS BOSONS? -- CHANCE FOR
 A^0 AT FNAL
- LHC? -- PRODUCE LOTS OF A^0, H^0, H^\pm
-- DETECTION? -- HARD TO SAY
UNTIL KNOW SPARTICLE
MASSES, SINCE BR (SPARTICLES)
IS LARGE IF ALLOWED

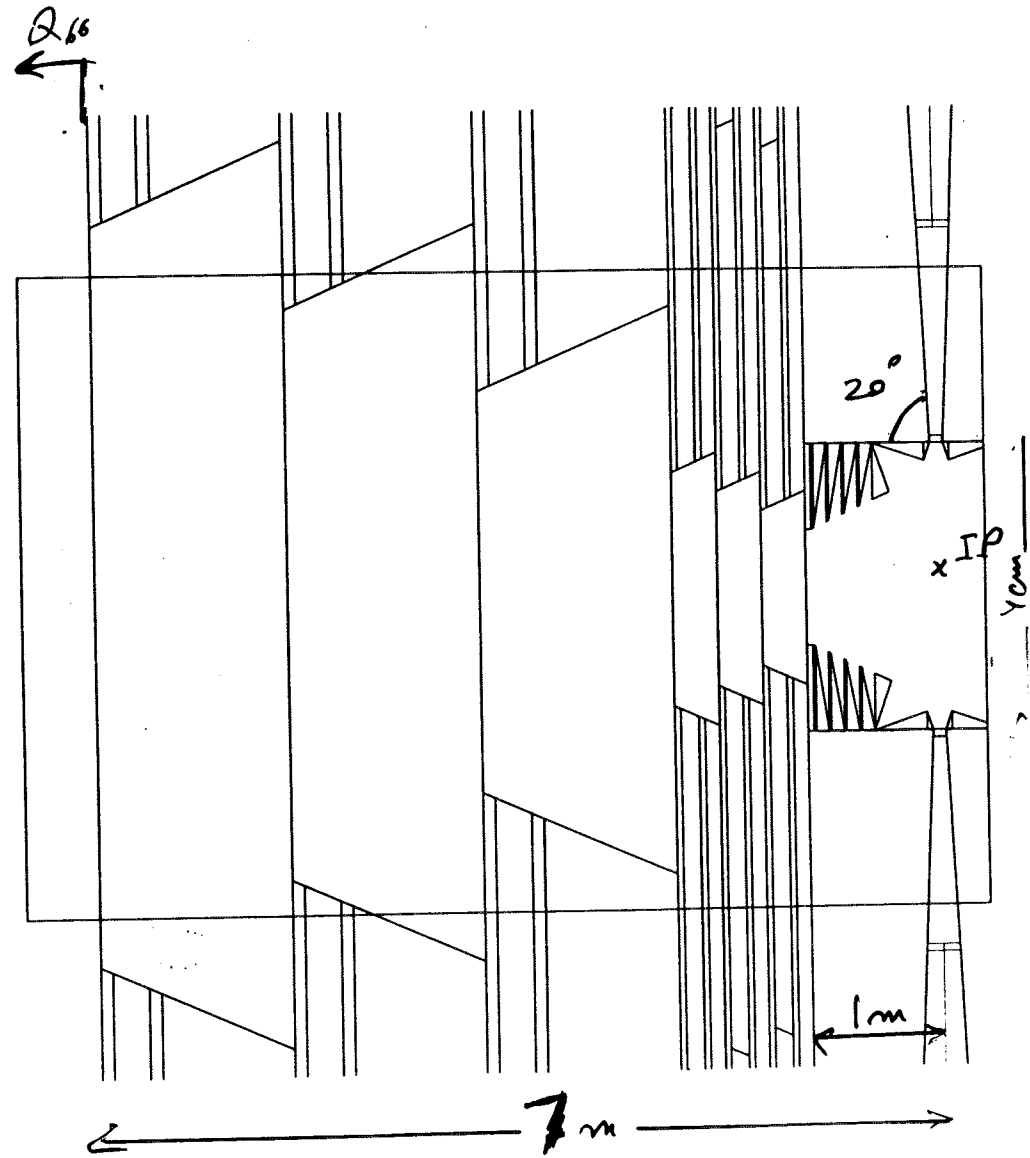
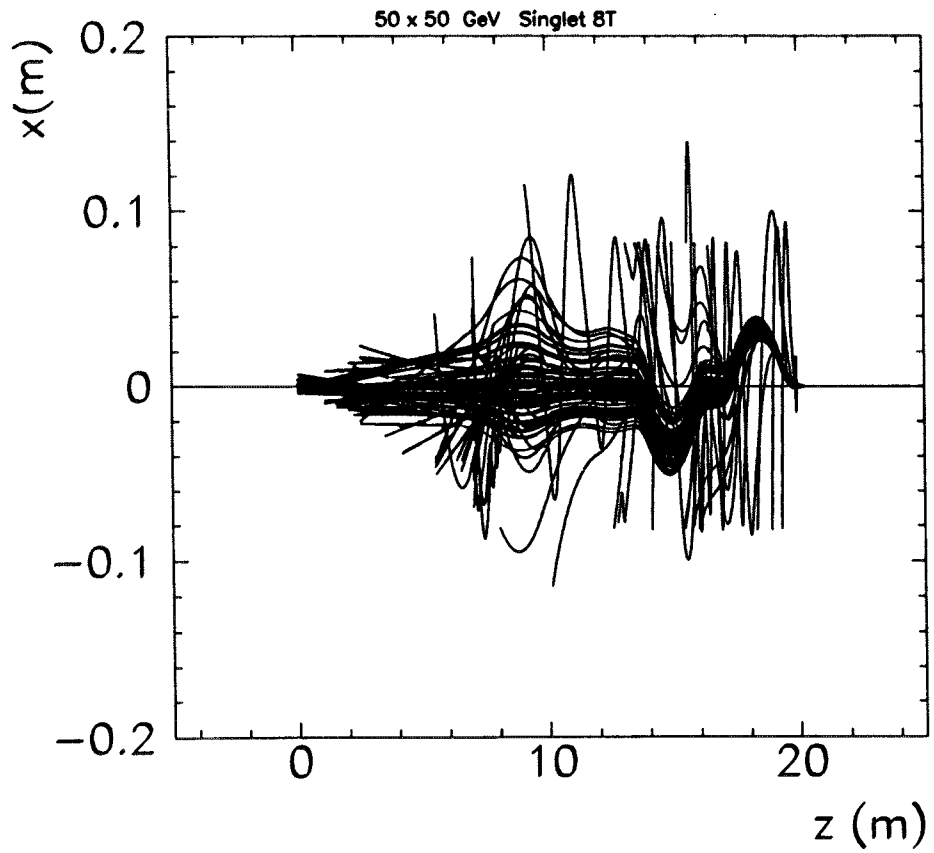
PROGRESS REPORTSF DEC 97
STUMERDETECTOR BACKGROUNDS

50 x 50 GeV

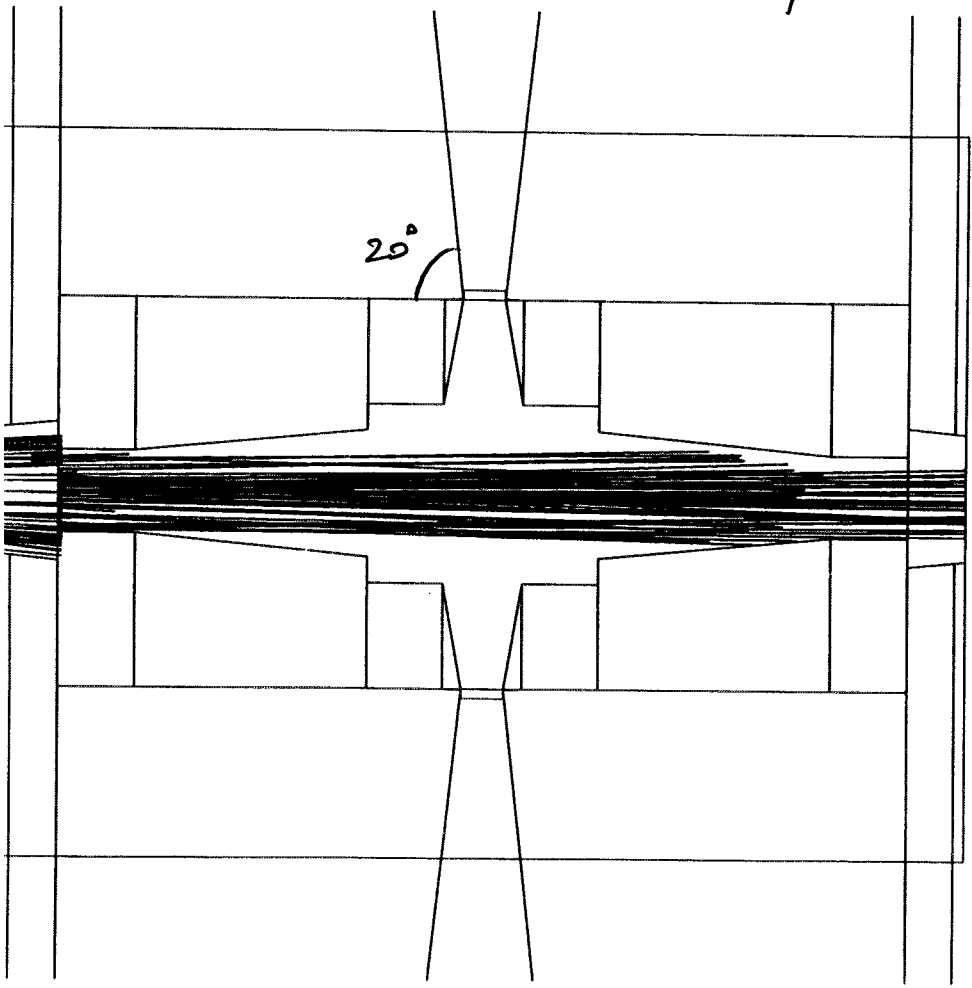
BENARY
KAHN
PALMER
STUMEROUTLINE

- IMPROVEMENTS ON 50 x 50 GeV
 - ① MOVE THE FIRST LIP TO 80 CM
 - ② ADD 4T DIPOLE AT 2.5-4 M
 - ③ RAISE SOLENOID TO 4T
 - ④ ADD FINS TO INNER CAVITY
- FLUENCES AT 2x2, 250x250, 50x50
- OCCUPANCIES " "
- RADIATION DAMAGE " "
- BETHE HEITLER μ 'S PROBLEM AND SOLUTIONS ??
- CONCLUSIONS

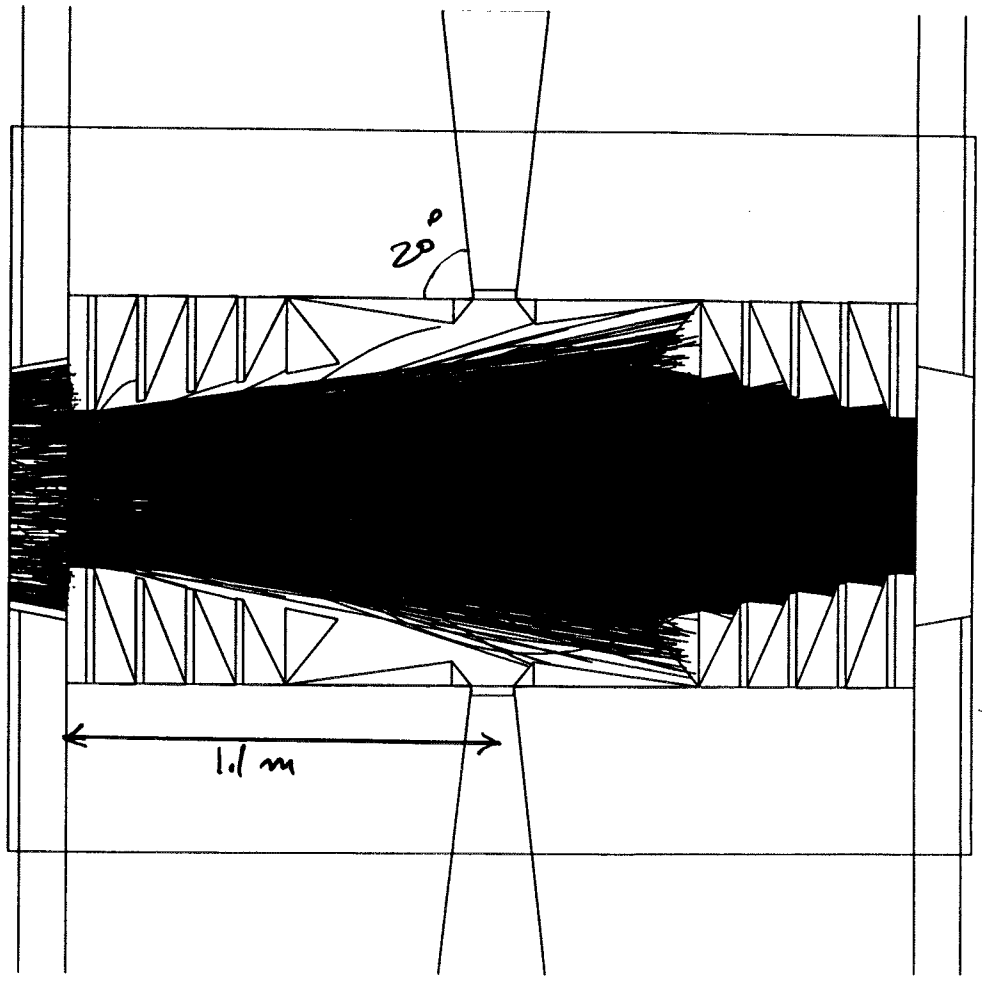


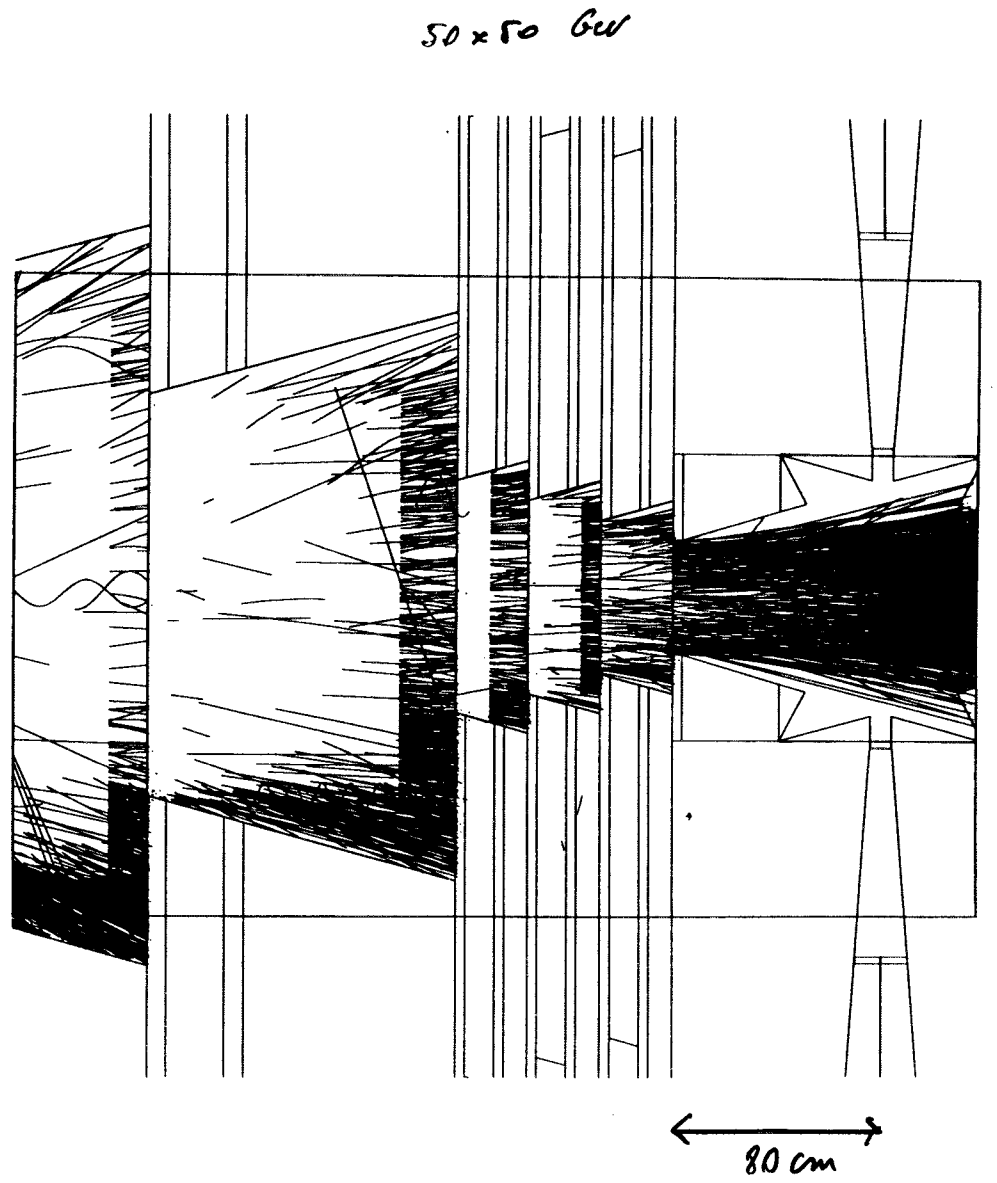
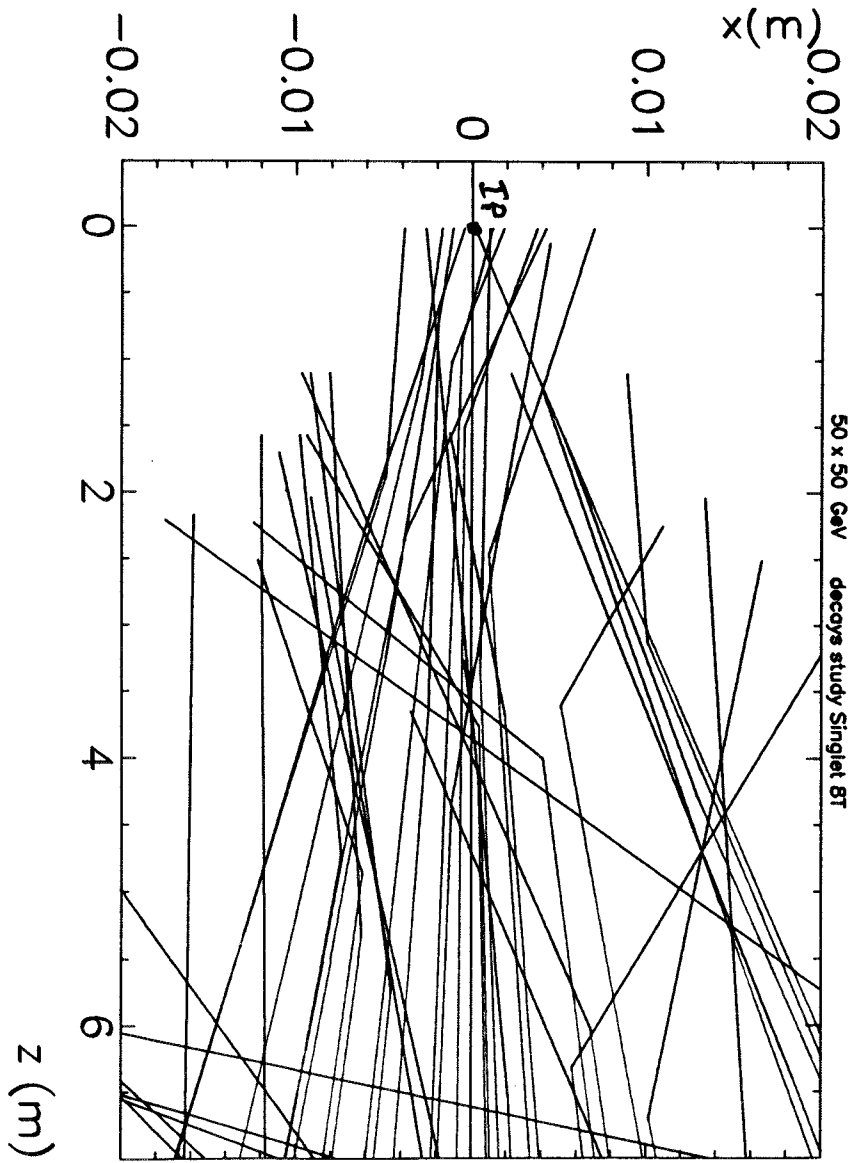


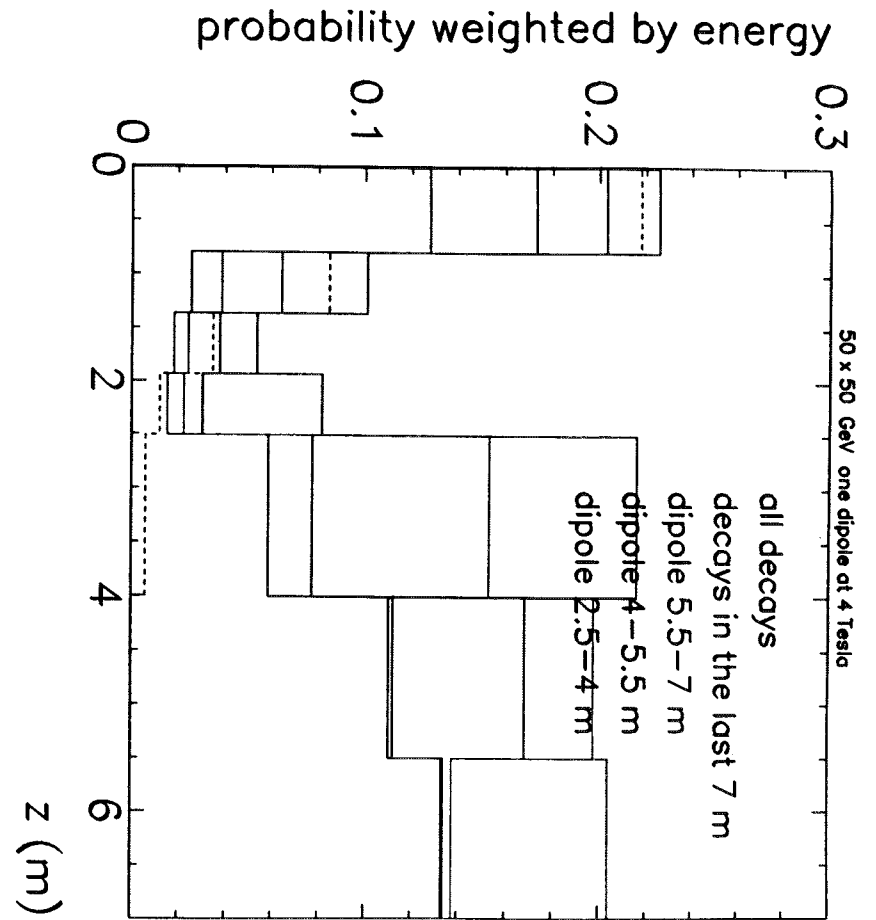
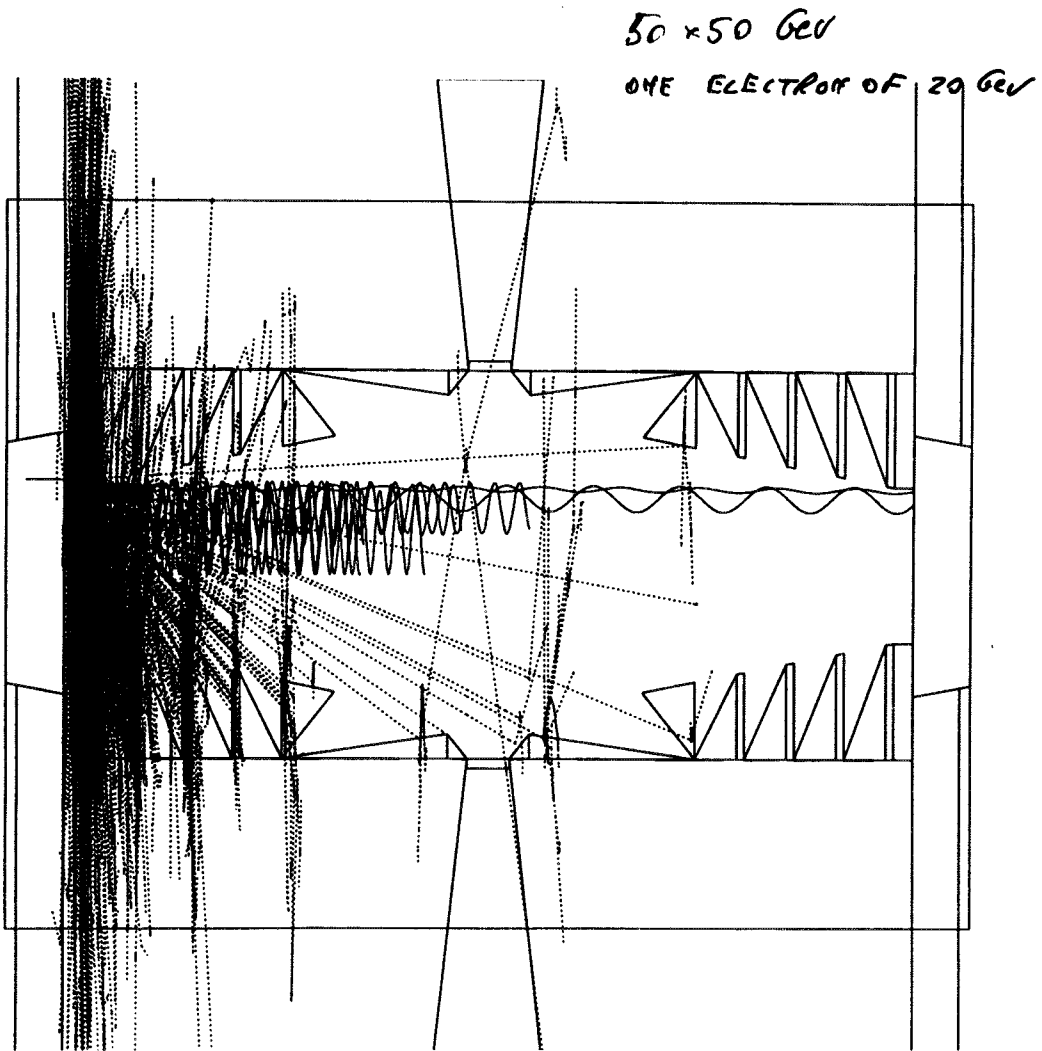
2x2 Tev

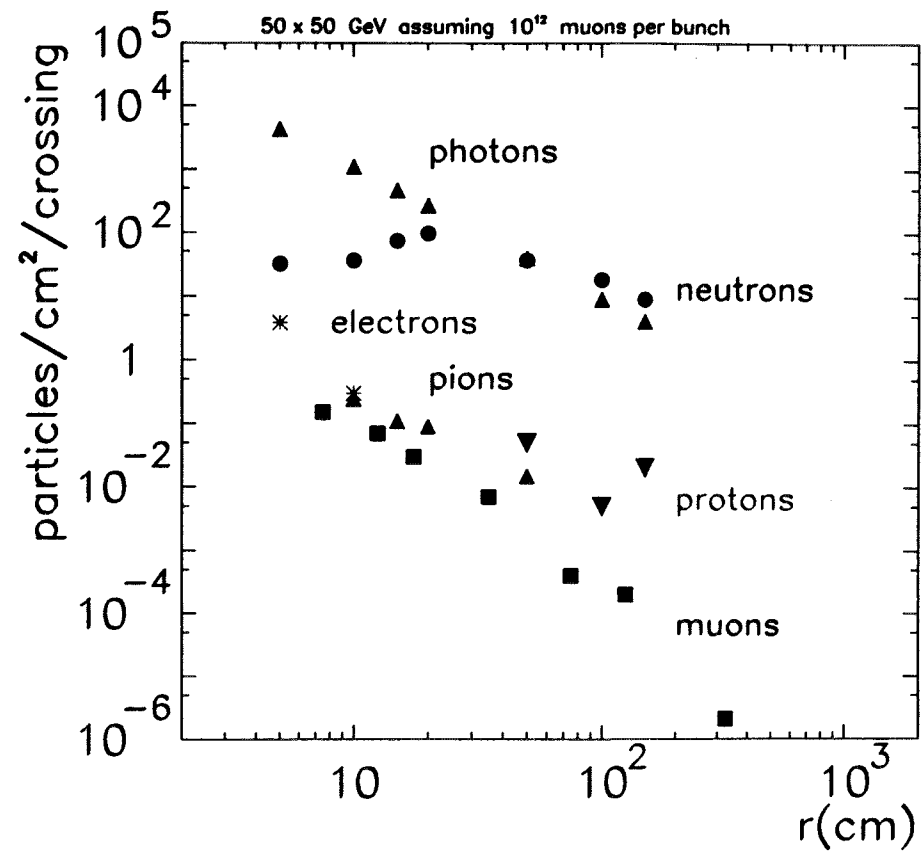
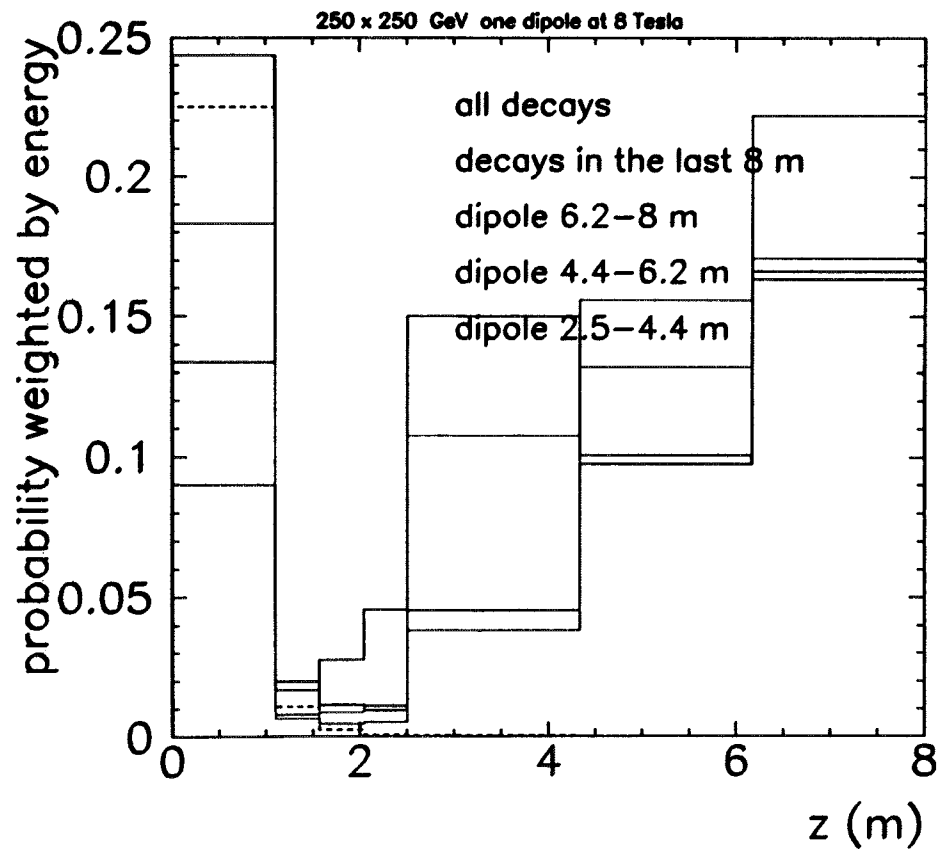


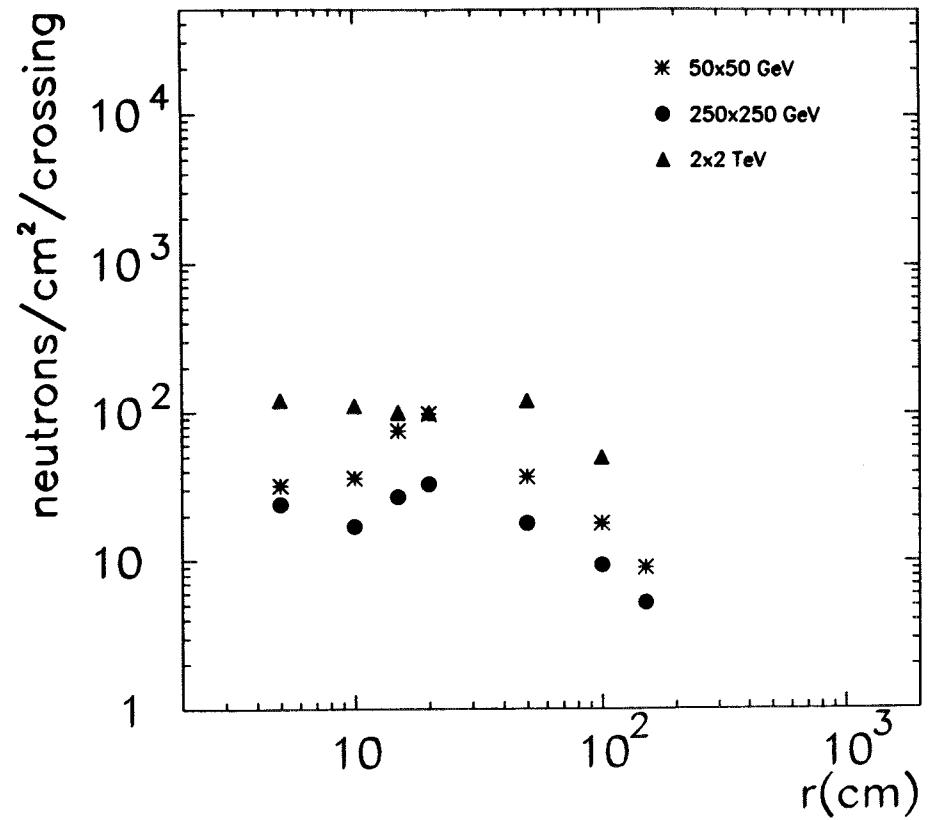
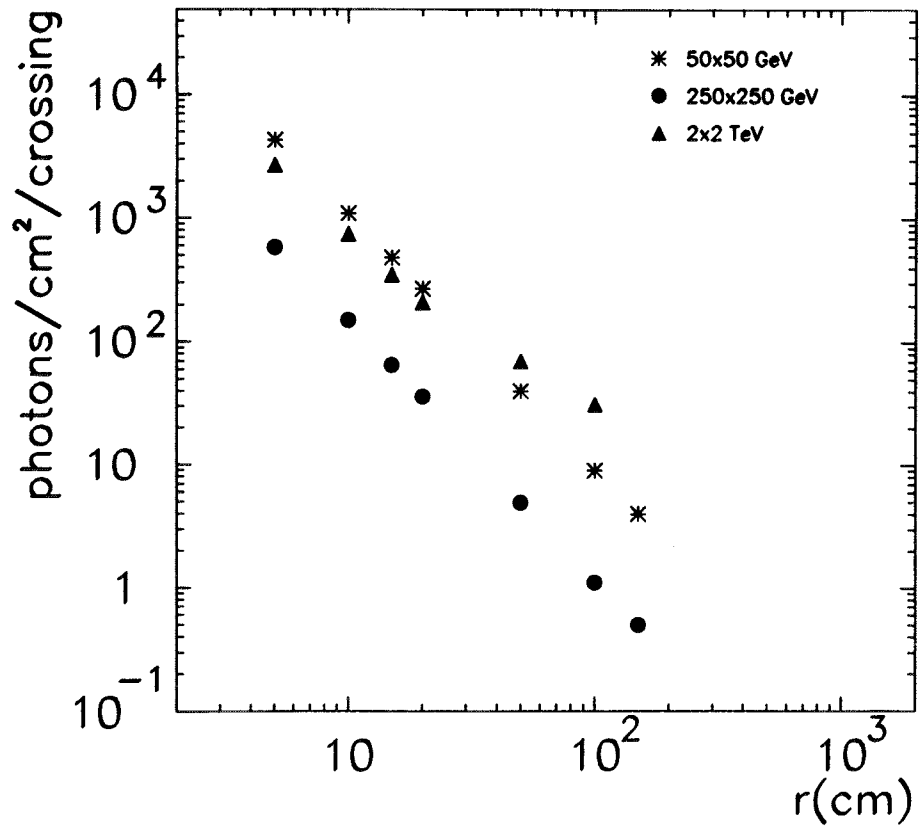
50 x 50 GeV











Background hits and occupancy at 50x50 TeV

Assume 2 bunches of $10^{12} \mu$'s each for hits, 4×10^{12} for occupancy

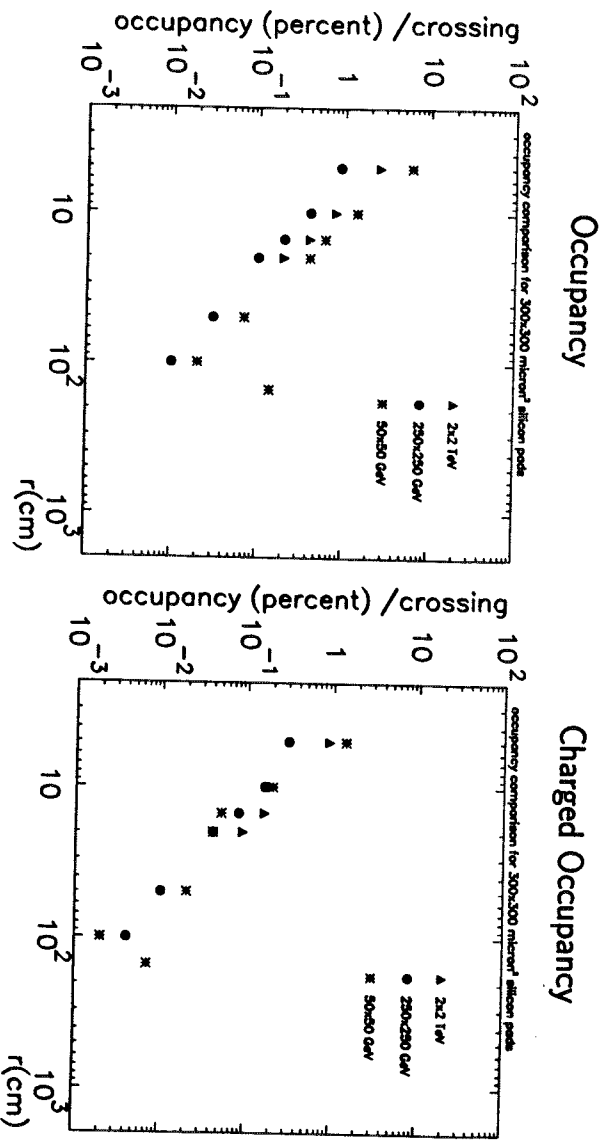
For silicon vertex assume 300x300 micron² pads

rad (cm)	photons (/cm ²)	neutrons (/cm ²)	charged (/cm ²)	Hits (/cm ²)	Occup all	Occup charged
5	13	0.03	4	17	6.1 %	1.4 %
10	3.3	0.04	0.6	4	1.4 %	0.2 %
15	1.4	0.07	0.14	1.6	0.6 %	0.05 %
20	0.8	0.1	0.10	1.0	0.4 %	0.04 %
50	0.1	0.03	0.065	0.2	0.07 %	0.02 %
100	0.03	0.02	0.005	0.06	0.02 %	0.002 %
150	0.01	0.01	0.02	0.04	0.014 %	0.007 %

Radial Fluences at 50x50 GeV

particles/cm²/crossing for two bunches of $10^{12} \mu$'s each

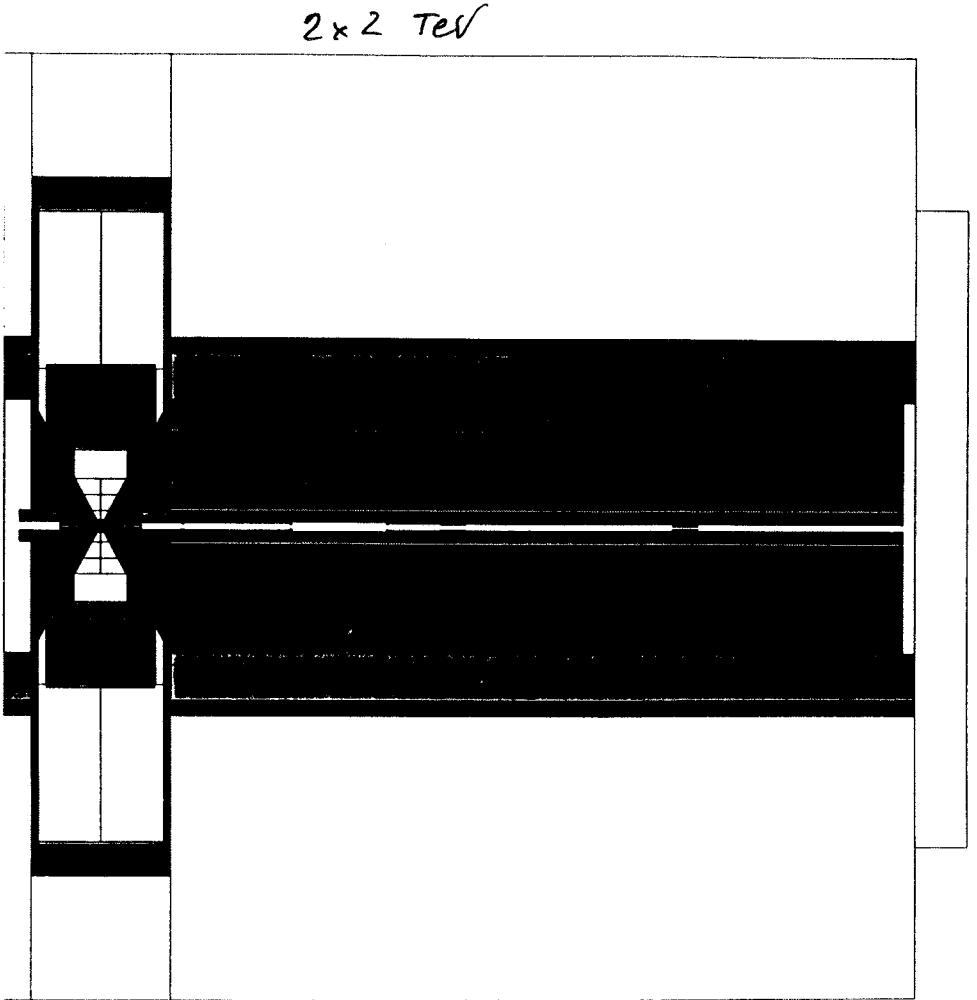
radius (cm)	photons	neutrons	protons	pions	electrons	muons
5	4300	32			3.8	0.15
10	1100	36		0.24	0.3	0.07
15	480	75		0.11		0.03
20	270	98		0.09		0.007
50	40	37	0.05	0.015		0.0004
100	9	18	0.005			0.0002
150	4	9	0.02			.21e-5
muon threshold	40 keV	40 keV	10 MeV	10 MeV		.24e-6



Radiation damage by neutrons on silicon detectors

assume 1000 loops , 15 Hz , 1 year = 10^7 seconds
 acceptable hits per year = $1.5 \cdot 10^{14}$

c.m. Tev	μ 's/bunch 10^{12}	neutrons/cm ² /crossing above 100 Kev	Hits/year 10^{13}	Lifetime years
4	2	100	3.	5
.5	4	50	3.	5
.1	4	30	1.8	8



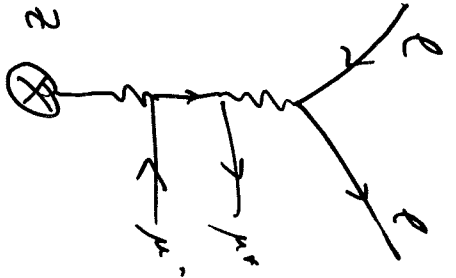
BECKE. HEITLER ROSEN II

$$P(e^+e^- \rightarrow \mu^+\mu^- \gamma\gamma) = 10^{-3}$$

500 GeV

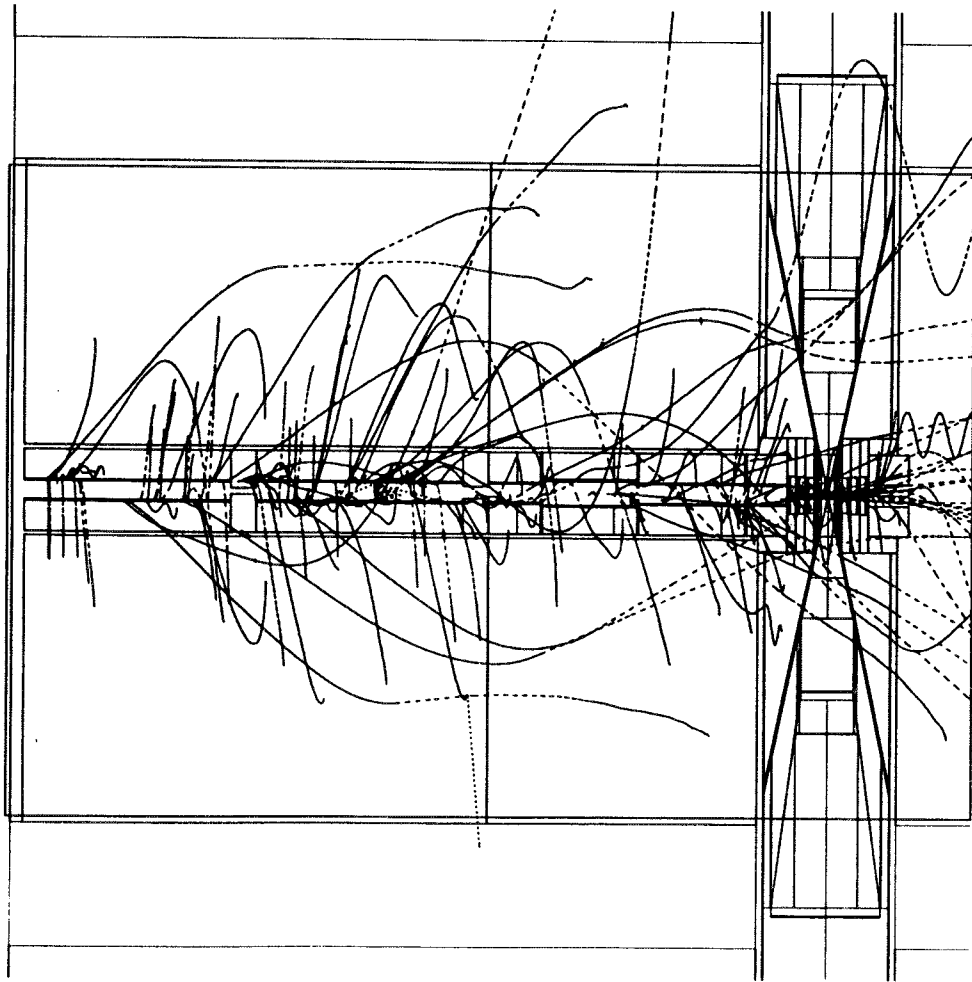
100 GeV = 10^{-4}

20 GeV = 10^{-5}

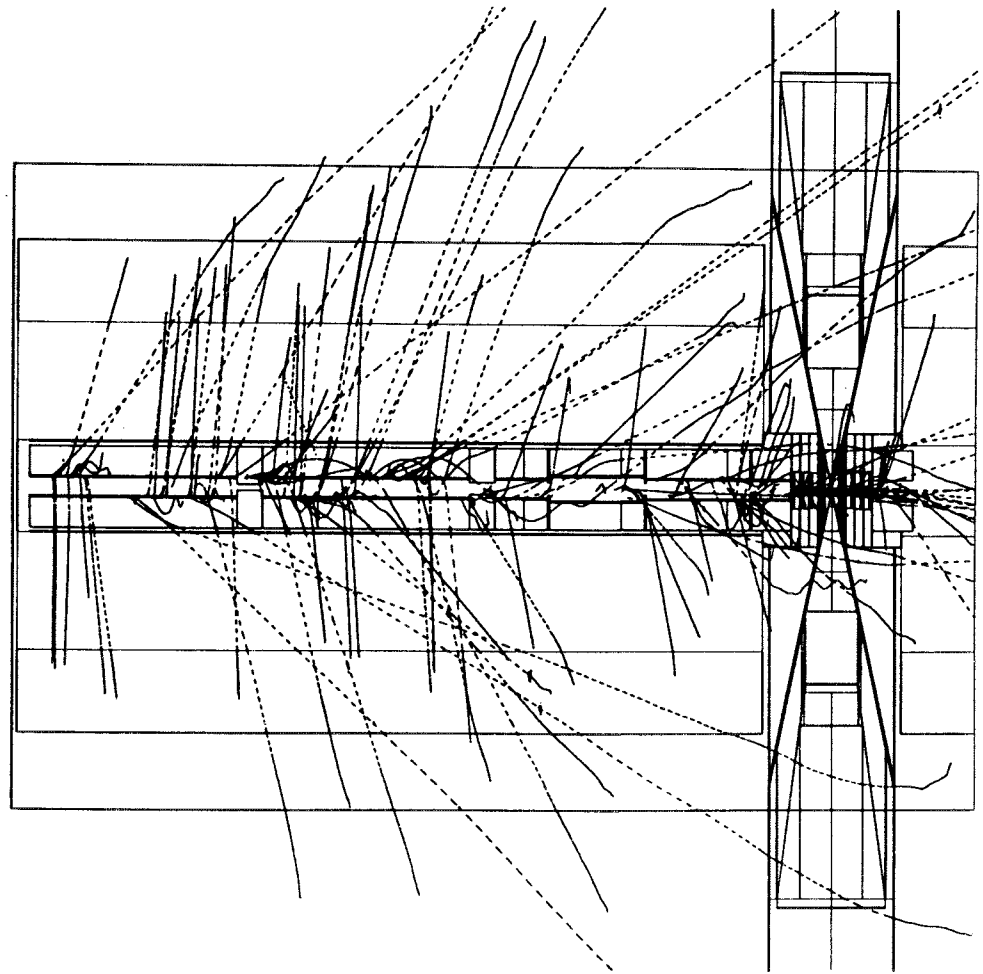


SIMULATION REQUIRES ALL
MAGNETIC FIELDS:
QUADS, DRIPPLES, TOROIDS, SOLENOIDS
AND THE RETURN YOKES.

2x2 TeV
~~250 x 250~~ Fe TOROID 2 Tesla

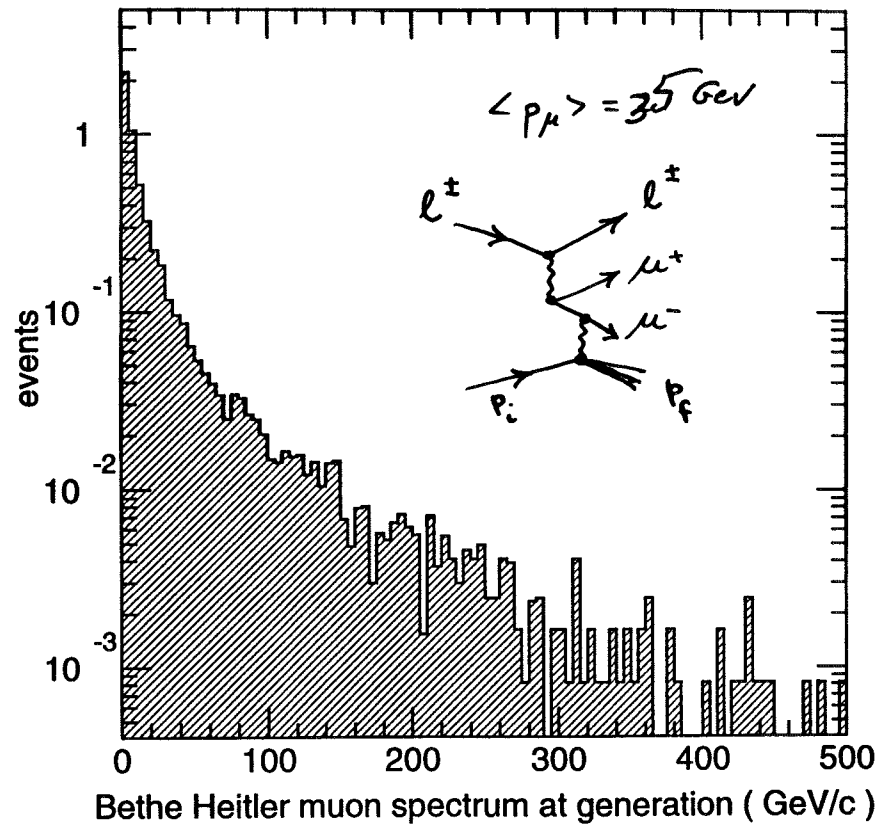
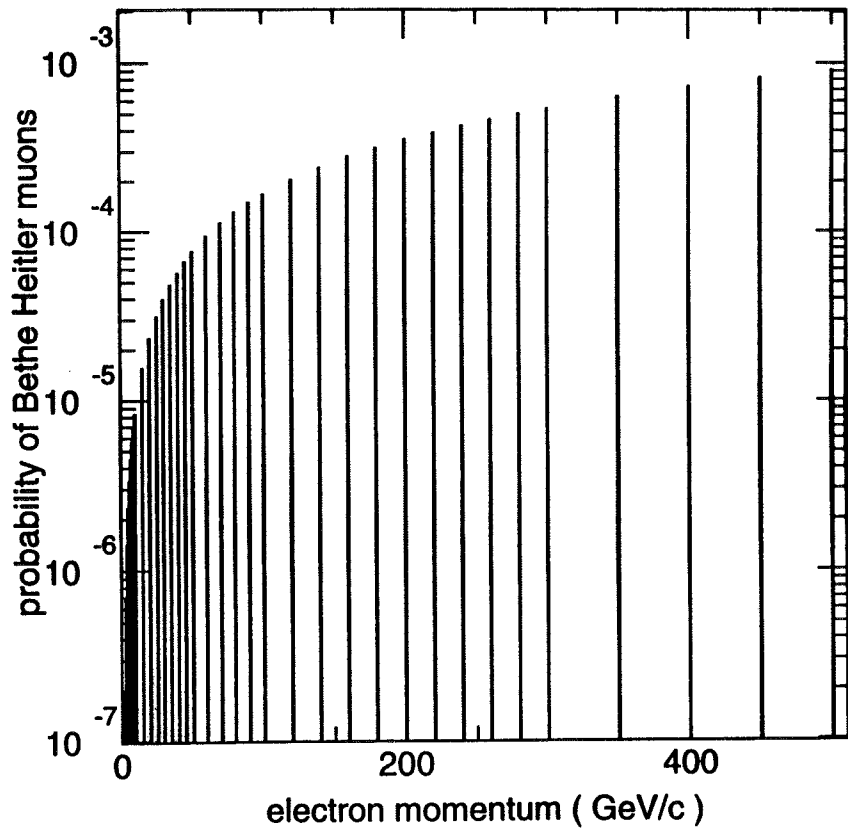


2x2 TeV
 BETHE HEITLER μ 'S REGULAR CNFTG.

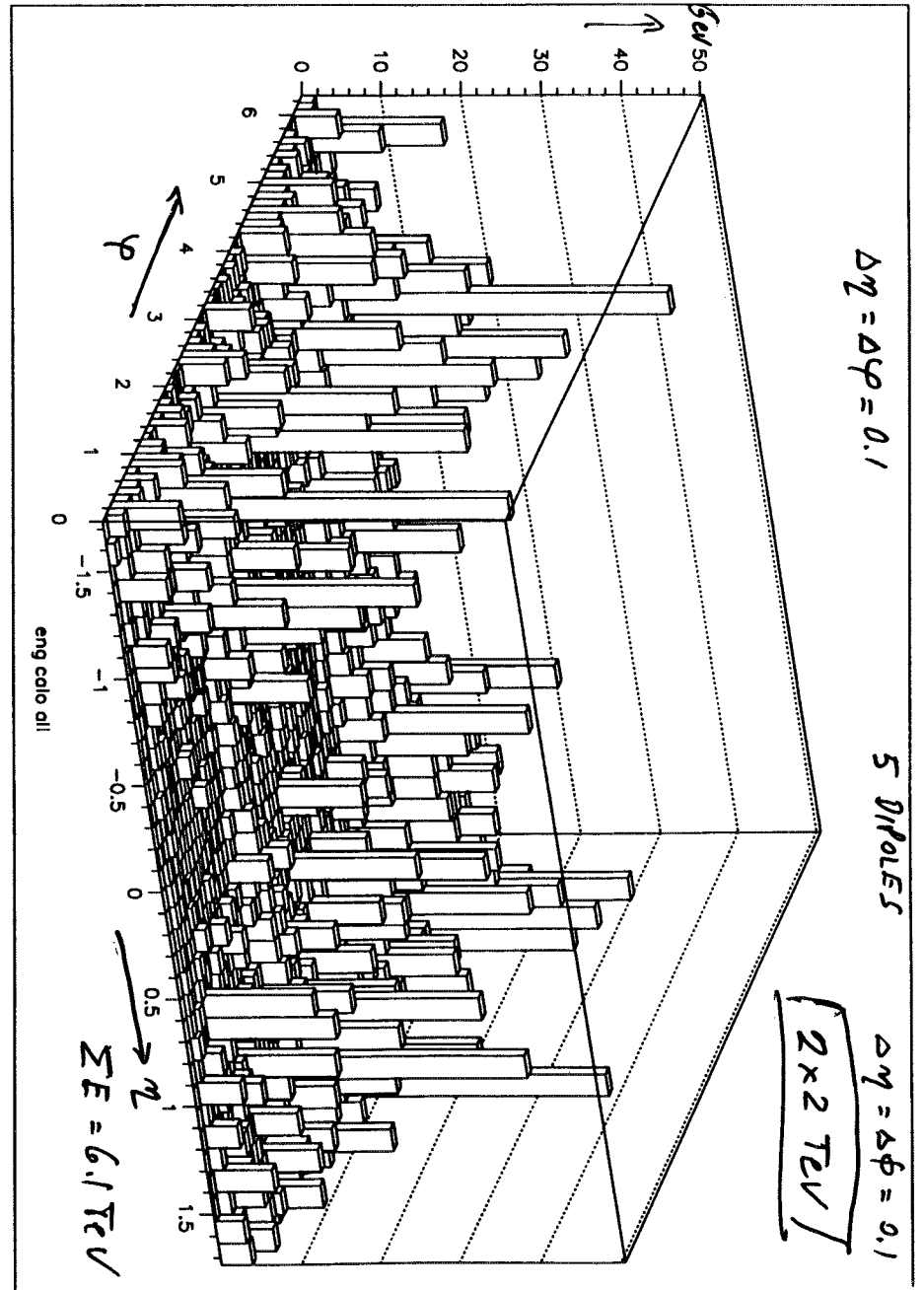
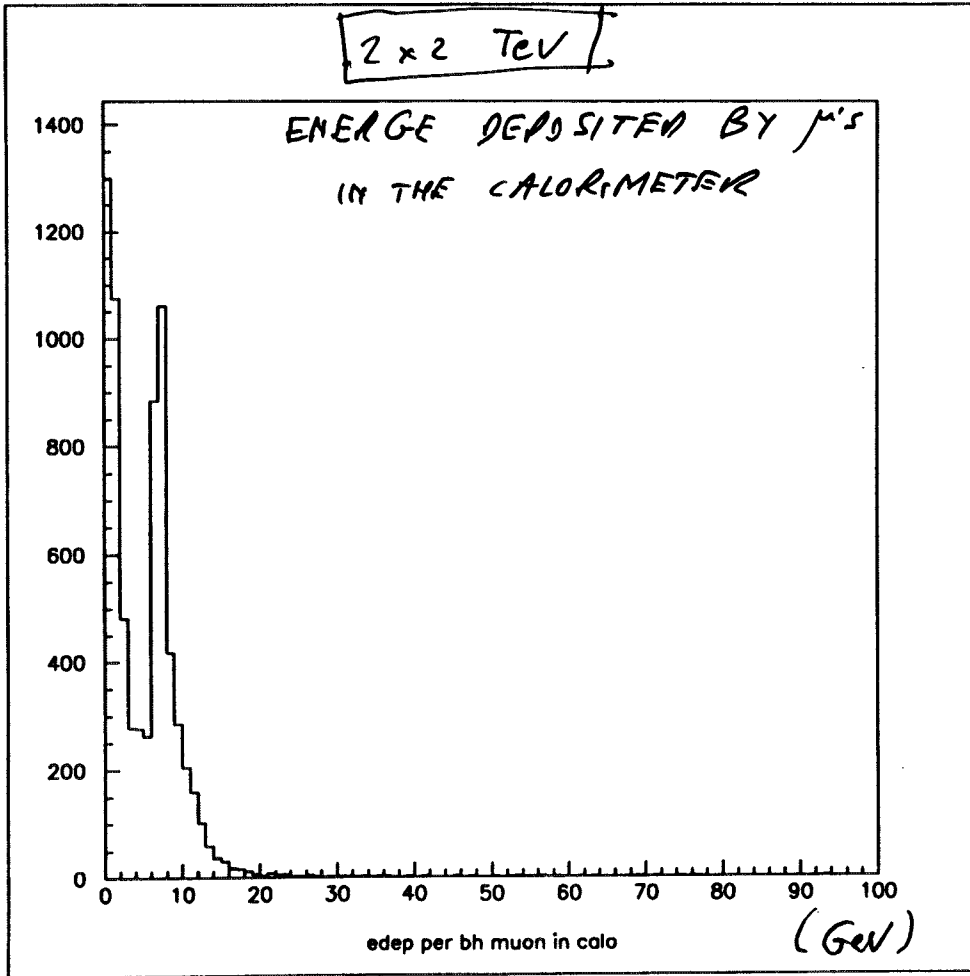


BETHE - HEITLER MUONS

2 x 2 TeV

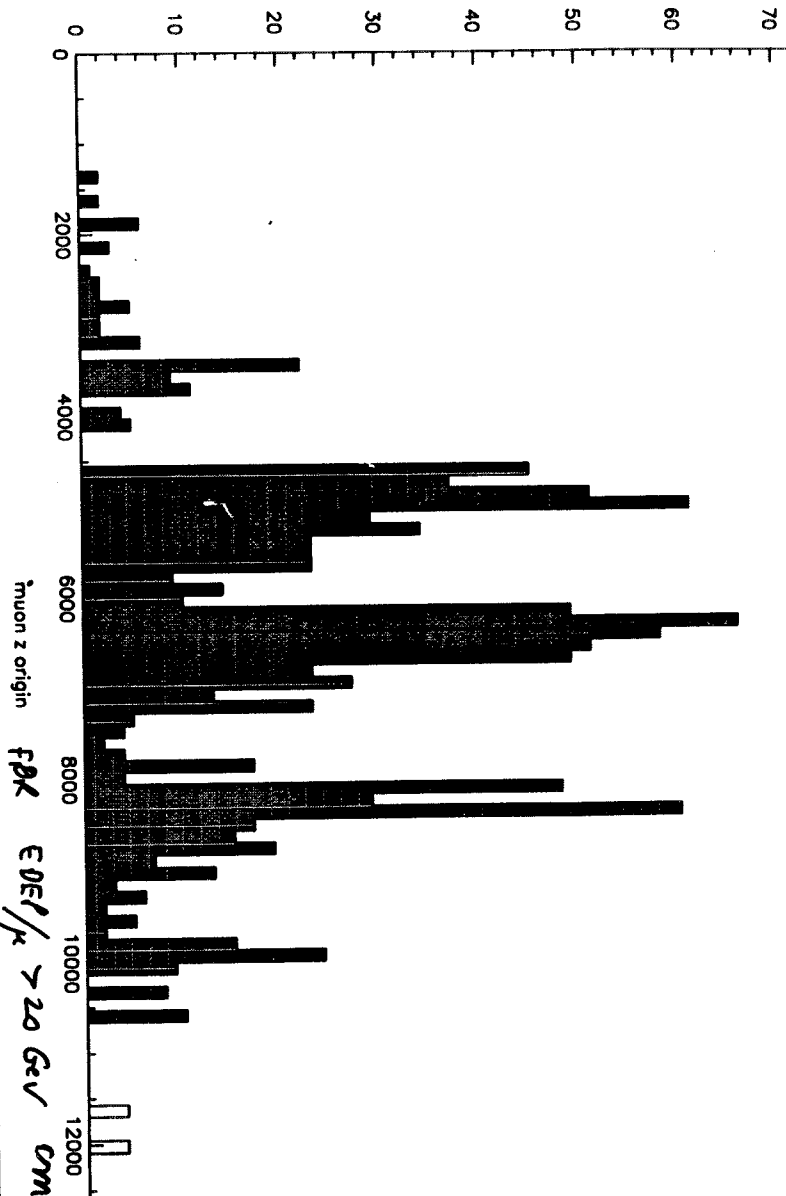


- NOTE: PROBABILITY FOR A 500 GeV e^- INCIDENT ON TUNGSTEN BLOCK TO PRODUCE A MUON IS $\sim 10^{-3}$
- THE BETHE-HEITLER MUONS ARE \approx PARALLEL TO THE BEAM DIRECTION



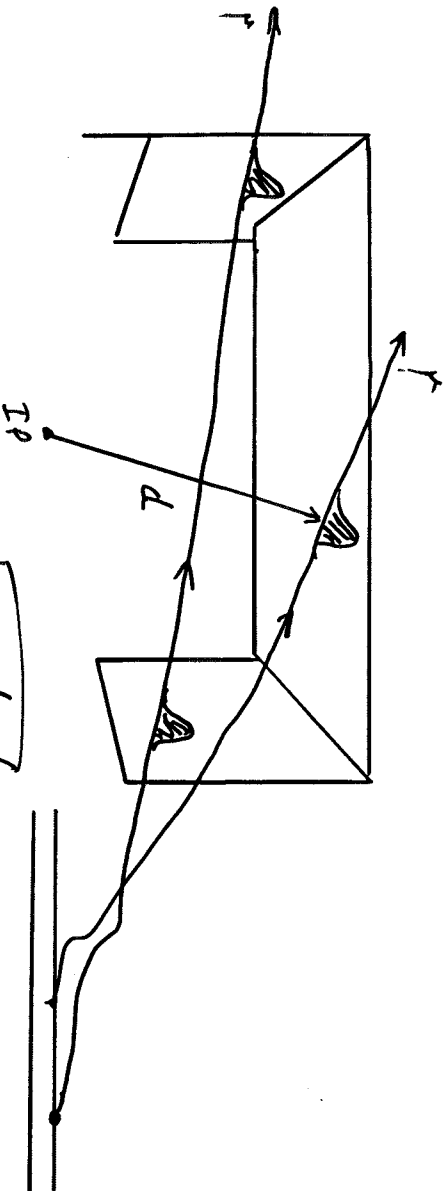
2x2 FeV

5 DIVICES



WAYS TO IMPROVE THE
SECONDARY MUONS PROBLEM

- ① MOVE THE CHARACTER AT $V_0 = 2.5 \mu$
- ② TIME OF FLIGHT CUT.
- ③ LOWER THE Q OF HARMONIC CHARACTER
AL + LIG ARON
- ④ USE A HIGH Z ABSORBER (H)
AROUND THE FF.
- ⑤ INSTALL A FE TOROID (2 TORI)
- ⑥ -----



— USE 1 nsec AS TIME UNIT

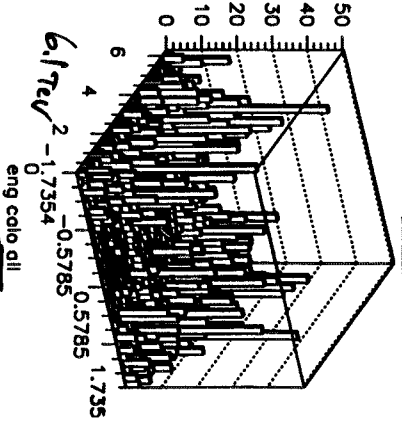
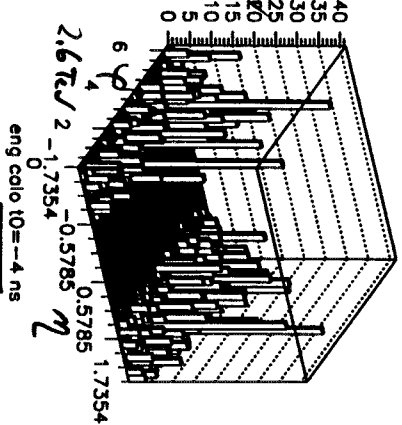
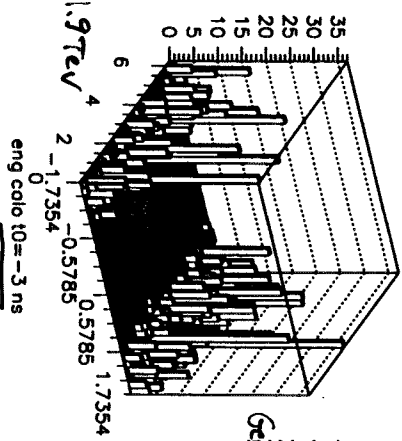
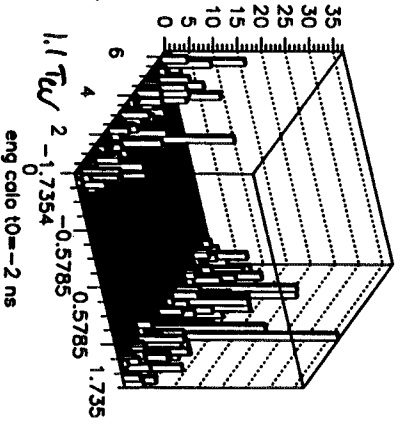
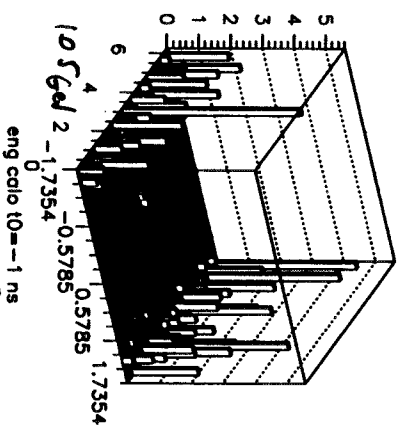
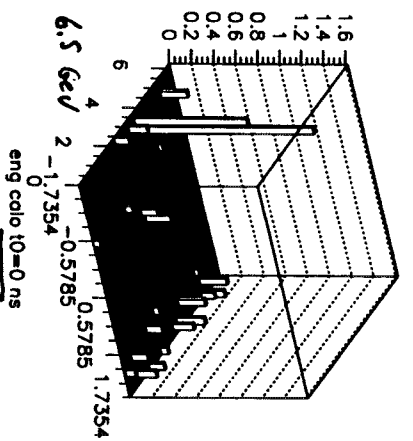
$$t_0 = \frac{d}{c}$$

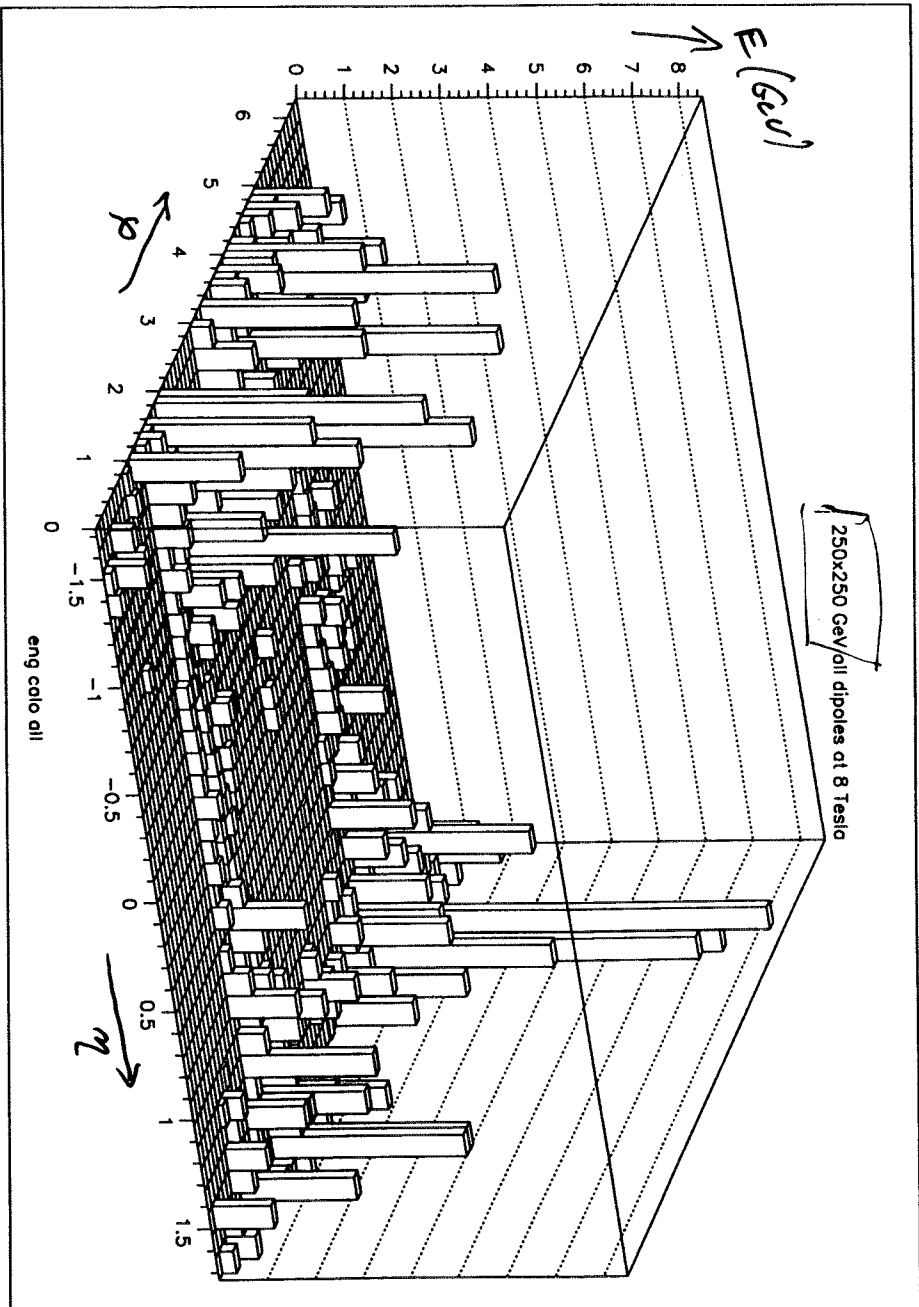
1 nsec \approx TIME DEVELOPMENT OF ELM SHOULD

\approx SIZE OF A HARMONIC CALORIMETER CELL.

2x2 TeV

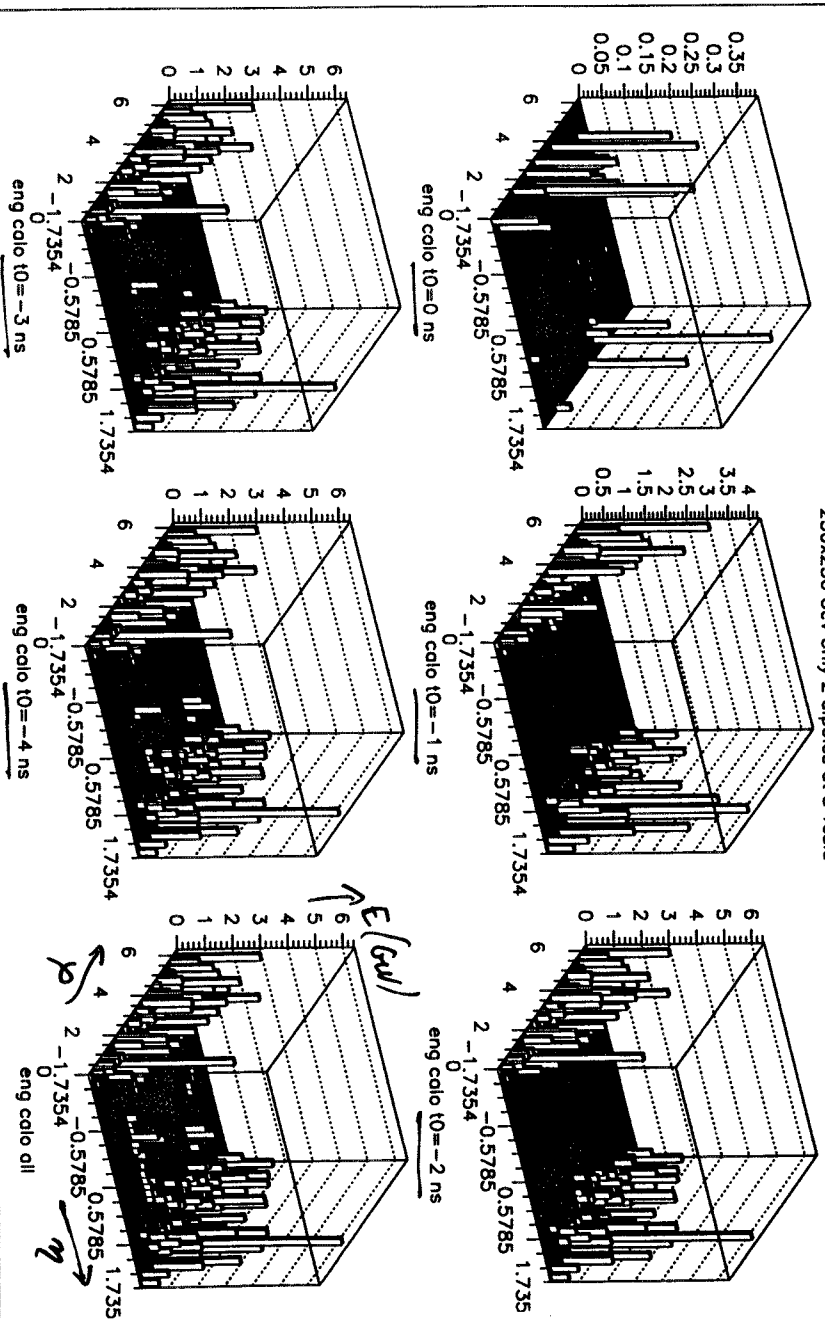
5 DIPOLES



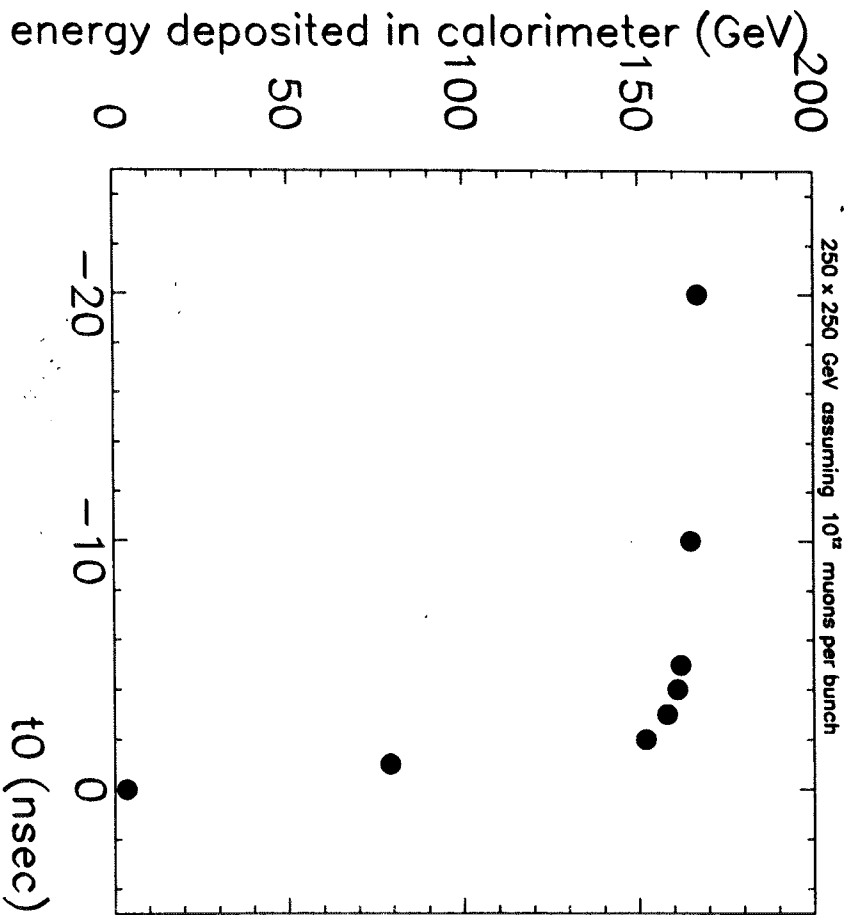
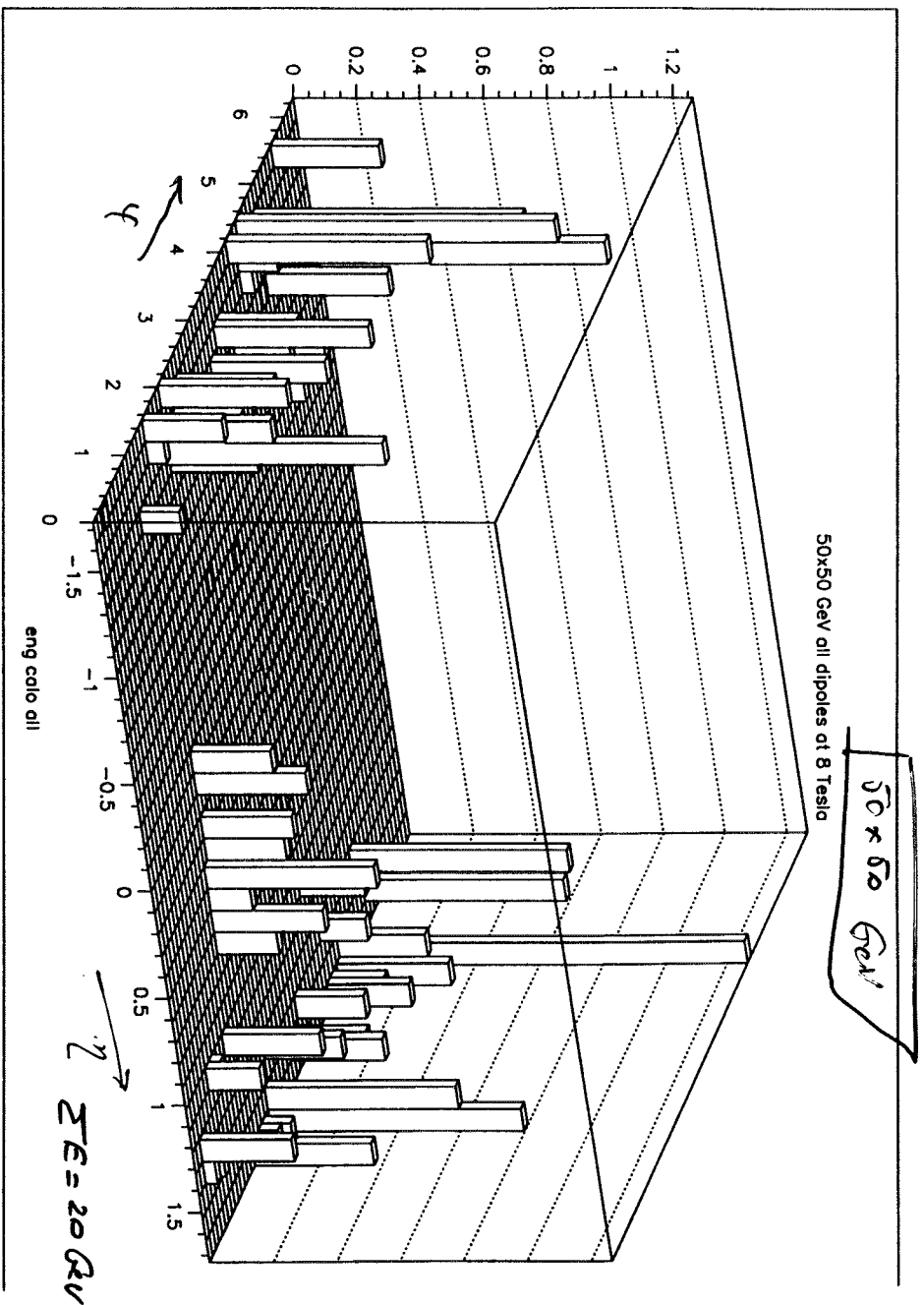


250 x 250 GeV

250x250 GeV only 2 dipoles at 8 Tesla

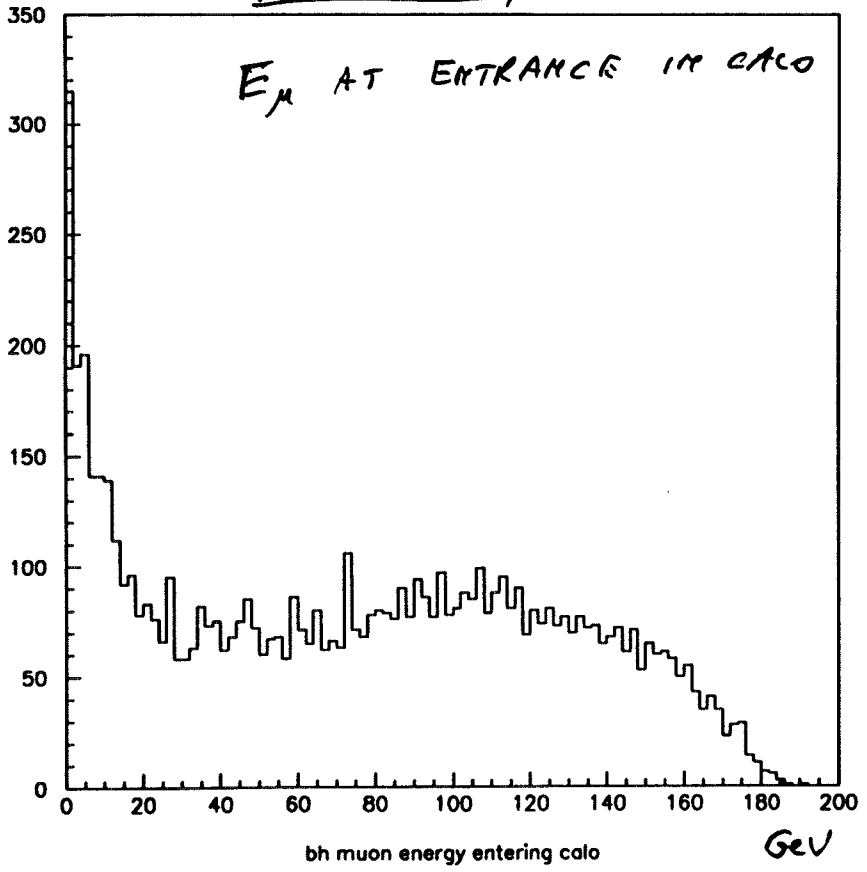


$E_{TOT} = 170 \text{ GeV}$



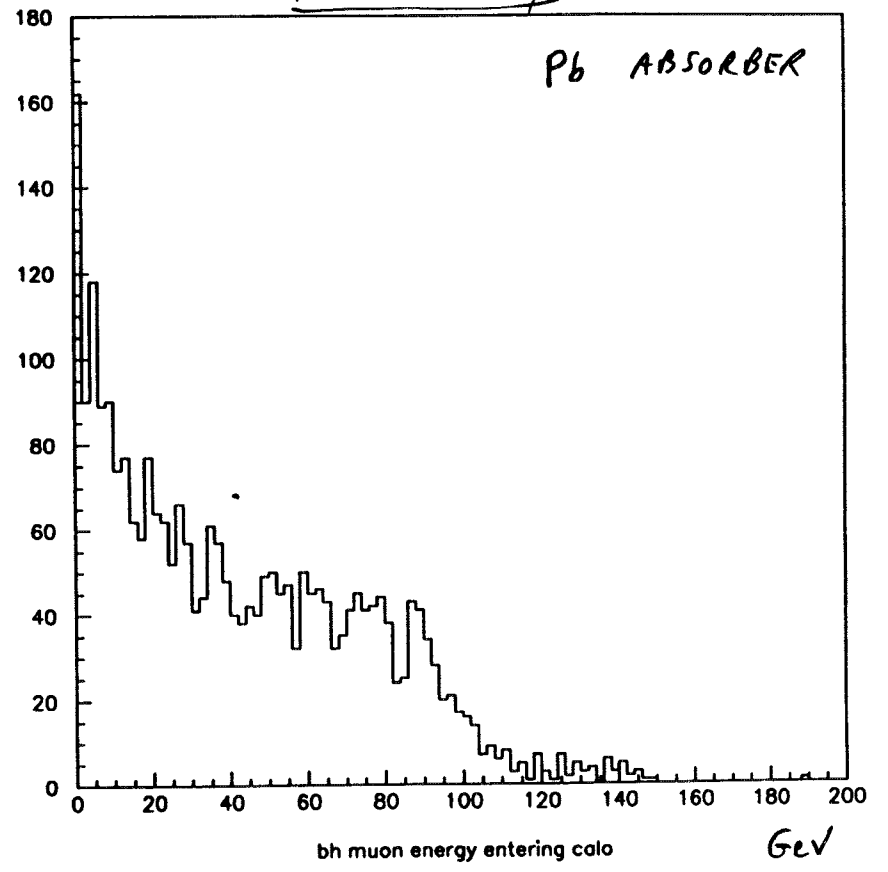
2 x 2 TeV

E_{μ} AT ENTRANCE IN CALO

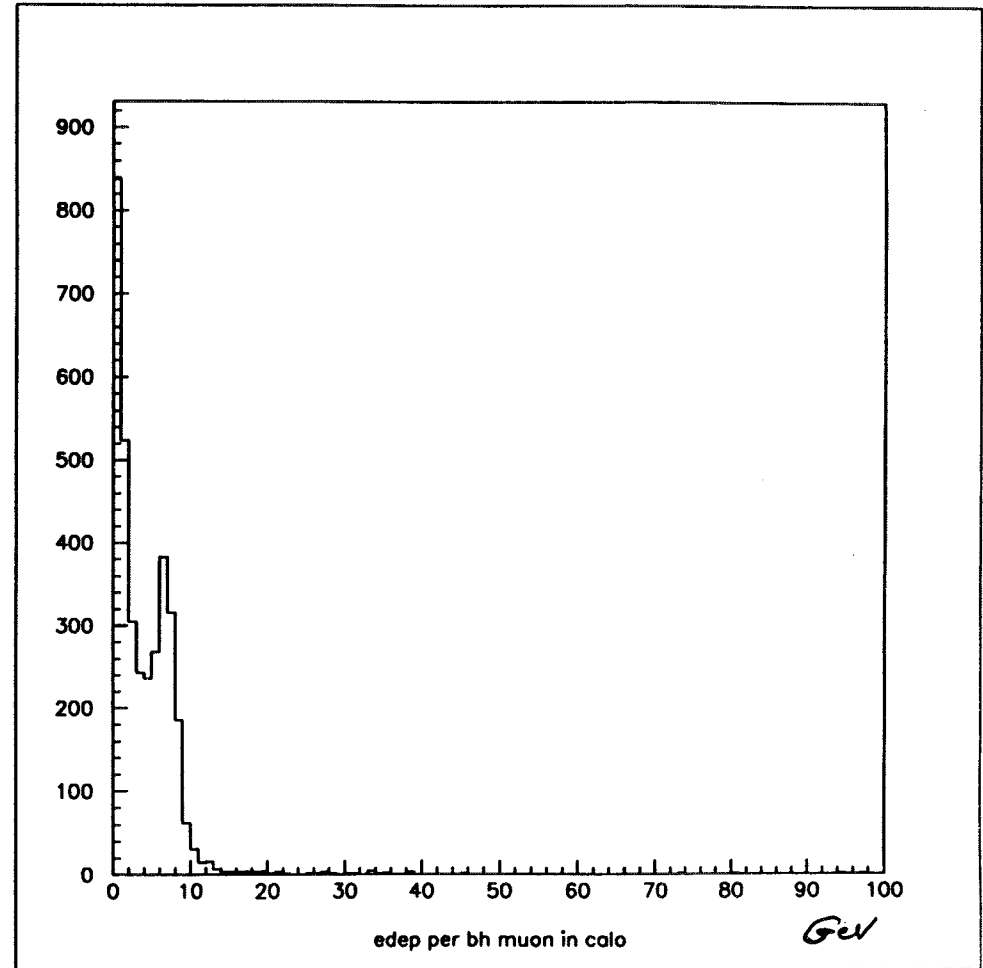
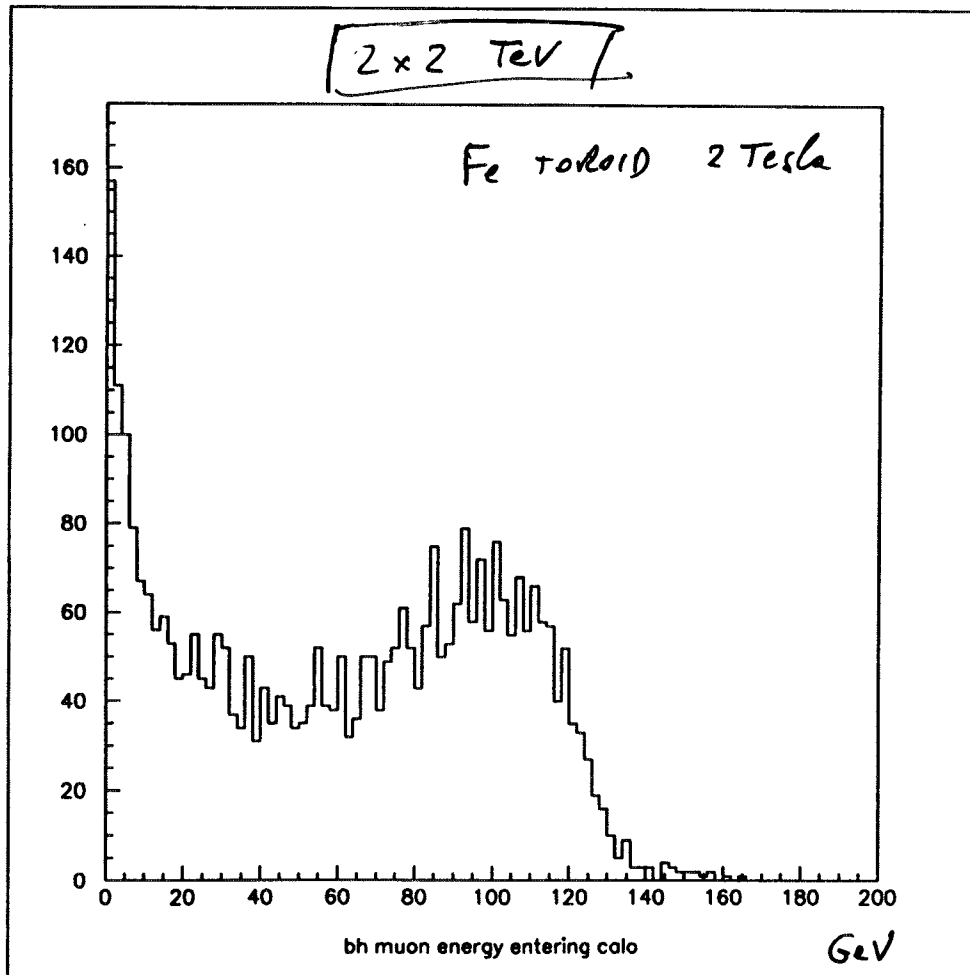


2 x 2 TeV

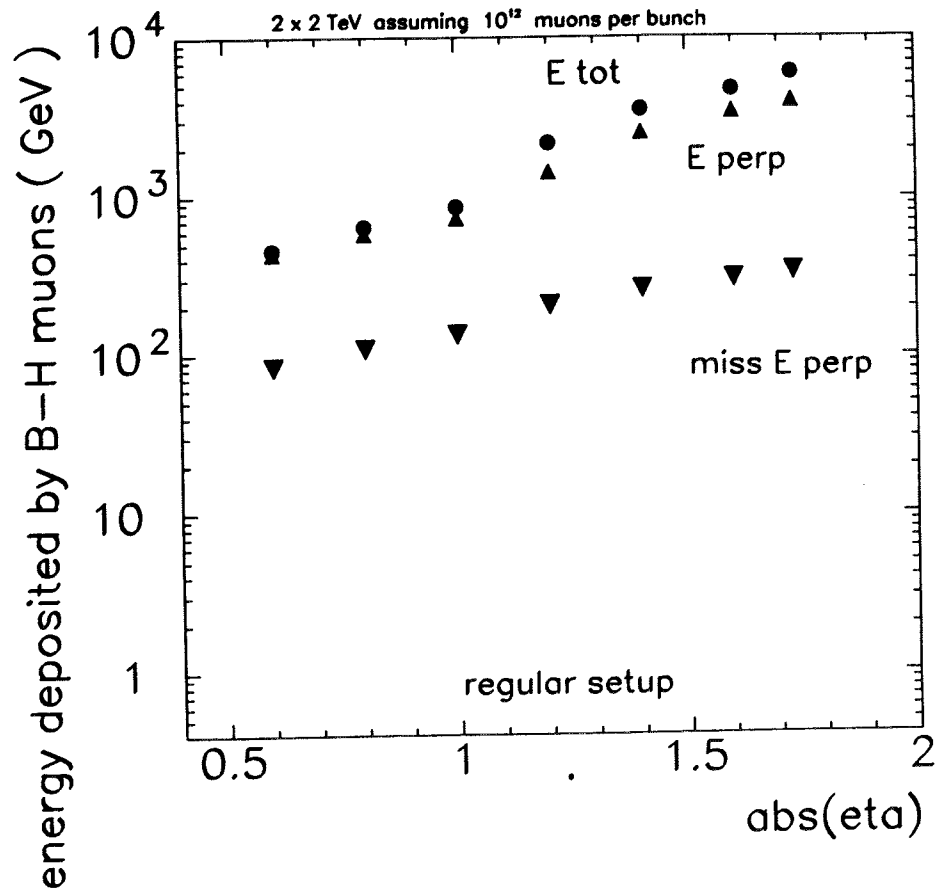
Pb ABSORBER

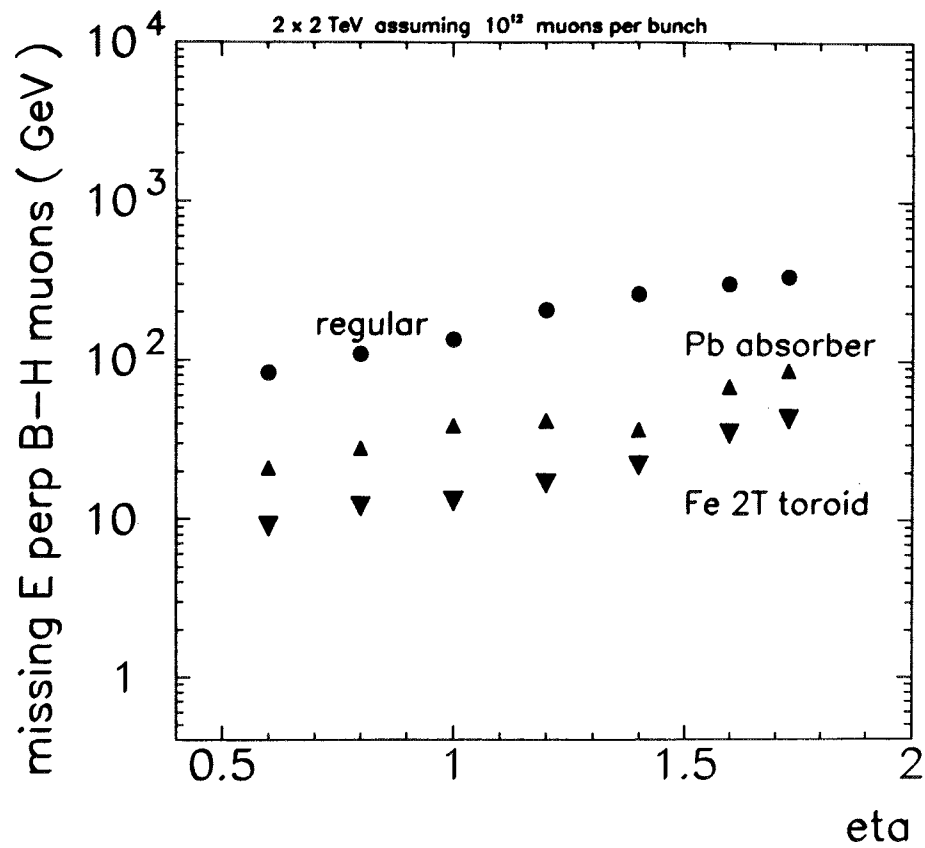
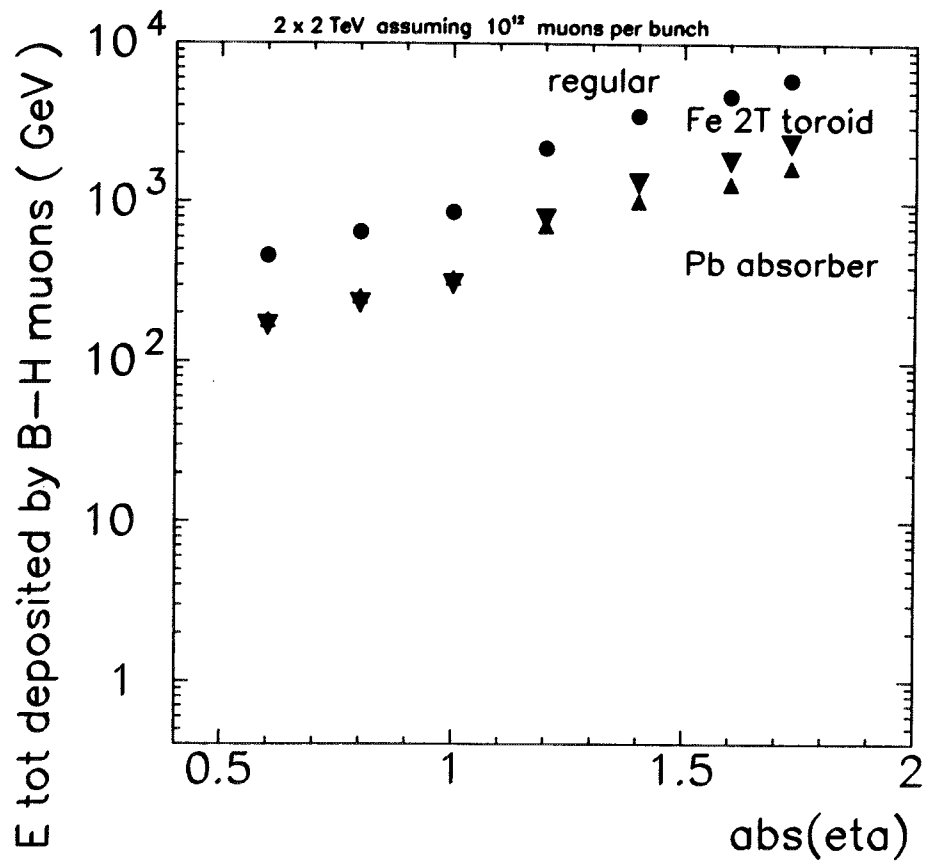


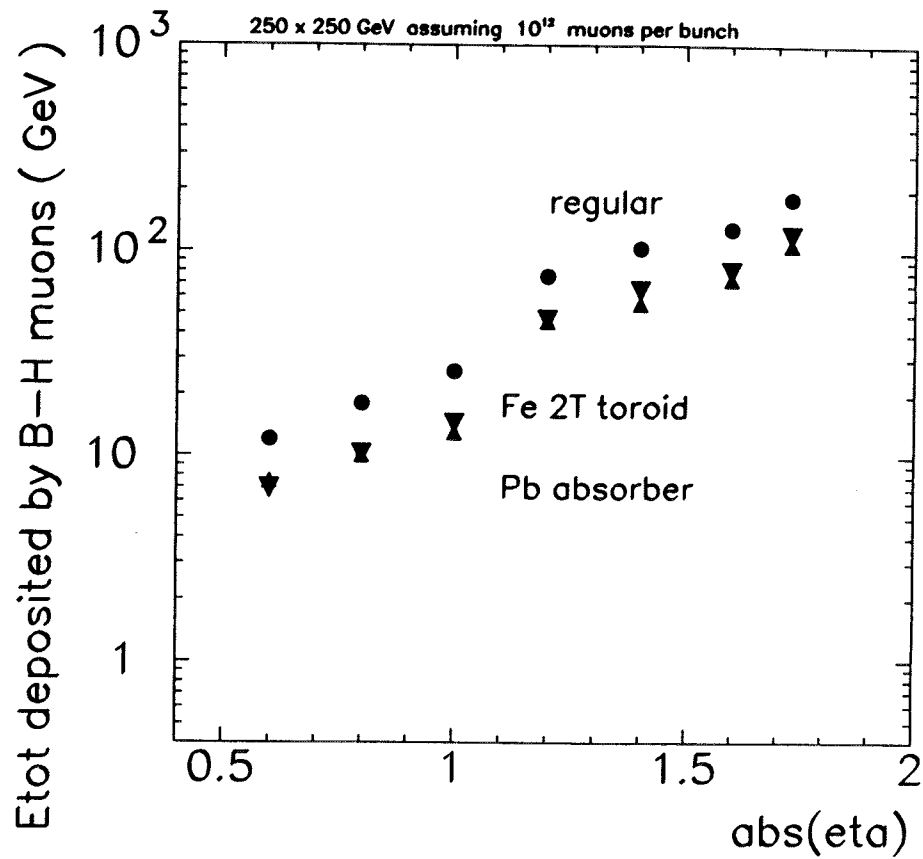
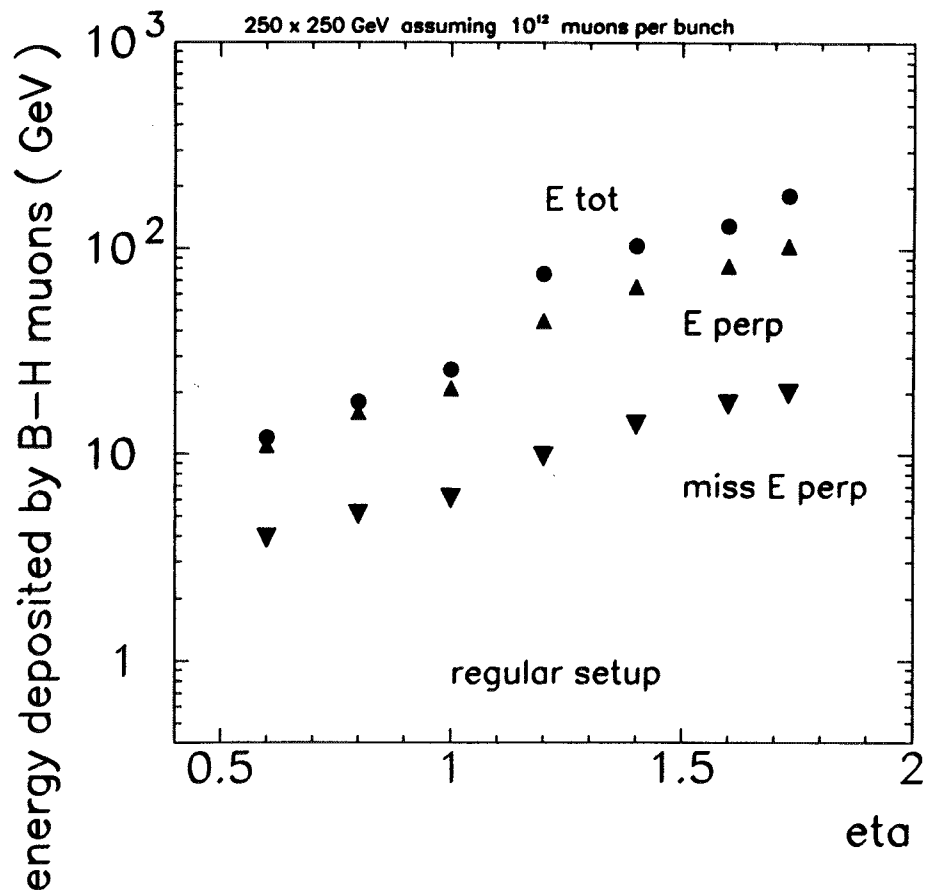
2 x 2 TeV

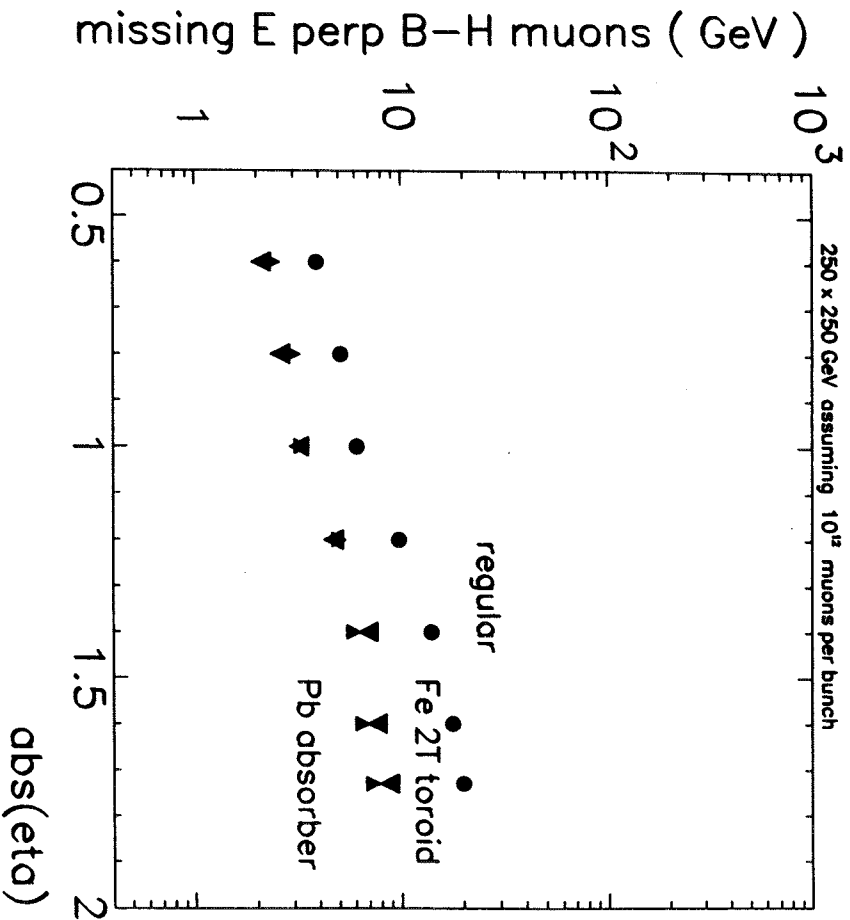


	2x2 TeV	2.5Dx2.1D GeV	5Dx1D GeV
# μ 's GENERATED $\langle p_{\mu} \rangle$	18.5 k 35 GeV	51 k 16 GeV	1k
# μ 's ENTER CALO. $\langle p_{\mu} \rangle$	1.3 k 76 GeV	94 11.2 GeV	58 1.8 GeV
$\langle E_{DEPOSITED} \rangle$	5.4 GeV	2.6 GeV	2.8 GeV
$\langle E_{TOT} \rangle$	6 TeV	200 GeV	20 GeV
<u>Pb ABSORBER</u>			
# μ 's ENTER CALO. $\langle p_{\mu} \rangle$	500 42 GeV	70 11. GeV	
$\langle E_{dep} \rangle$	3.9 GeV	2 GeV	
$\langle E_{TOT} \rangle$	1.6 TeV	109 GeV	
<u>Fe TOROID (2T)</u>			
# μ 's ENTER CALO $\langle p_{\mu} \rangle$	640 62 GeV	74 10.9 GeV	
$\langle E_{dep} \rangle$	4.2 GeV	2 GeV	
$\langle E_{TOT} \rangle$	2.4 TeV	121 GeV	









CONCLUSIONS

NOX

DETECTORS

MAY-97
JULY-97
DEC 97

BACK GROUNDS

RANGE	SHORT	MEDIUM	LONG	VERY LONG
	γ, e	n, π, ρ	BR μ 's	$\mu, \nu, \bar{\nu}$

$e, 2T\mu$	V	V	i	?	V	SIL VTX
						TPC
						CALO

$50 \times 100 \text{ GeV}$	X V	V	X i	?	V	SIL VTX VTX
						CALO

$50 \times 50 \text{ GeV}$	X V	V	V	?	V	SIL VTX VTX
						CALO

**BEAM HALO VS BEAM DECAYS IN $\mu^+ \mu^-$
COLLIDERS:**

EFFECT ON DETECTOR AND MACHINE DESIGNS

by **N. Mokhov**

A.I. Drozhdin, G.J. Johnstone, N.V. Mokhov
Fermilab
A. Garren
LBNL

N. Mokhov, Fermilab

478

OUTLINE

- Beam halo handling
- Extraction of 2 TeV halo
- Extraction and collimation at 50 GeV
- Beam loss and backgrounds
- Protection of lattice components
- Conclusion

N. Mokhov, Fermilab

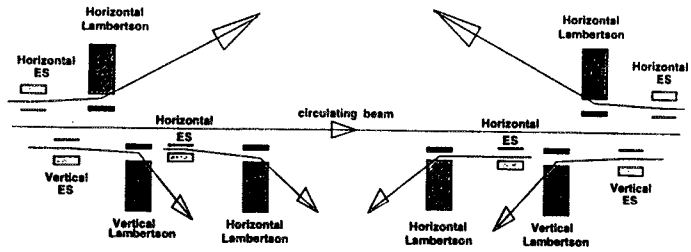


Figure 1: General view of the muon collider beam collimation system.

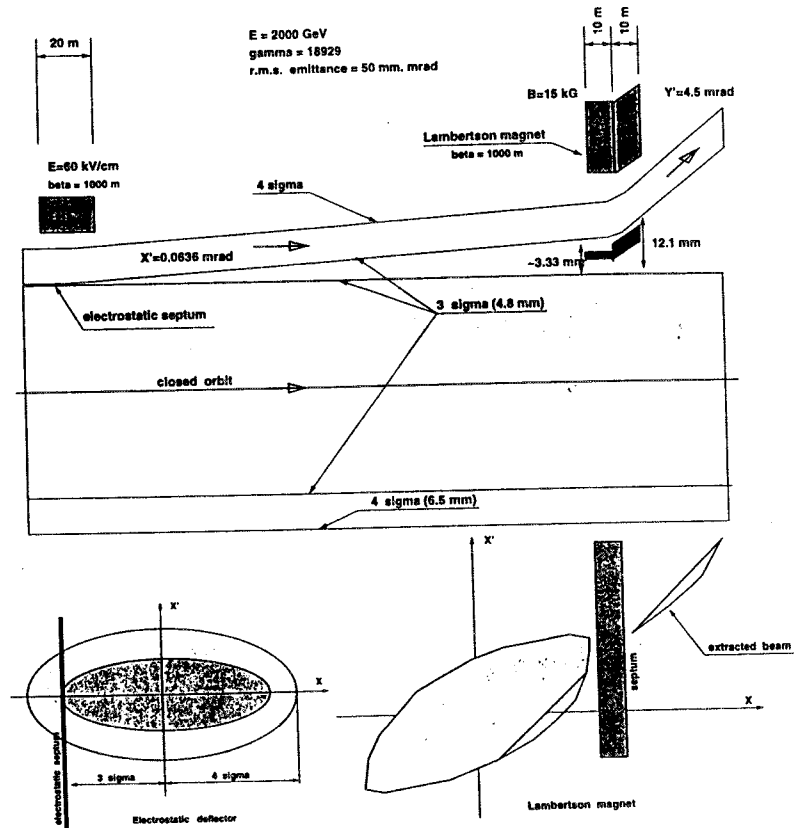


Figure 2: Halo cleaning scheme.

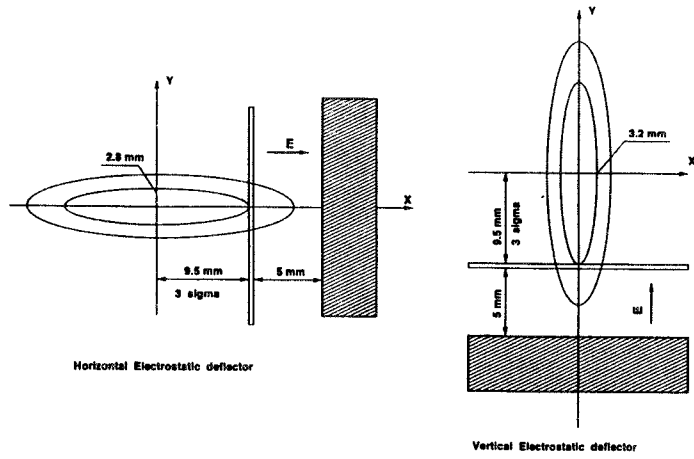


Figure 2: Electrostatic deflectors cross section.

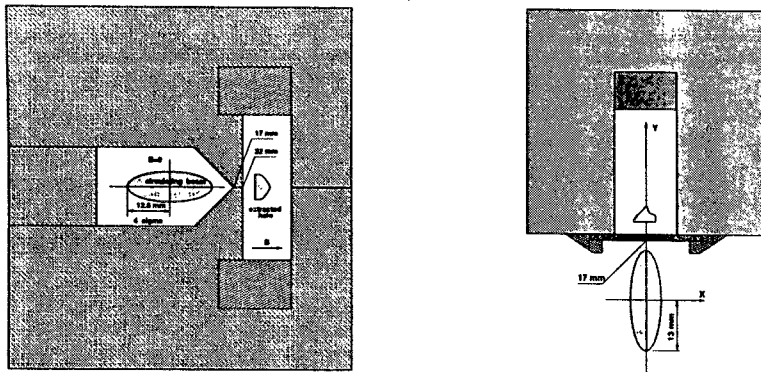


Figure 3: Lambertson and septum-magnet cross section.

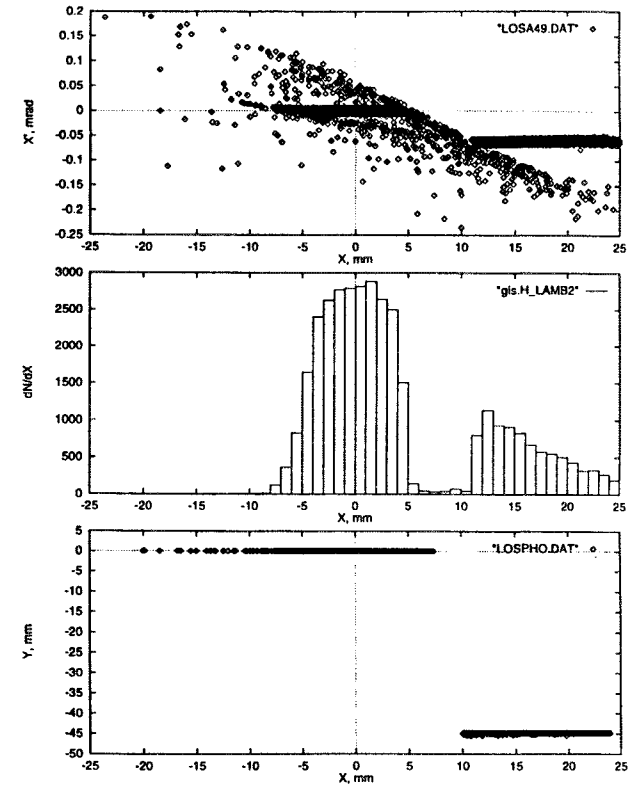


Figure 15: Halo phase plane at the second Lambertson magnet entrance (top and middle), and exit (bottom).

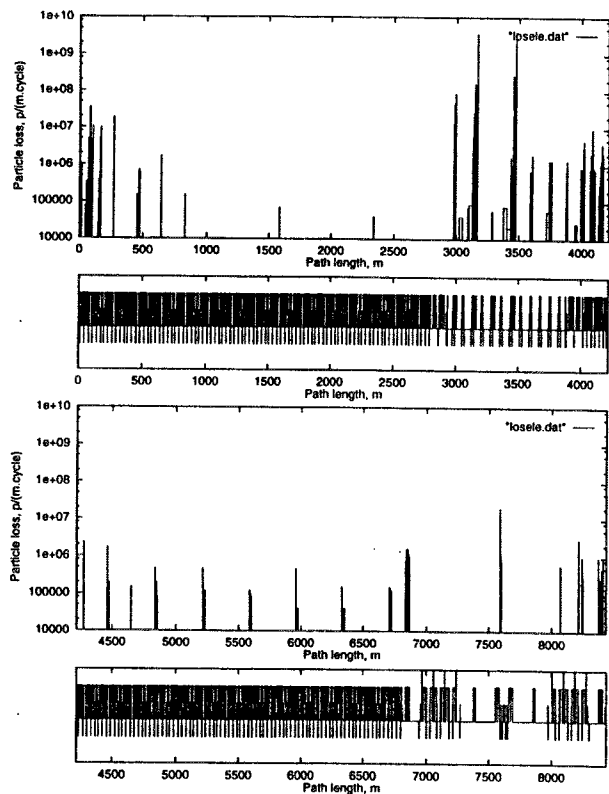


Figure 16: Beam loss at collimation.

50 X 50 GeV $\mu^+\mu^-$ Collider Beam Collimation System*

A. I. Drozhdin, C. Johnstone, N. V. Mokhov

Fermi National Accelerator Laboratory

P.O. Box 500, Batavia, Illinois 60510

A. Garren

Lawrence Berkeley National Laboratory

Berkeley, CA 94720

December 8, 1997

1 Abstract

Summary of studies is presented towards the possibility of beam halo collimation in the 50 X 50 GeV $\mu^+\mu^-$ collider using absorbers or electrostatic deflector for scrapping the circulating beam. It is shown based on Monte-Carlo simulations that traditional scheme with 5m long steel absorber permits to suppress losses in the IP by three order of magnitude, to 0.07% of the scraped beam.

2 Introduction

The halo originated background in the detector arise from muons which come to the aperture restrictions of the collider. In proton and electron accelerators particles which are lost away from the interaction region do not produce considerable background in the detector as they can be intercepted locally. High-energy muons can traverse several tens meters of lattice or shielding. Therefore, muons lost from the beam anywhere along the collider are candidates for background production in the detector. Muons which induce electromagnetic or hadronic showers either upstream or inside of the detector

*Presented at the *International Conference on Physics Potential and Development of $\mu^+\mu^-$ Colliders*. San Francisco, California, December 10-12, 1997

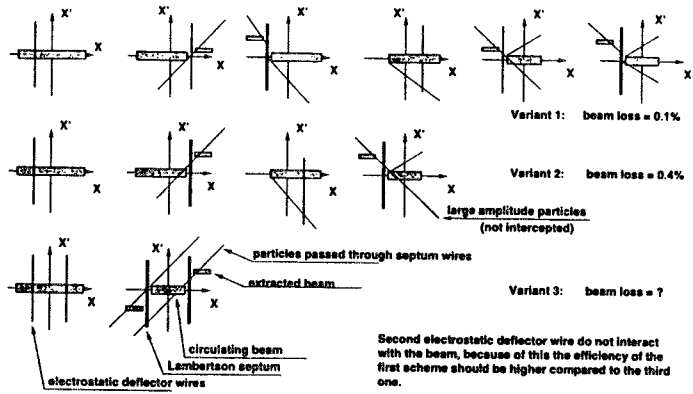


Figure 4: Different schemes of muon collider beam collimation.

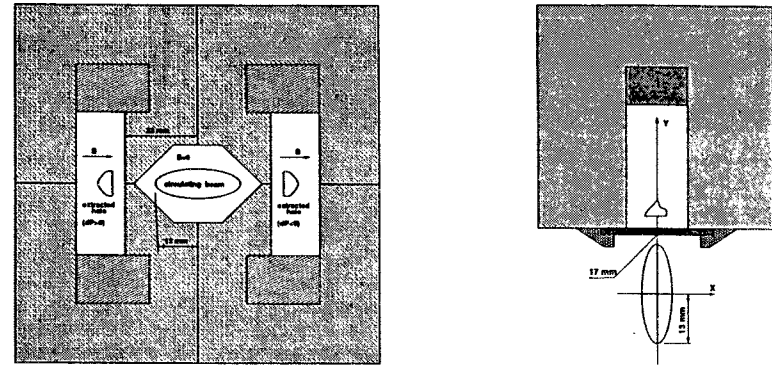


Figure 6: Symmetric Lambertson and septum-magnet cross section.

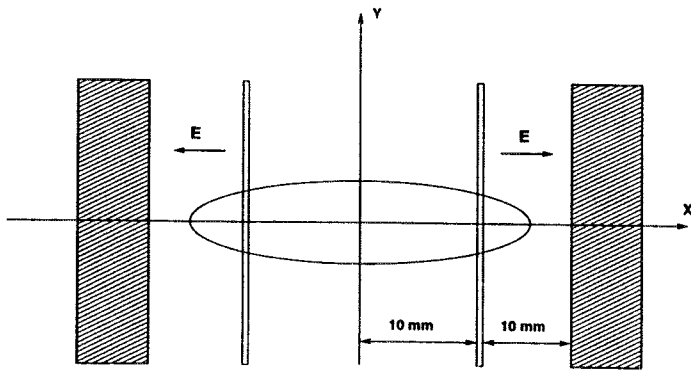


Figure 5: Symmetric electrostatic deflectors cross section.

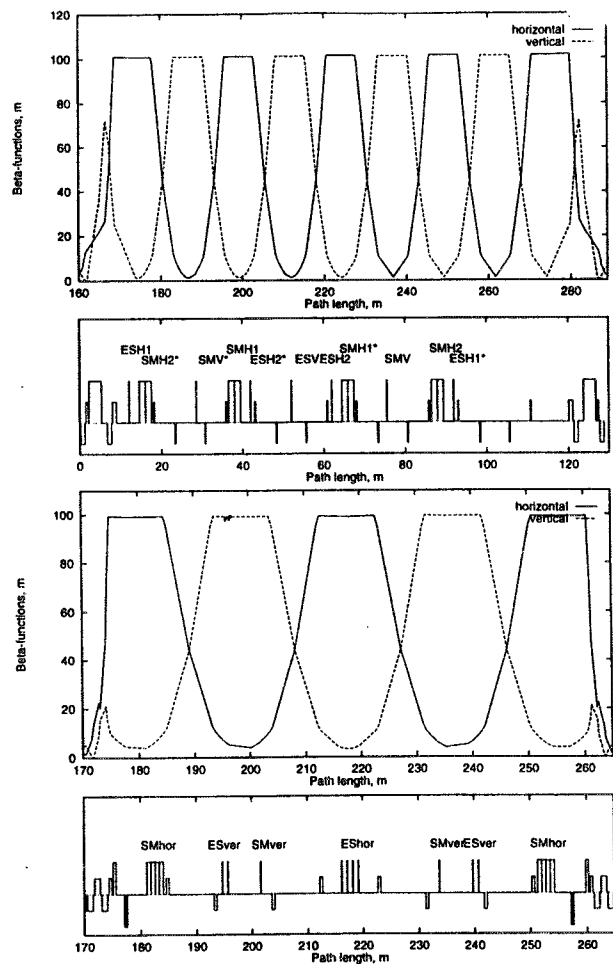


Figure 8: Collimation section beta functions and possible collimation schemes.

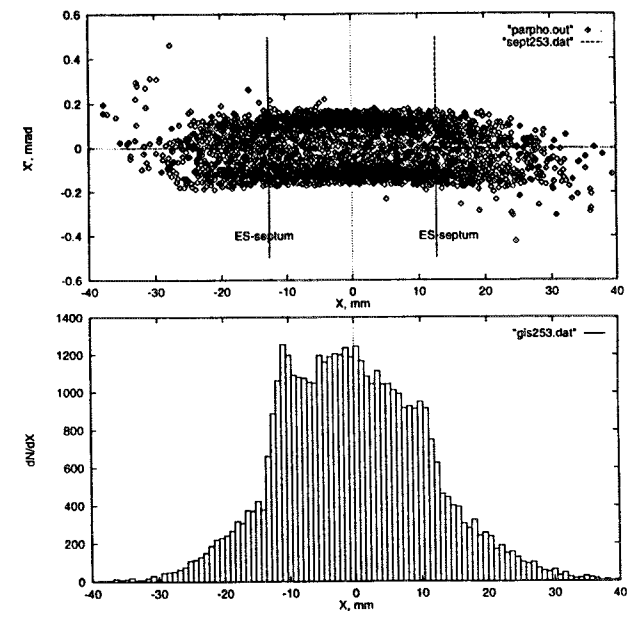


Figure 9: Halo phase plane at the horizontal electrostatic deflector entrance in the symmetric scheme.

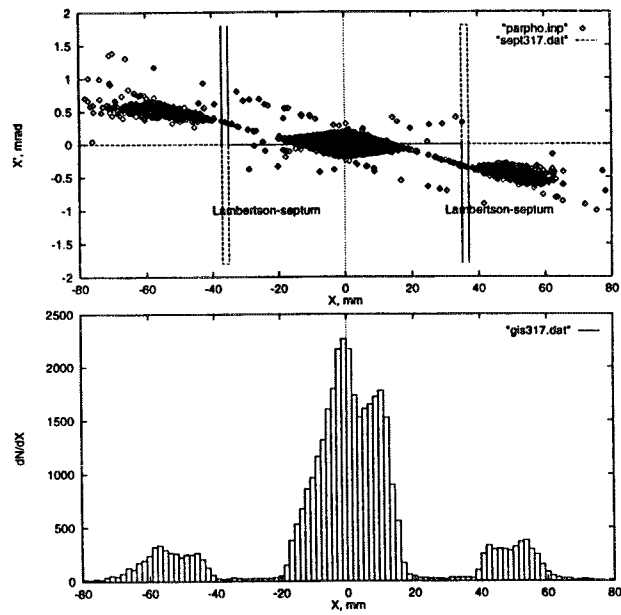


Figure 10: Halo phase plane at the Lambertson magnet entrance in the symmetric scheme.

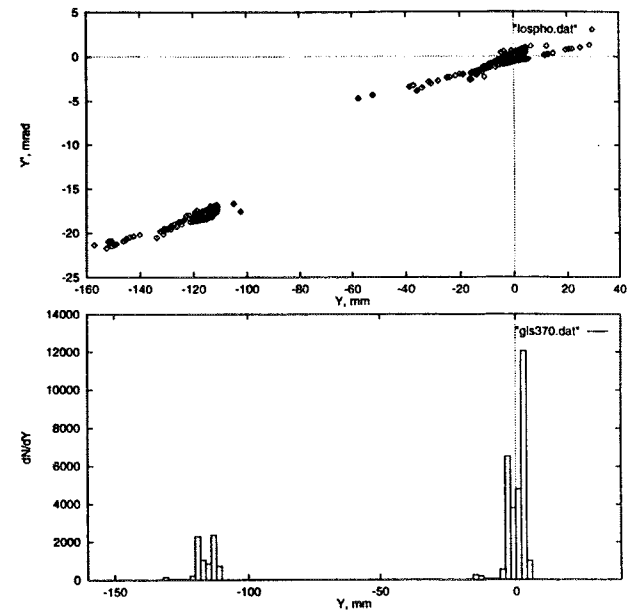


Figure 11: Halo phase plane at the the Lambertson magnet exit in the symmetric scheme.

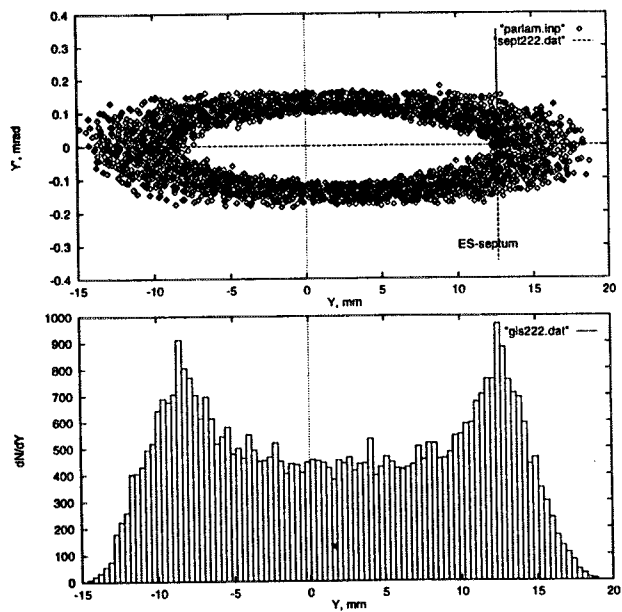


Figure 12: Halo phase plane at the vertical electrostatic deflector entrance in the symmetric scheme.

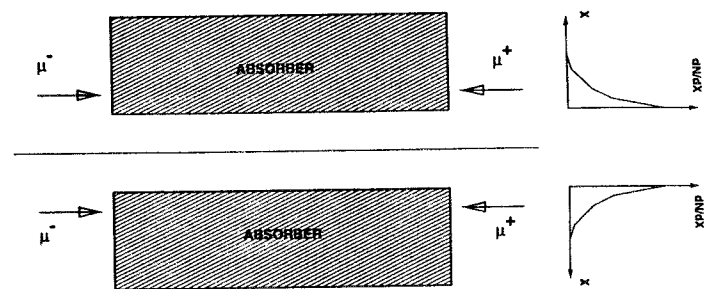
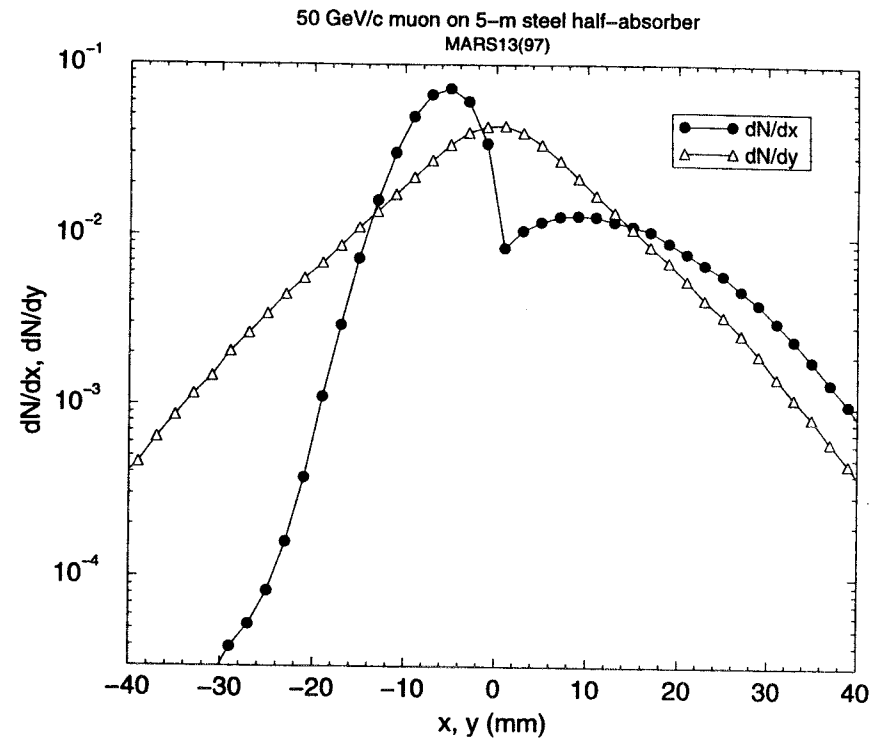
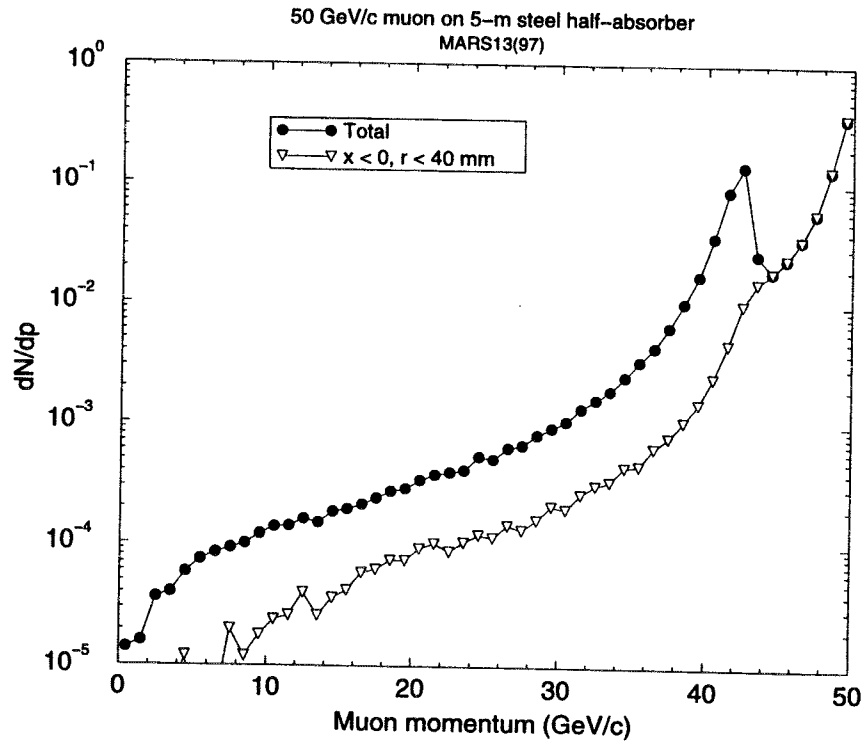


Figure 15: Halo collimation with 5m steel absorber.



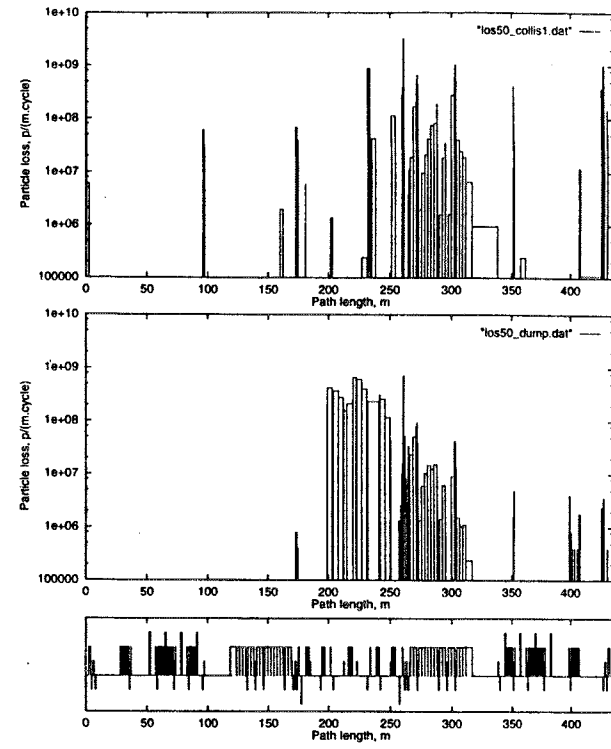
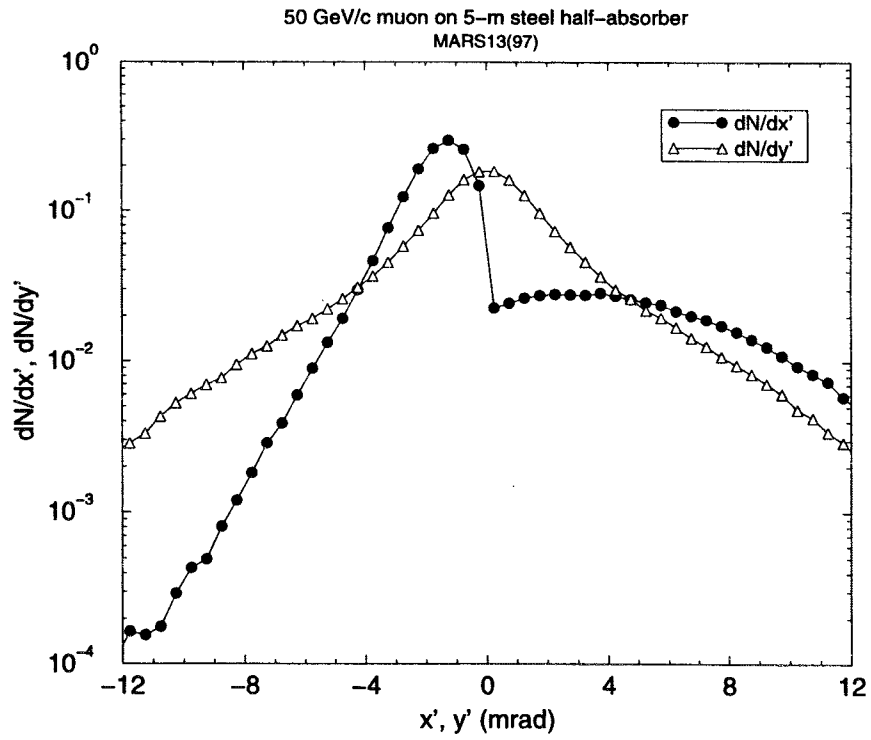


Figure 16: Beam loss at collisions with halo extraction (top) and halo dumping at internal absorber (bottom). One percent of the beam intensity is collimated at collisions.

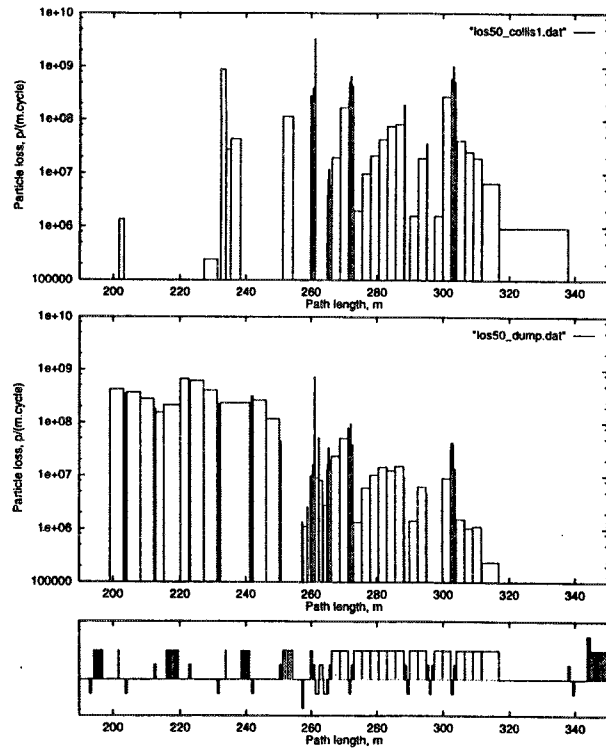
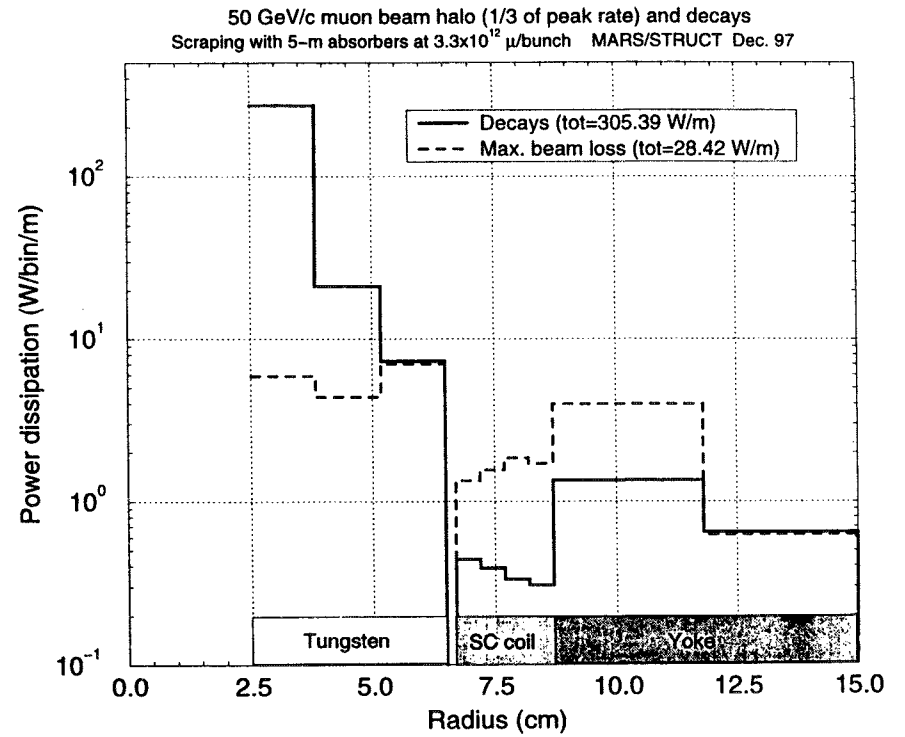
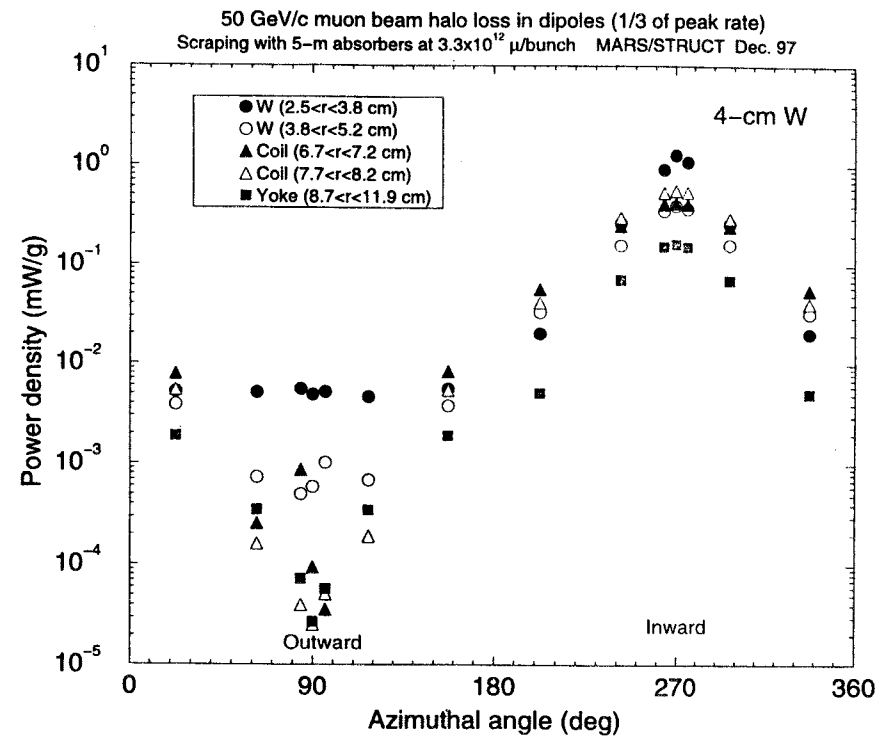
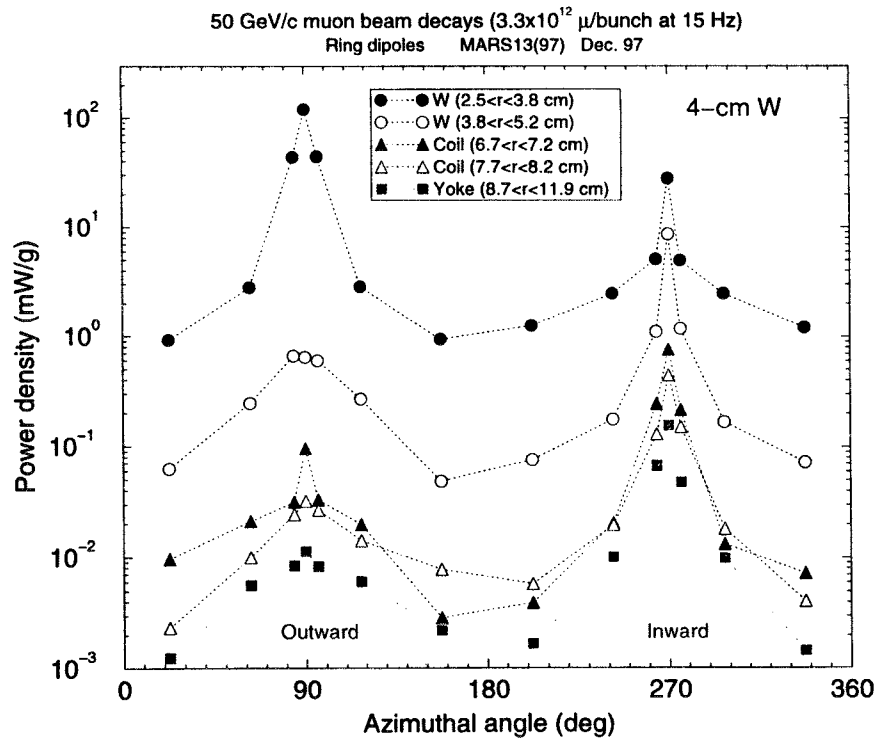
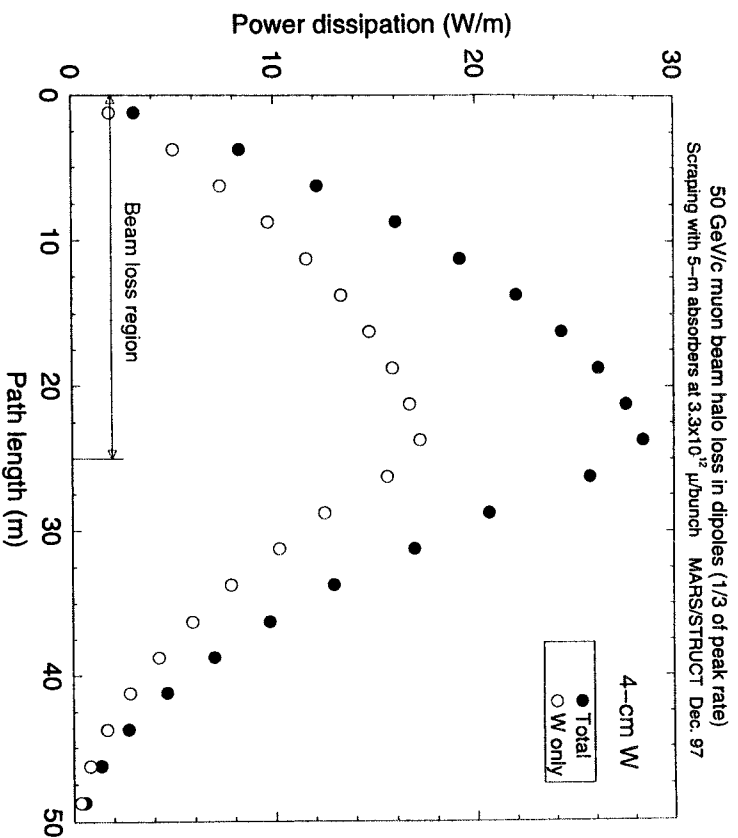


Figure 17: Beam loss at collisions with halo extraction (top) and halo dumping at internal absorber (bottom). One percent of the beam intensity is collimated at collisions.



50 GeV/c muon beam halo (1/3 of peak rate) and decays
Scraping with 5-m absorbers at 3.3×10^{12} μ /bunch MARS/STRUCT Dec. 97





CONCLUSION

- Beam cleaning system is a mandatory in muon colliders
- At 2 TeV, extraction of beam halo reduces loss rate in IR by three orders of magnitude; efficiency of an absorber-based system is much much lower
- At 50 GeV, a five meter long steel absorber does an excellent job, eliminating halo-induced backgrounds in detectors
- At 50 GeV, a 4-cm tungsten liner or a design with iron/coils completely separated on the mid-plane are needed to protect SC magnets against both beam halo (locally!) and beam decays



Determining the energy scale of the 50 GeV First Muon Collider using g-2 precession

Rajendran Raja, Alvin Tollestrup
Fermilab

Workshop on Physics at the First Muon
Collider and Front end of the FMC ,
November 6-9, 1997

Format of talk

- Describe g-2 method.
- Planar ideal accelerator
- Explore fractional error in measurement Lorentz factor $\delta\gamma/\gamma$ of muon as a function of number of electrons sampled and polarization.
- Explore variation of $\delta\gamma/\gamma$ as a function of momentum spread $\delta p/p$ of muons
- Examine effects of departures from ideal case.
- Assume that a) Polarized muons can be delivered to the collider ring and b) The polarization can be adequately maintained for 1000 turns.

Bargmann-Michel-Telegdi equation

$$\frac{d\vec{S}}{dt} = \vec{\Omega} \times \vec{S}$$

$$\vec{\Omega} = -\frac{e}{m\gamma} \left((1 + \alpha\gamma)\vec{B}_{\perp} + (1 + a)\vec{B}_{\parallel} - \left(\alpha\gamma + \frac{\gamma}{1 + \gamma} \right) \vec{\beta} \times \frac{\vec{E}}{c} \right)$$

$$\vec{\Omega} = \vec{\Omega}_{\text{cycl}} (1 + \alpha\gamma)$$

$$a = (g - 2) / 2$$

B_{\perp}, B_{\parallel} are the components of magnetic field perpendicular and parallel particle direction

This equation controls the evolution of the spin vector \vec{S} . Polarization is the average of the spin vectors over the muon ensemble. Per revolution spin rotates by $\alpha\gamma 2\pi$ radians more than momentum

Definitions

In the muon rest frame, E is the energy of the electron. Its fractional energy expressed in terms of the maximum energy ($m_{\mu}/2$) is x. N is the number of muon decays. θ is the angle of the electron in the muon center of mass

w.r.t muon direction. $\langle E \rangle$ is the average electron energy and $\langle PL \rangle$ is the average longitudinal electron momentum in the muon rest frame.

P is the z component of the muon polarization along the muon direction. \hat{P} is charge*P of the muon.

Electron energy distribution

$$x = 2E / m_\mu$$

$$\frac{d^2N}{dx d\cos\theta} = N(x^2(3-2x) - \hat{P}x^2(1-2x)\cos\theta)$$

$$\langle E \rangle = \frac{m_\mu}{2N} \iint x \frac{d^2N}{dx d\cos\theta} dx d\cos\theta = \frac{7}{10} \frac{m_\mu}{2}$$

$$\langle P_L \rangle = \frac{m_\mu}{2N} \iint x \cos\theta \frac{d^2N}{dx d\cos\theta} dx d\cos\theta = \frac{\hat{P}}{10} \frac{m_\mu}{2}$$

Decay distributions

$$\langle E_{lab} \rangle = \frac{7}{20} E_\mu \left(1 + \frac{\beta}{7} \hat{P}\right)$$

$$E(t) = N e^{-\alpha t} \left(\frac{7}{20} E_\mu \left(1 + \frac{\beta}{7} (\hat{P} \cos\omega t + \phi)\right) \right)$$

$$\omega = \gamma \frac{g-2}{2} 2\pi$$

$$\alpha = \frac{t_{circ}}{\gamma t_{life}} = \frac{2\pi m_\mu}{0.3 B c t_{life}}$$

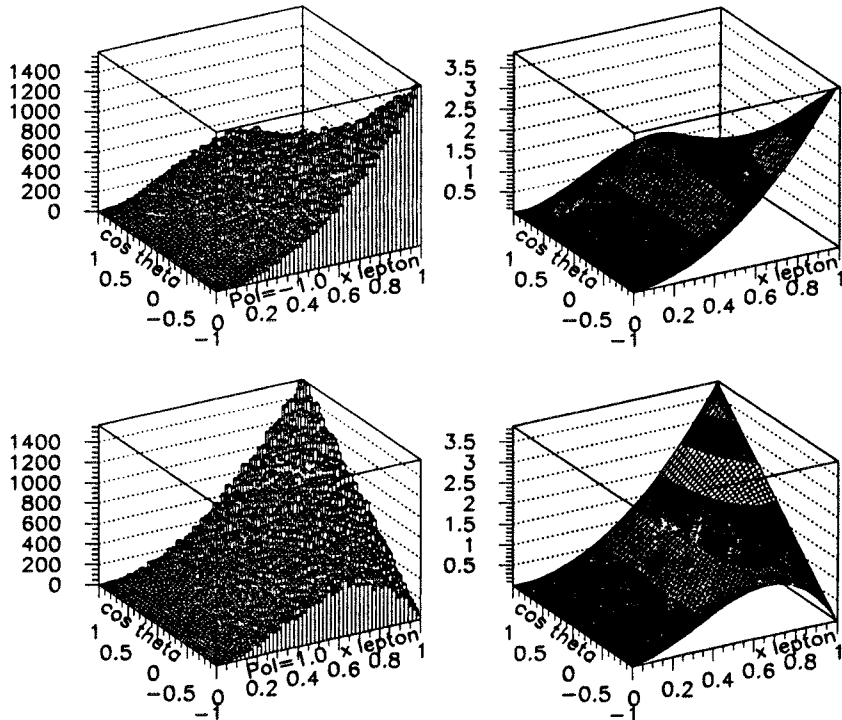
$$f(t) = A e^{-Bt} (C \cos(D + Et) + F)$$

$\langle E_{lab} \rangle$ is the average electron energy in lab. $E(t)$ is the total electron energy during turn t . Determine ω to get γ . γ information also present in α .

$f(t)$ is the fitting function. MINUIT used to fit and extract information.

*Electron energy and angle distributions in
muon rest frame
Polarization = -1.0 and 1.0*

19/08/97 14.24

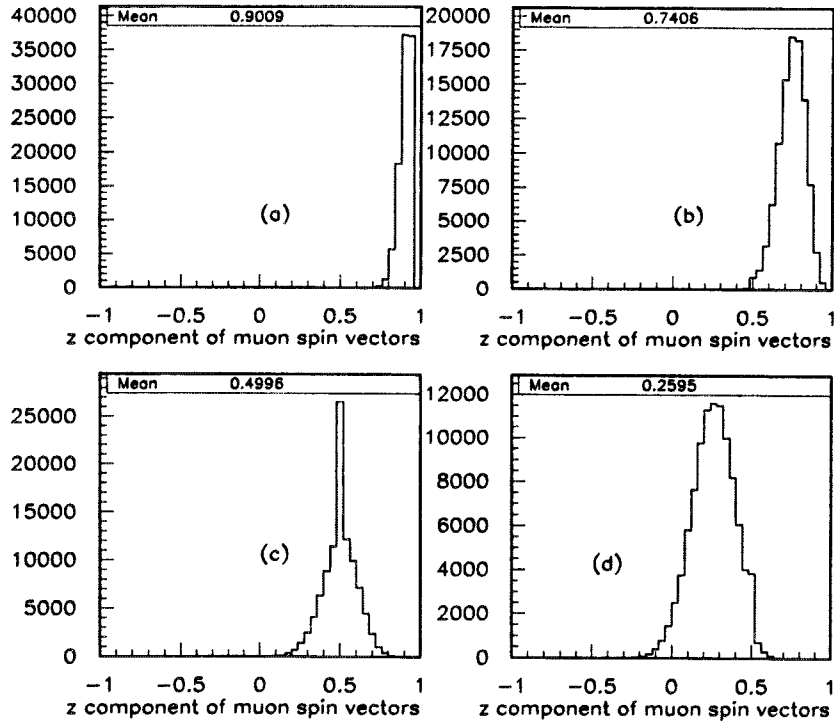


Variation in spin vectors

The electron energy sampled depends only on \hat{p} which is the average of the z component of the individual spin vectors. If all the muons had the same momentum, then the variation of the individual spin vectors is unimportant. Only the average matters. However, $\delta p/p$ is non-zero and the individual spins precess slightly differently turn to turn and a dilution in polarization results. We generate \hat{p} as a binomial distribution about a given average.

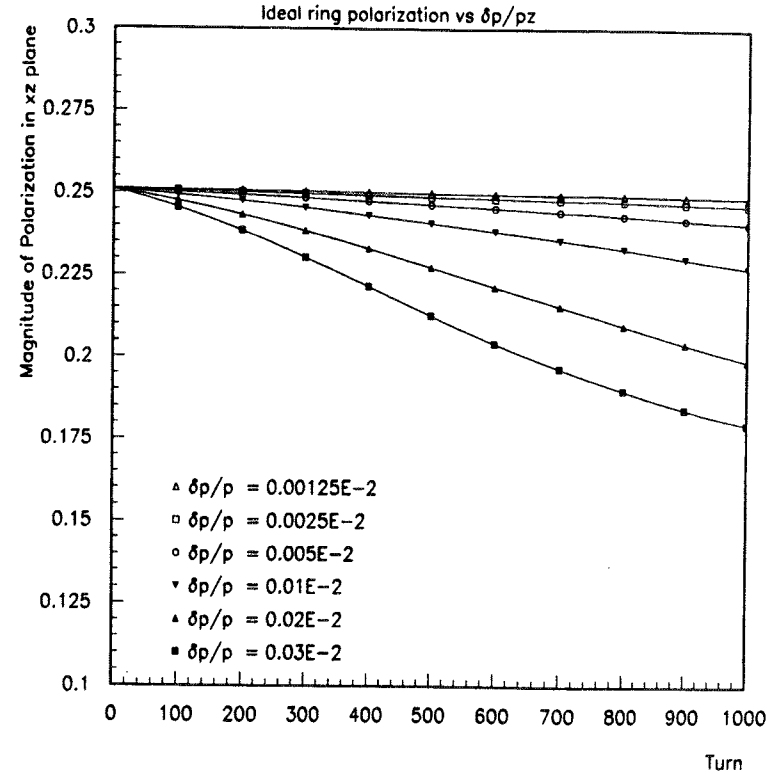
Muon Spin vector generation

05/09/97 10.28



Polarization vs turn for various $\delta p/p$

05/11/97 10.57



Idealized collider ring model

In order to simulate the decays, we assume an idealized planar collider ring made up of 4.0 Tesla average bending field. This results in the following parameters.

Muon Energy	= 50 GeV
Lorentz factor γ	= 473.22
Spin precession per turn	= 3.4667 radians
Magnetic field	= 4 Tesla
Ring Radius	= 41.667 meters
Circulation time	= 0.873E-6 sec
Dilated muon life time	= 0.104E-2 sec
Turn by turn decay constant α	= 0.8399E-3

Generation of decays

We generate an ensemble of 100K muons with appropriate spin and momentum vectors, precess them and decay them for 1000 turns. The measurement errors are added later as appropriate.

The 100K ensemble of muons represent the beam and are re-used every turn, after precessing. Each individual muon is precessed by the appropriate amount determined by its individual γ . After each turn, the number of muons is reduced by the amount expected by exponential decay. No fluctuations in this are made at this point.

We will generate muons with $\delta p/p=0.03E-2$ for most of the study and then will explore the dependence of the results on $\delta p/p$.

We will explore the effect of measurement errors due to sampling fluctuations in the number of electrons.

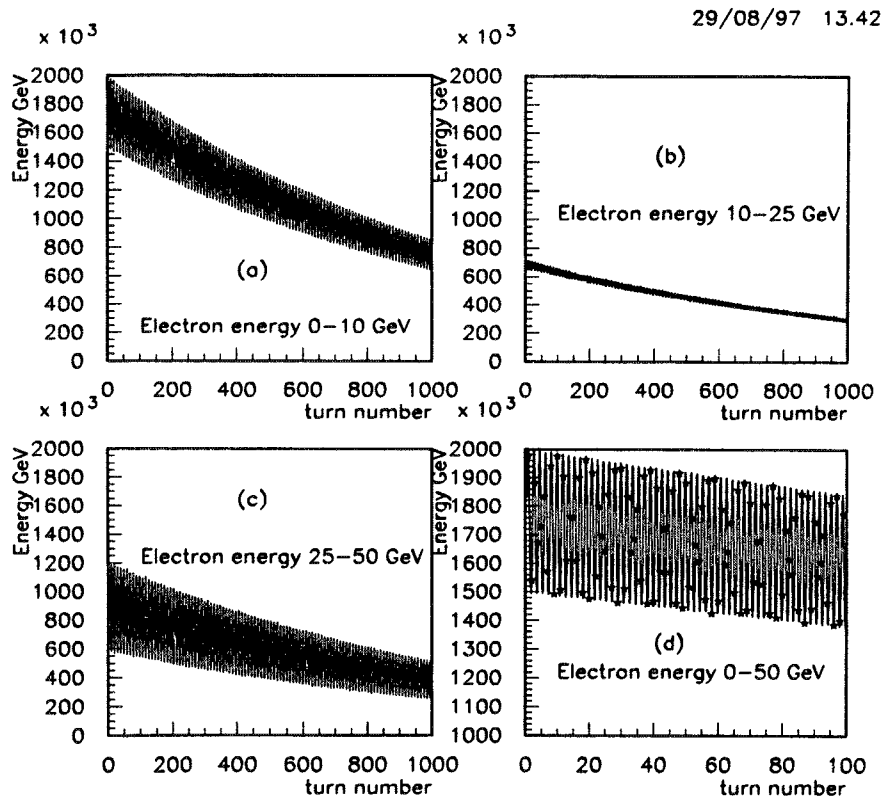
We will explore the accuracy obtainable in $\delta\gamma/\gamma$ from measuring α , the turn by turn decay constant.

Electron lab energy spectrum

Pol=1.0, 100K decays

Explanation of previous plot

The variation of the total lab electron energy seen in a calorimeter will depend on the electron energy cut made. Figure (d) has no electron energy cut. For 100 turns, we compare the predictions of the theory with the generated events. Excellent agreement. The amplitude of the oscillations depend on the polarization as well as the average value of $\cos \theta$ sampled. A cut on lab electron energy imposes a selection on $\cos \theta$. Electron energy 10-25 GeV for 50 GeV muons samples $\cos \theta = 0$, i.e. 90 degrees in muon rest frame.



Measurement errors

We need an EM calorimeter that measures total energy deposited per bunch from turn to turn. In addition, it would also be useful to have the number of particles going into the calorimeter. This can be done by having a scintillating fiber front end to the calorimeter that measures mips. This can lead to two sets of measurements. Total Electron energy and average electron energy.

We would also like to make cuts on the momenta of electrons being summed over. This can be done by a spectrometer in front of the calorimeter. With such a device, we can show that...

Measurement errors

For total energy E, N electrons and average individual electron energy $\langle e \rangle$, for a calorimeter with Constant Sampling and Noise terms (C,S, η) the fractional resolution in E is given by

$$\frac{\sigma_E^2}{\langle E \rangle^2} \approx \frac{1}{N} \left(1 + \frac{\sigma_e^2}{\langle e \rangle^2} \right) + C^2 + \frac{S^2}{N \langle e \rangle} + \frac{\eta^2}{N^2 \langle e \rangle^2}$$

For 50 GeV muons, $\langle e \rangle = 34.05$ GeV, $\sigma_e = 6.046$ GeV. For calorimeter, $S = 0.15 \text{ GeV}^{1/2}$ and η may be neglected for large N. If $C=0$, then

Measurement errors

$$\frac{\sigma_E^2}{\langle E \rangle^2} \approx \frac{1}{N} (1 + 0.03153 + 0.000661)$$

Neglecting sampling term,

$$PERR^2 \equiv \frac{\sigma_E^2}{\langle E \rangle^2} \approx \frac{1.03153}{N}$$

PERR=0.5E-2, 1.0E-2, 2.0E-2, 3.0E-2

imply, N=41261, 10315, 2579 and 1146
electrons sampled with $e > 25$ GeV.

For a beam intensity of 10^{12} muons,
there are 3.2E6 decays per meter.

Constant term has to be of order 0.32E-2
for 100,000 electrons sampled.

Measurement errors, using average energy

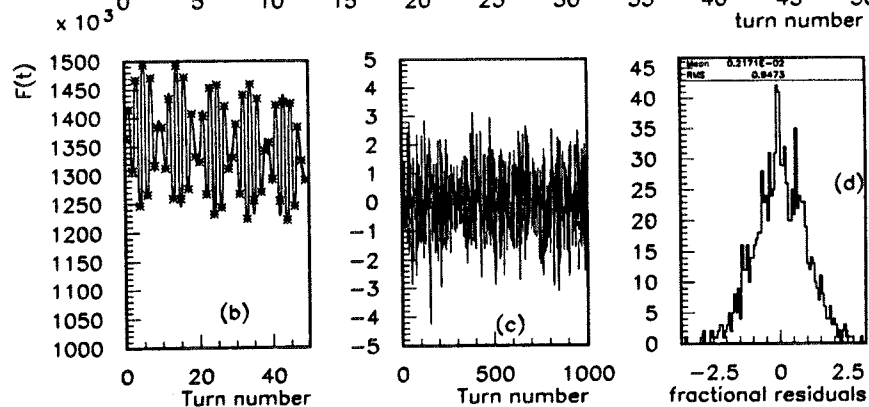
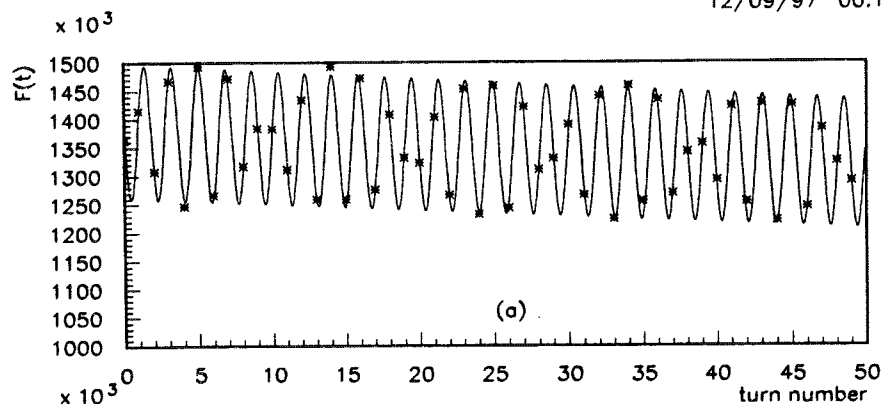
If the number of electrons as well as their total energy is measured, then one can use the average energy. Average energy has lower percentage error, since the error due to the fluctuations in N are removed.

$$\frac{\sigma_{E_{av}}^2}{\langle E_{av} \rangle^2} \approx \frac{1}{\langle N \rangle} \left(\frac{\sigma_e^2}{\langle e \rangle^2} \right) \dots \approx \frac{0.03153}{N}$$

The other advantage of using average energy is that one does not have to model the intensity decay function.

Fit to 50 GeV μ^- , $P=0.26$ $\delta p/p=0.03E-2$

12/09/97 00.13



$\delta\gamma/\gamma$ vs measurement error and Polarization $\delta p/p=0.03E-2$

12/09/97 00.20

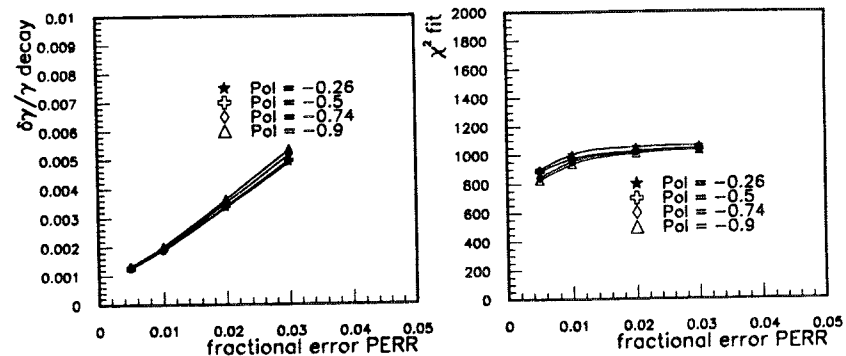
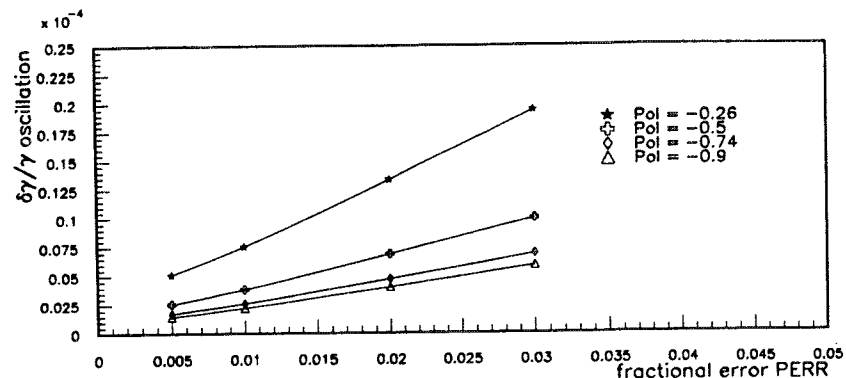
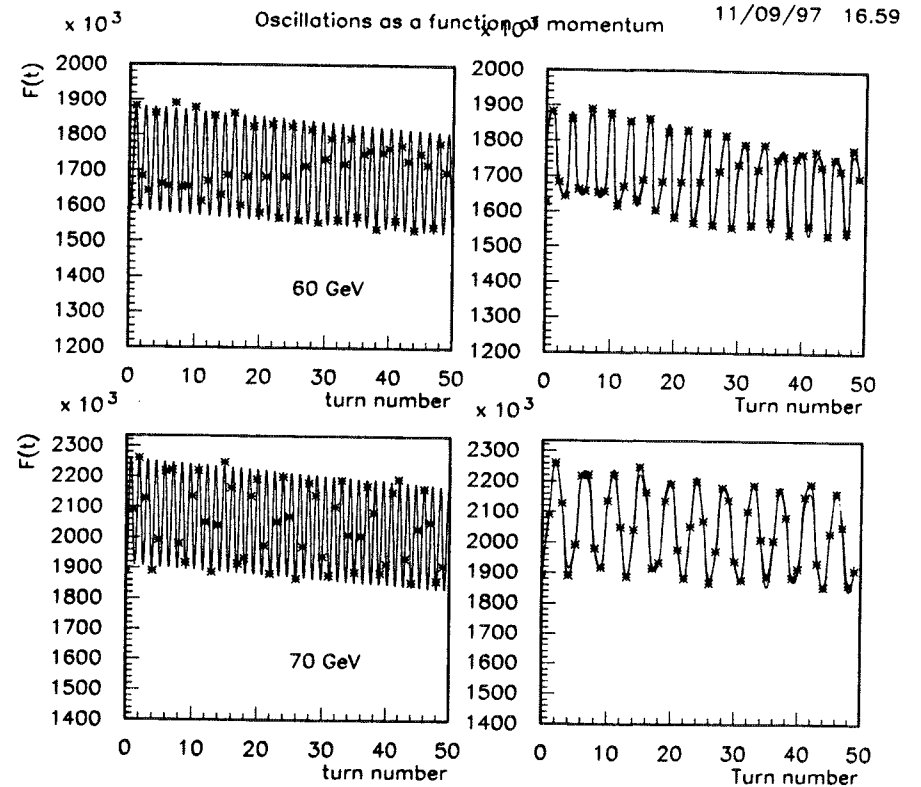


Table of fit parameters

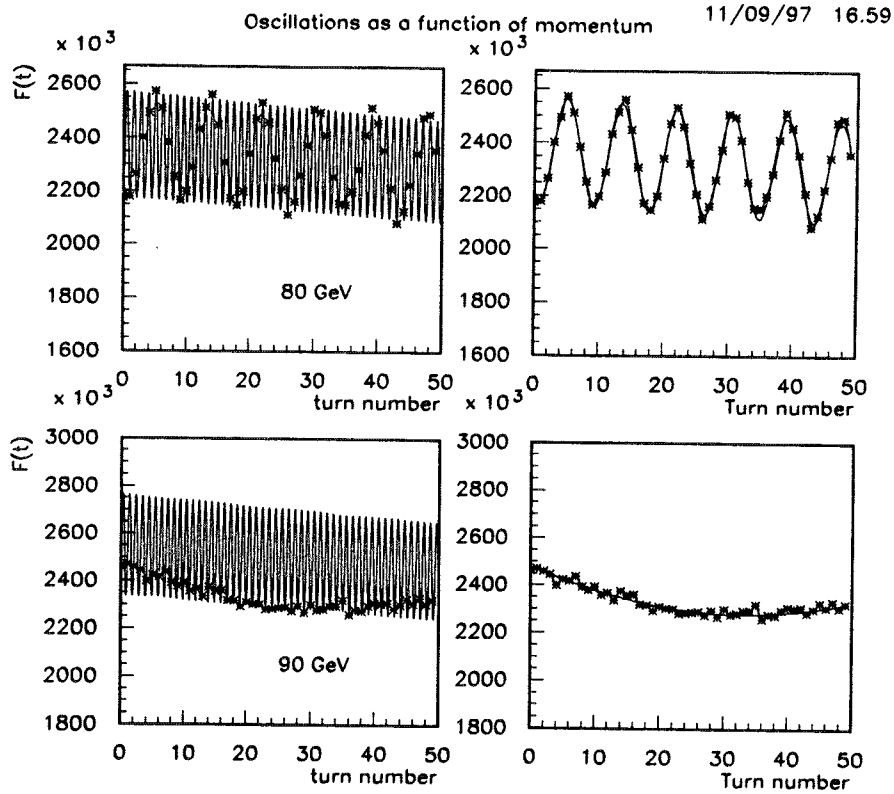
\hat{P}	PERR	Number of electrons sampled	$\delta\gamma/\gamma_{oscillations}$	$\delta\gamma/\gamma_{decay}$	χ^2 for NDF=1000
-0.90	0.50E-02	41261	0.14568E-05	0.13227E-02	824.
-0.90	0.10E-01	10315	0.22147E-05	0.20124E-02	936.
-0.90	0.20E-01	2579	0.39999E-05	0.36398E-02	1009.
-0.90	0.30E-01	1146	0.58659E-05	0.53457E-02	1030.
-0.74	0.50E-02	41261	0.17418E-05	0.13019E-02	843.
-0.74	0.10E-01	10315	0.26183E-05	0.19591E-02	954.
-0.74	0.20E-01	2579	0.46981E-05	0.35229E-02	1021.
-0.74	0.30E-01	1146	0.68765E-05	0.51672E-02	1039.
-0.50	0.50E-02	41261	0.25903E-05	0.12813E-02	888.
-0.50	0.10E-01	10315	0.38407E-05	0.19029E-02	973.
-0.50	0.20E-01	2579	0.68338E-05	0.33972E-02	1026.
-0.50	0.30E-01	1146	0.99744E-05	0.49749E-02	1041.
-0.26	0.50E-02	41261	0.51242E-05	0.12688E-02	898.
-0.26	0.10E-01	10315	0.75317E-05	0.18791E-02	1004.
-0.26	0.20E-01	2579	0.13324E-04	0.33447E-02	1053.
-0.26	0.30E-01	1146	0.19380E-04	0.48950E-02	1061.

TABLE I. Results of fits for $\delta\gamma/\gamma$ as a function of polarization \hat{P} and noise PERR. Also shown is the χ^2 of the fit for 1000 turns.

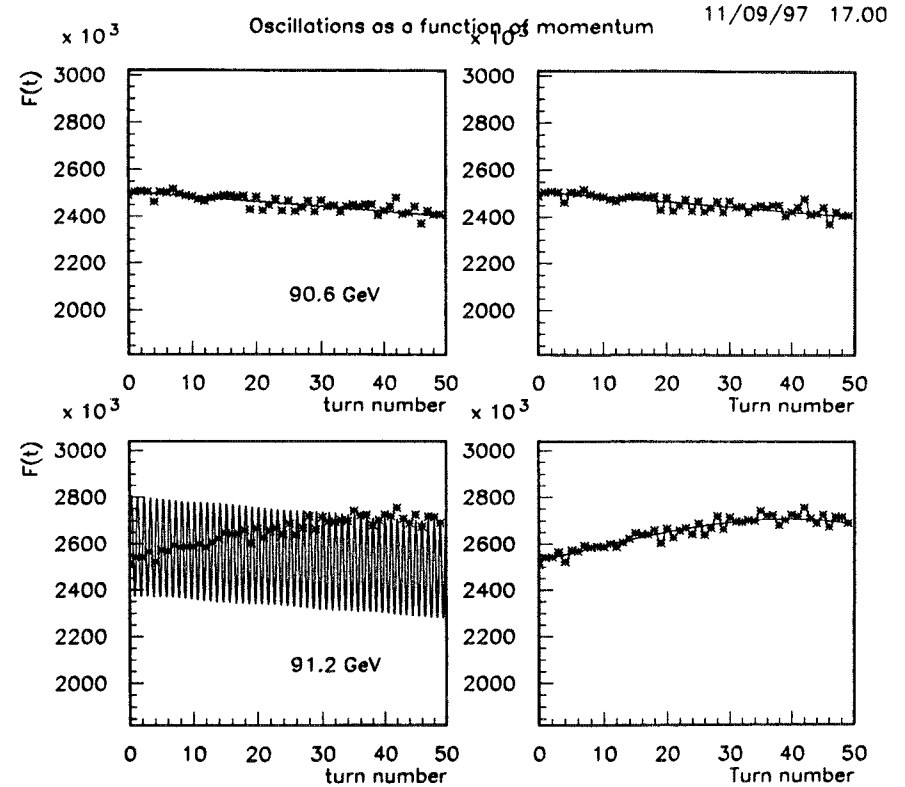
Fits for 60Gev/c and 70 Gev/c muon momenta



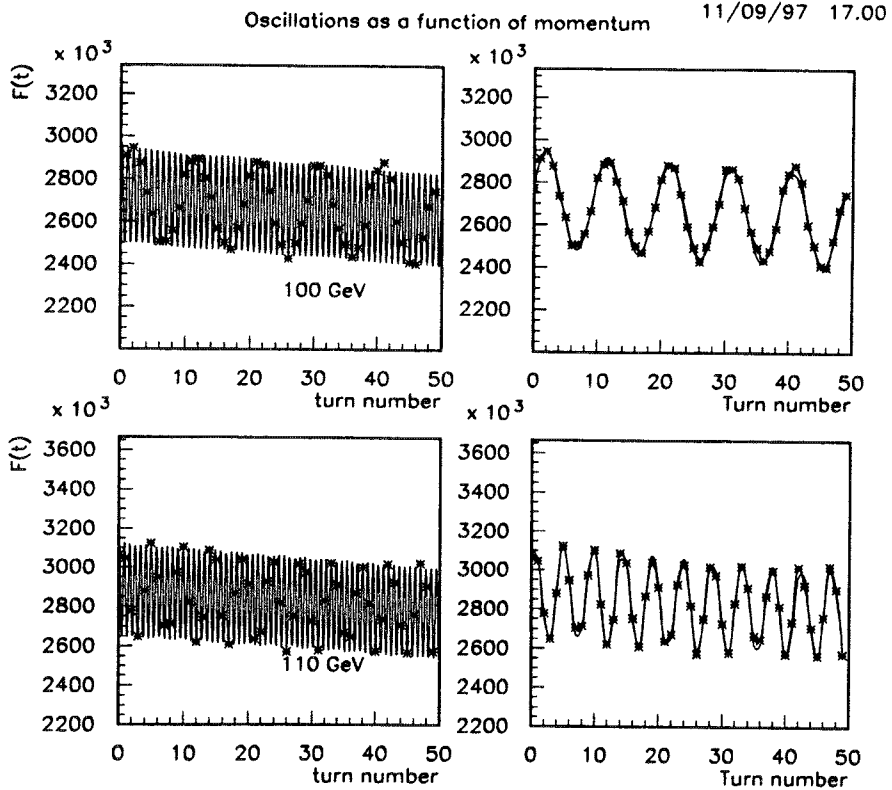
Fits for 80 GeV/c and 90 GeV/c muon momenta



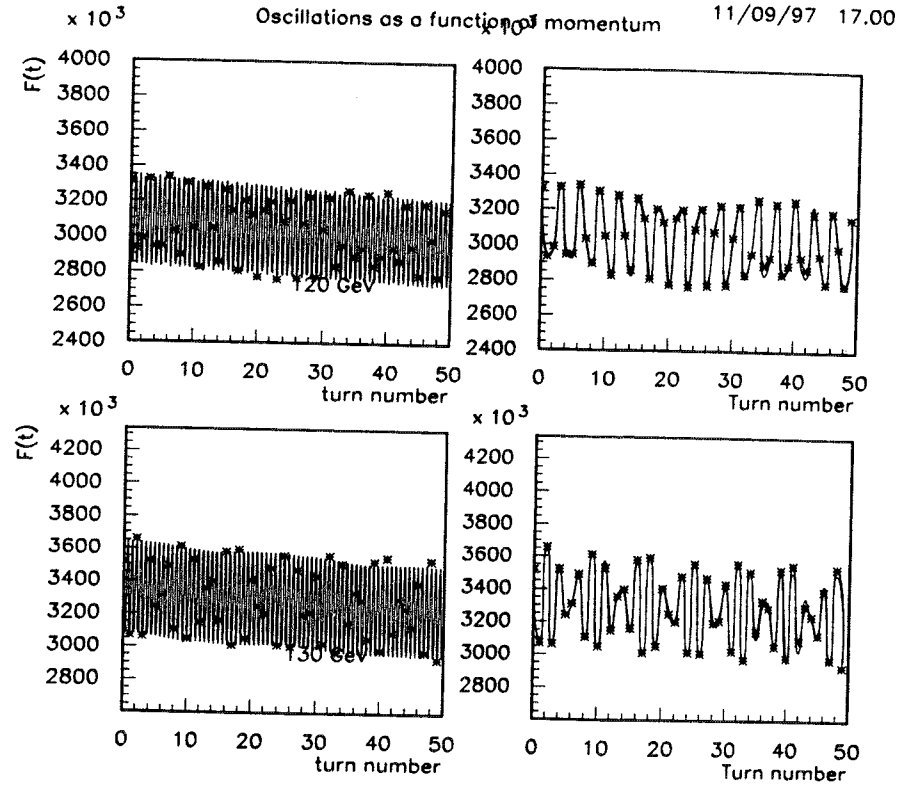
Fits for 90.622 GeV/c and 91.2 GeV/c muon momenta



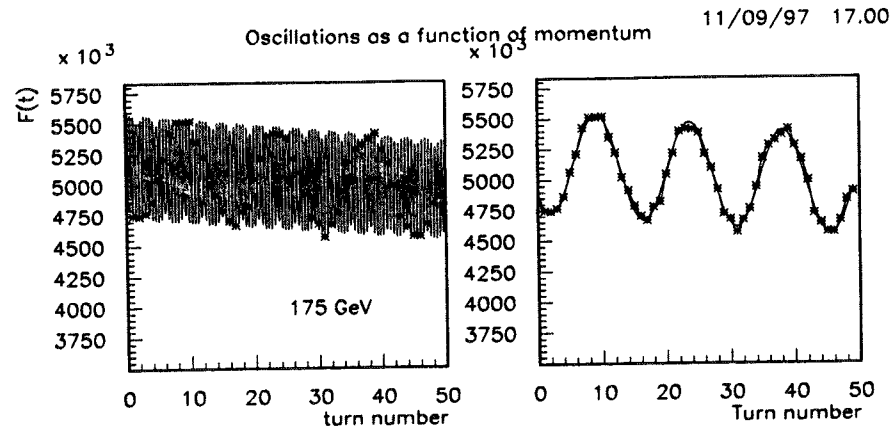
Fits for 100 GeV/c and 110 GeV/c muon momenta



Fits for 120 GeV/c and 130 GeV/c muon momenta

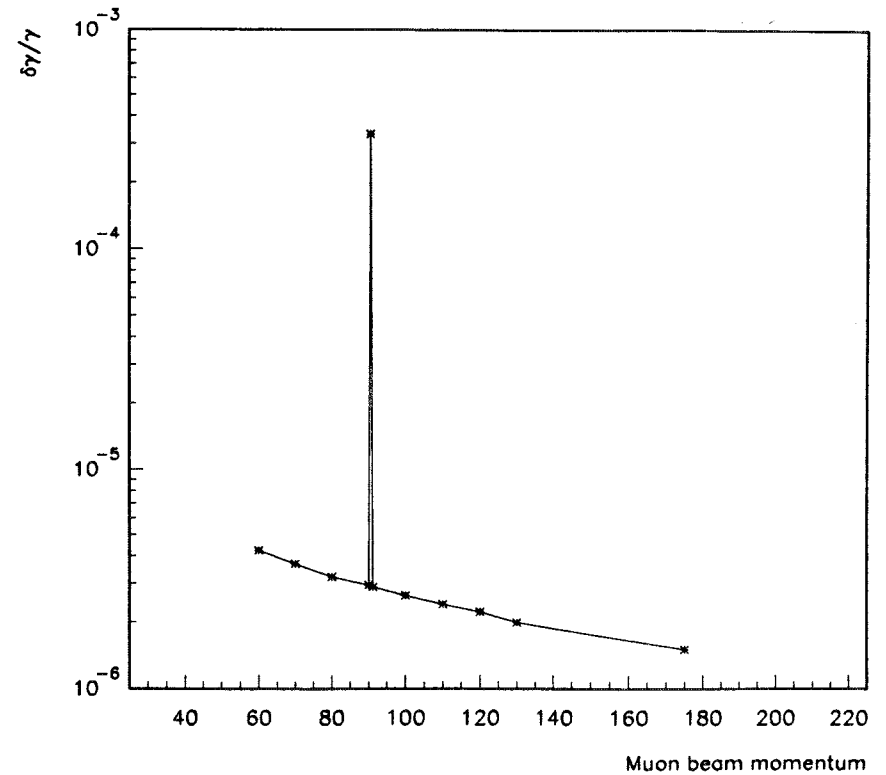


Fit for 175 GeV/c muon momenta



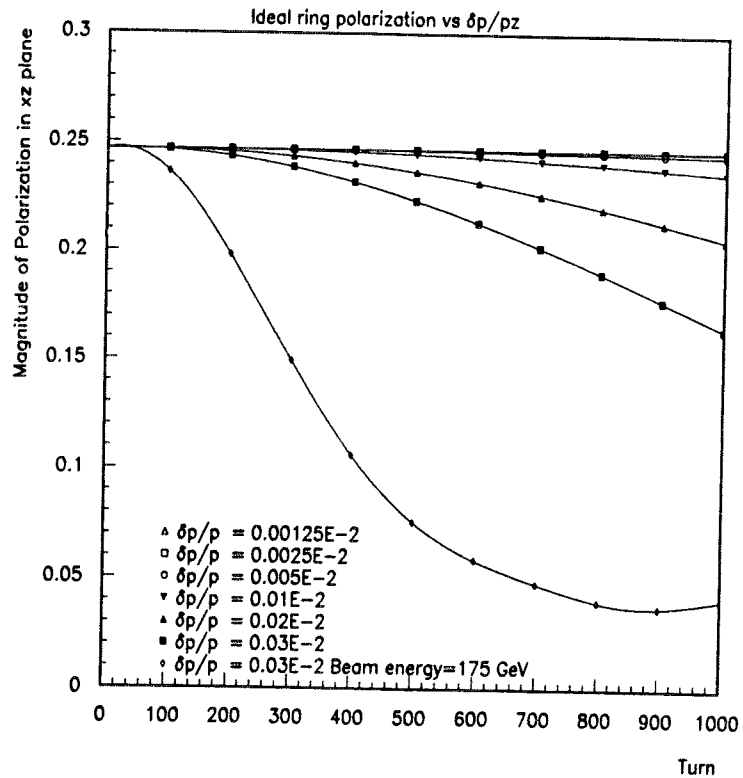
$\delta\gamma/\gamma$ vs muon beam momentum

11/09/97 16.59



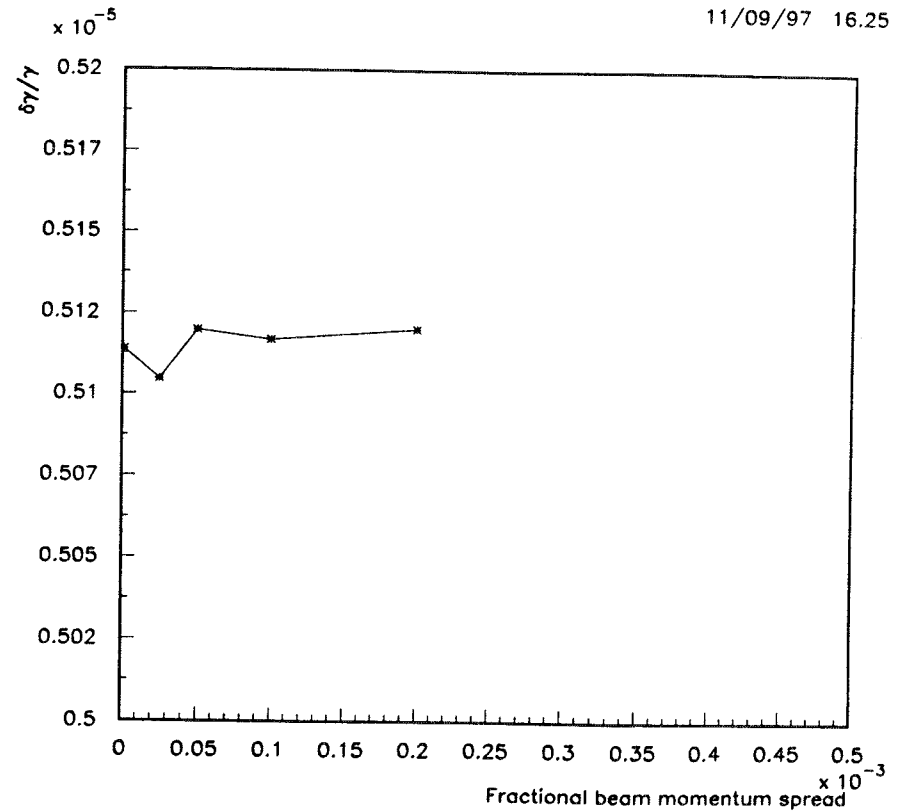
Polarization vs turn for various $\delta p/p$

23/11/97 19.40



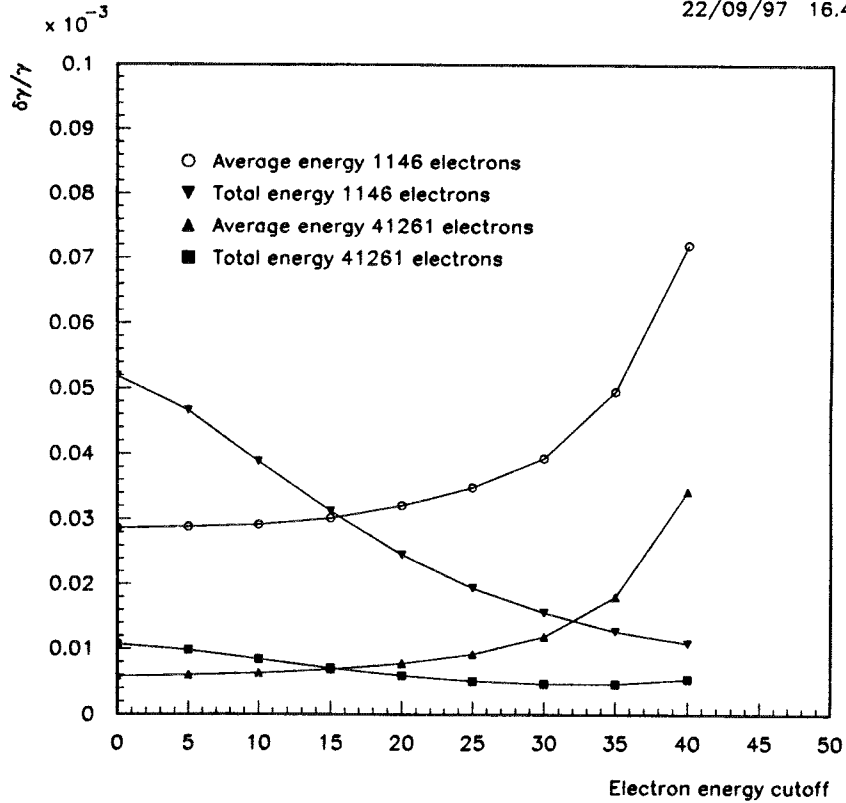
$\delta\gamma/\gamma$ vs $\delta p/p$ for 50 GeV/c μ^- . $P_{err}=0.05$ $P=0.26$

11/09/97 16.25



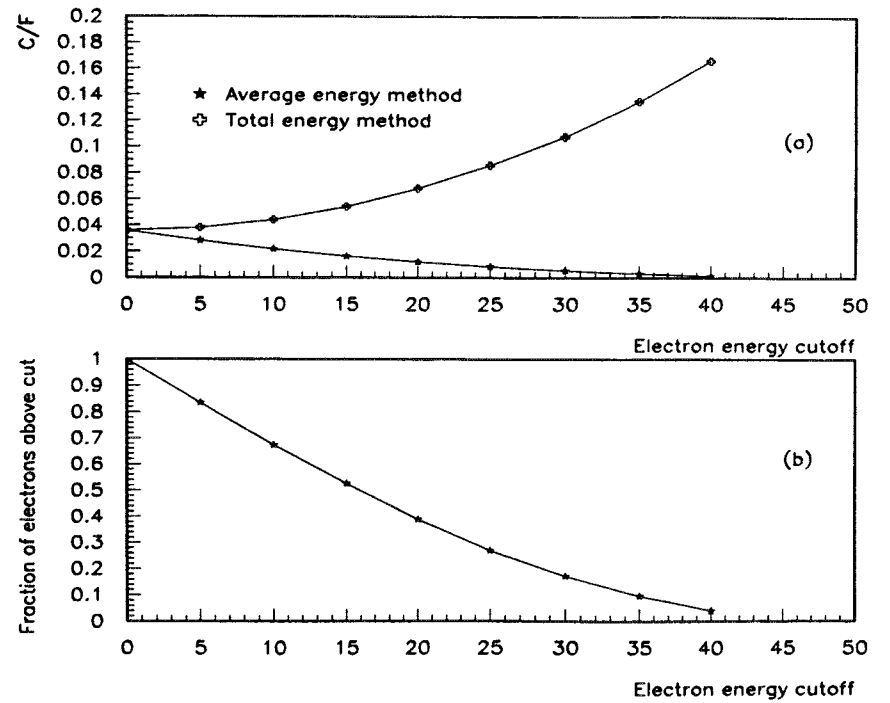
**$\delta\gamma/\gamma$ vs electron energy cut
for a sample of 40K and 1.1K
electrons**

22/09/97 16.49



**a) Variation of C/F vs electron
energy cut
b) fraction of electrons that
survive cut**

15/09/97 17.37



Departures from ideal case

- Electric fields. Collider ring will have RF but electrostatic separators are not envisaged at present. BMT equation tells that longitudinal electric fields have no spin precession effect since $\vec{\beta} \times \vec{E} = 0$
- Effects of radial magnetic fields
 - » Quadrupole misalignments. FODO
 - » Quad radial magnetic field followed by Horizontal dipole bend followed by reverse quad radial field has a net effect. (Assmann and Koutchouk LEP)

$$\nu_0 = \gamma (g - 2) / 2$$

$$\langle \delta \nu \rangle = \frac{\cot \pi \nu}{8\pi} \nu_0^2 (n_Q (Kl_Q)^2 \sigma_y^2 + n_{cv} \sigma_{\theta cv}^2)$$

$$\sigma_{\delta \nu} = \frac{\langle \delta \nu \rangle}{\cos \pi \nu_0}$$

Departures from ideal case

- Correction elements may be neglected. These effects are less for the muon collider than for LEP because a) LEP has more quadrupoles b) Muon is 200 times heavier than electron.

Machine	Spin tune ν_0	Quadrupoles	RMS Kl_Q meters ⁻¹	σ_y meters	$\delta \nu$	$\sigma_{\delta \nu}$
46 GeV LEP	100.47	≈ 600	0.032	0.5E-3	5.7E-6 $\equiv 3\text{KeV}$	6.1E-5 $\equiv 30\text{KeV}$
50 GeV Muon Collider	0.5517	70	0.274	0.5E-3	-0.26E-8 $\equiv -0.24\text{KeV}$	1.66E-8 $\equiv 1.46\text{KeV}$

TABLE I. Predictions for spin tune shift $\delta \nu$ and spread in spin tune shift $\sigma_{\delta \nu}$ caused by quadrupoles for LEP compared to the 50 GeV muon collider ring

Effects due to Experimental area solenoid

- Consider a solenoid 1.5 Tesla - 6 meters long = 9Tesla -meters.

$$\theta_s = -\frac{e}{\gamma m_\mu} (1 + a) B_s = -(1 + a) \frac{B_s l}{B \rho}$$

$$\nu + \delta\nu = \frac{1}{\pi} \arccos(\cos(\pi\nu) \cos(\frac{\theta}{2}))$$

θ is the angle of rotation due to solenoid.
For 9 Tesla-meters, this is 3.09 degrees per turn. This yields $\delta\nu/\nu = -1.72$ MeV. LEP will have 200 times less effect, since the tune is 200 times larger. LEP corrects with vertical bumps and horizontal bends. 200 times harder to do for muons. Bucking solenoids optimal.

COSY studies

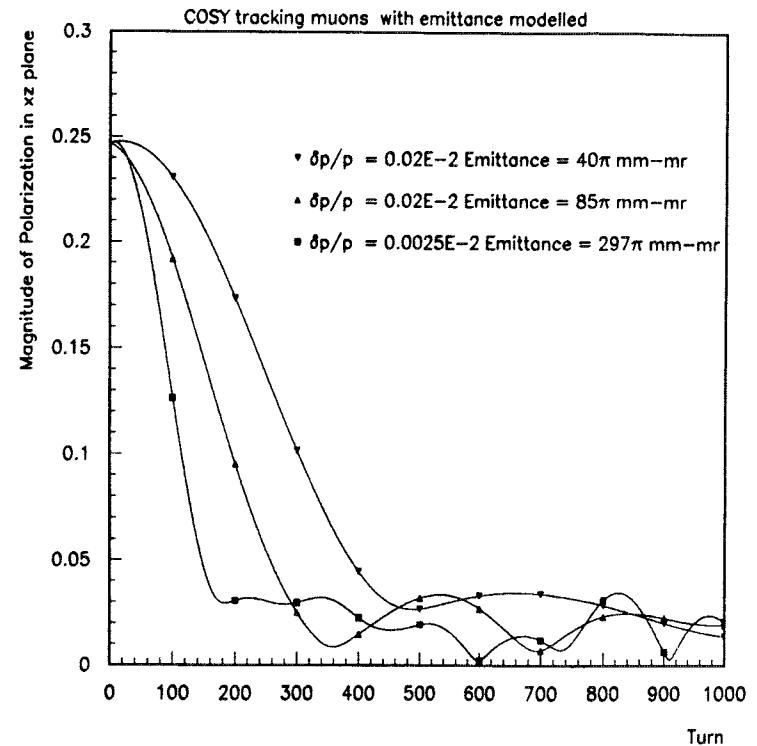
- COSY- Infinity has spin precession in it as well as higher order effects. Differential algebra techniques. Usin current 50 GeV design (C. Johnstone, W. Wan)
- 3 cases
 - » emittance = 297π mm-mr, $\delta p/p = 0.0025E-2$
 - » emittance = 85π mm-mr, $\delta p/p = 0.02E-2$
 - » emittance = 40π mm-mr, $\delta p/p = 0.02E-2$
- Spin tune studied as a function of 5 variables
 - » $x = x$ position ; $x' = p_x/p$
 - » $y = y$ vertical position; $y' = p_y/p$
 - » $\kappa = \delta$ kinetic energy/nominal kinetic energy
- Spin tune is then given by $\nu = 0.5517 + 0.5915\kappa - 64,61x^2 - 0.1017x'^2 - 69.81y^2 - 0.1088y'^2 - 8.341x\kappa - 0.3921\kappa^2$ to second order

Cosy Studies

- Track 1000 muons in COSY with
- polarization of 0.25 and emittance and $\delta p/p$ modelled for the three cases.
- Conclude that the non-linear aperture causes polarization loss for large emittances rather than momentum spread. Need to optimize design.

Polarization of 1000 muons vs turn number in COSY

22/11/97 18.43



Conclusions

- We have shown that IF
 - » it is possible to deliver polarized muons to the ring
 - » and that it is possible maintain the polarization for 1000 turns
- g-2 precession can be used to obtain precisions of the order of a few parts per million in the energy of the bunches.
- This is true for a range of $\delta p/p$ that covers the two options considered here.
- Method can be used to scan a narrow Higgs, Measure the W mass etc...

Dec.11, 1997

M.Atac, FNAL/UCLA

**TRACKING CONCEPTS OF HIGH LUMINOSITY
MUON COLLIDERS**

OUTLINE

1. FINAL FOCUS DESIGN AND COMPUTED BACKGROUNDS
2. SHIELDING FOR NEUTRONS AND GAMMAS
3. GENERAL PURPOSE STRAWMAN DETECTOR CONCEPTS
 - a. VERTEX TRACKING
 - b. INNER TRACKING
 - c. OUTER TRACKING
 - d. EM AND HADRON CALORIMETERS
 - e. MUON CHAMBERS
4. CONCLUSION

DETECTORS AND BACKGROUND

- Since muons decay, background levels at a muon collider are expected to be high.
- Understanding the backgrounds levels and how these backgrounds affect the performance of a strawman detector is a crucial part of assessing the feasibility of doing physics at a muon collider.
- Therefore, within the muon collider collaboration, there has been a significant effort devoted to:
 - (i) Designing the final focus to minimize backgrounds in the detector.
 - (ii) Understanding the remaining backgrounds in the detector, and identifying the critical background-related detector issues.
 - (iii) Developing a feasible strawman detector and assessing its performance in the predicted backgrounds.

Fermilab people (M. Atac, A. Bross, T. Diehl, S. Geer, C. Johnstone, P. Lebrun, N. Mokhov, R. Rajendran, A. Tollestrup) in collaboration with BNL people (D. Benary, S. Kahn, D. Lissauer, M. Murtagh, F. Paige, V. Polychronakos, P. Rehak, I. Stumer, V. Tchernatine), and R. Roser (Univ. Illinois).

Muon Decay Backgrounds

Background List

2 x 2 TeV Muon Collider

- 2×10^{12} muons/bunch
- 2×10^5 decays / m
- Mean decay electron energy = 700 GeV

Decay Backgrounds:

Two detailed complementary calculations have been performed: GEANT calculation (I. Stumer, BNL), MARS calculation (N. Mokhov, FNAL). The assumed final focus system and shielding configurations assumed for the two calculations are similar in general, but the details are very different.

Both the GEANT and MARS calculations track all particles through the final focus and 2 Tesla detector solenoidal fields and fully simulate:

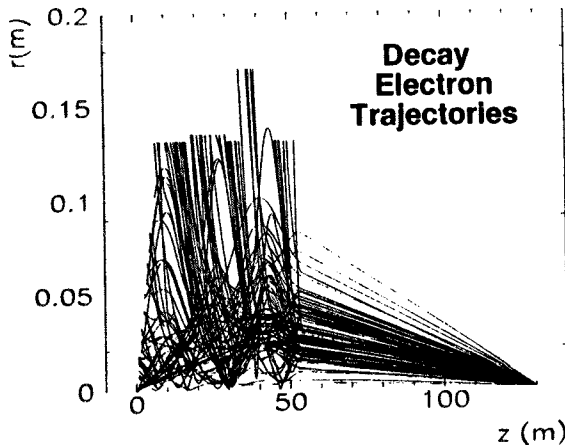
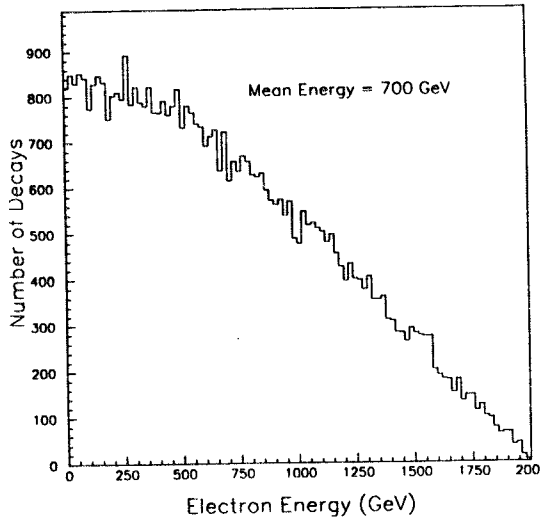
- Electron showers
- Synchrotron radiation
- Photonuclear interactions
- Bethe-Heitler muon pair production

Beam Halo:

Beam halo model and beam scraping design being developed, but no results yet.

Beam-Beam Interactions:

Believed to be small compared with other backgrounds

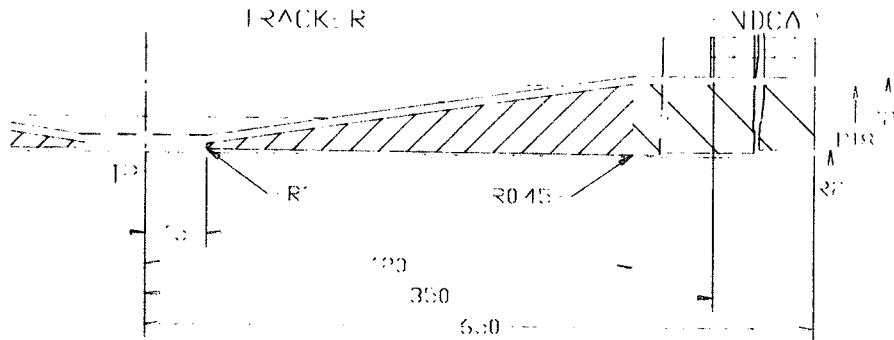


Electron decay angles are $O(10)$ microradians.

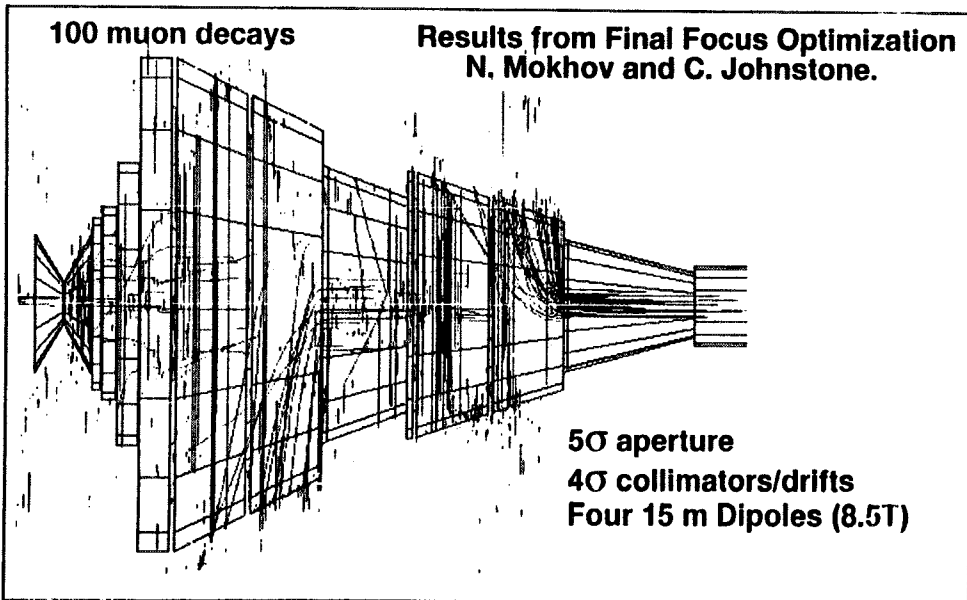
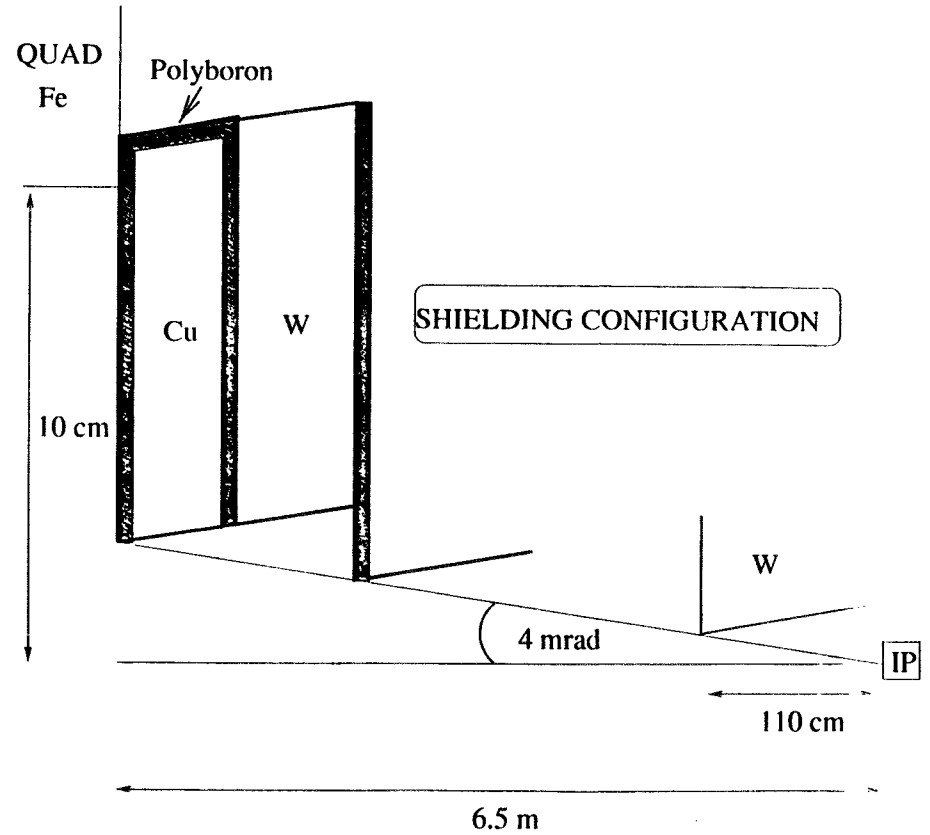
Therefore, in the final focus section, decay electrons tend to stay in the beampipe until they see the final focus Quad fields etc.

MARS Calculation

Uses a somewhat different shielding configuration than the GEANT calculation:



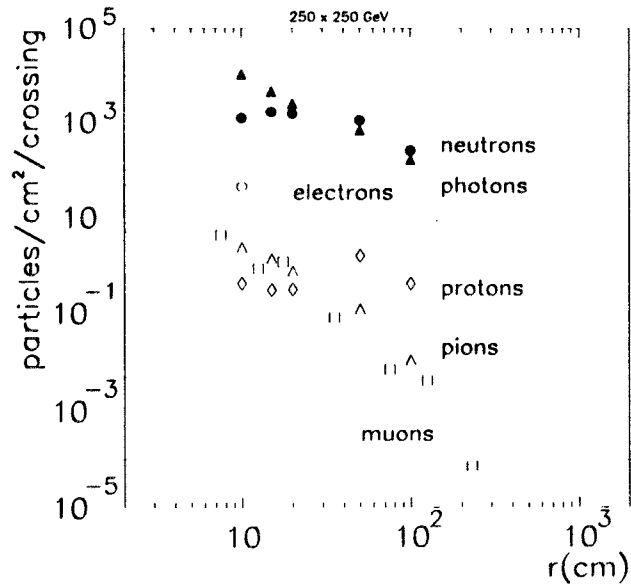
Shielding Configuration Implemented in GEANT Background Calculation



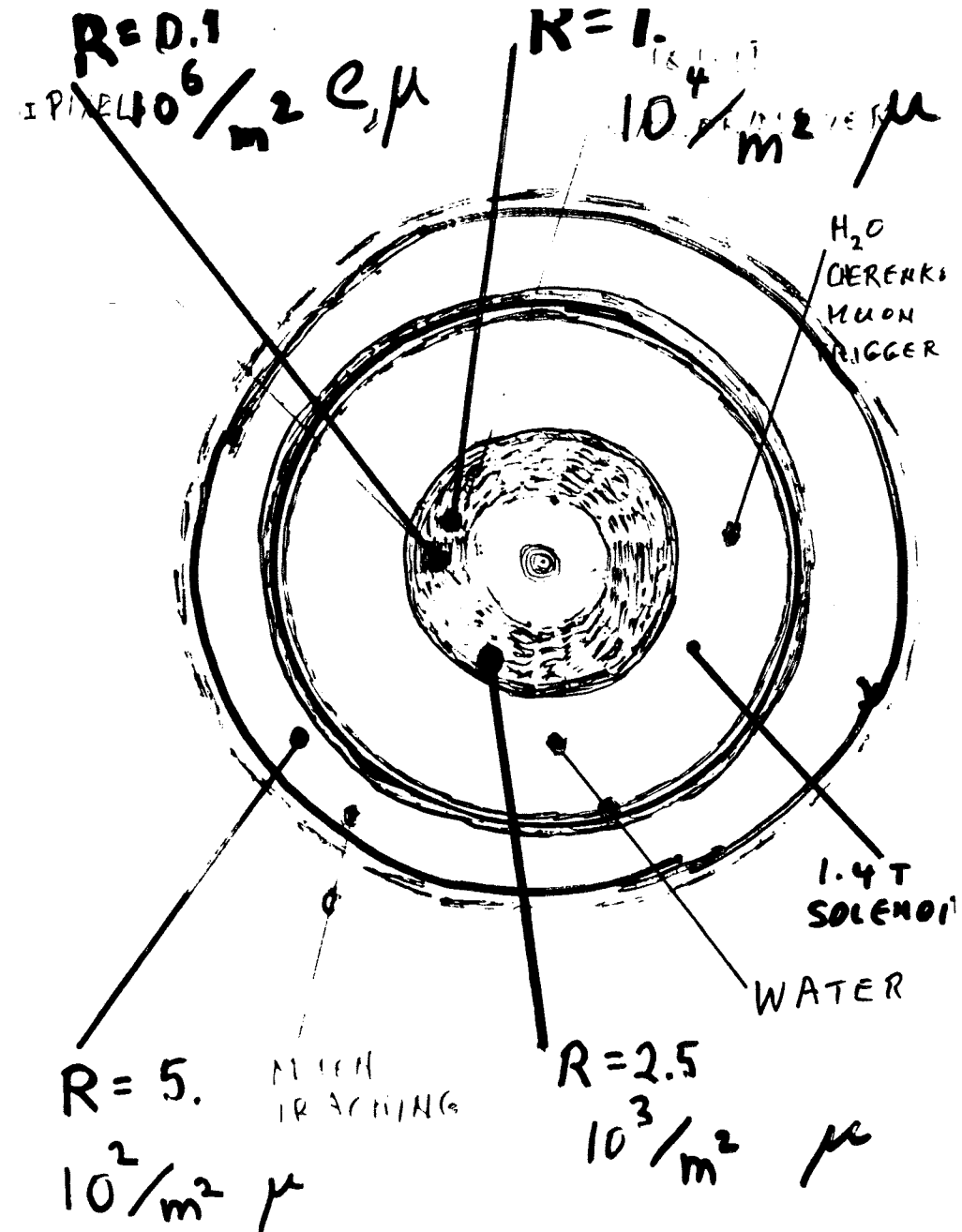
First Muon Collider

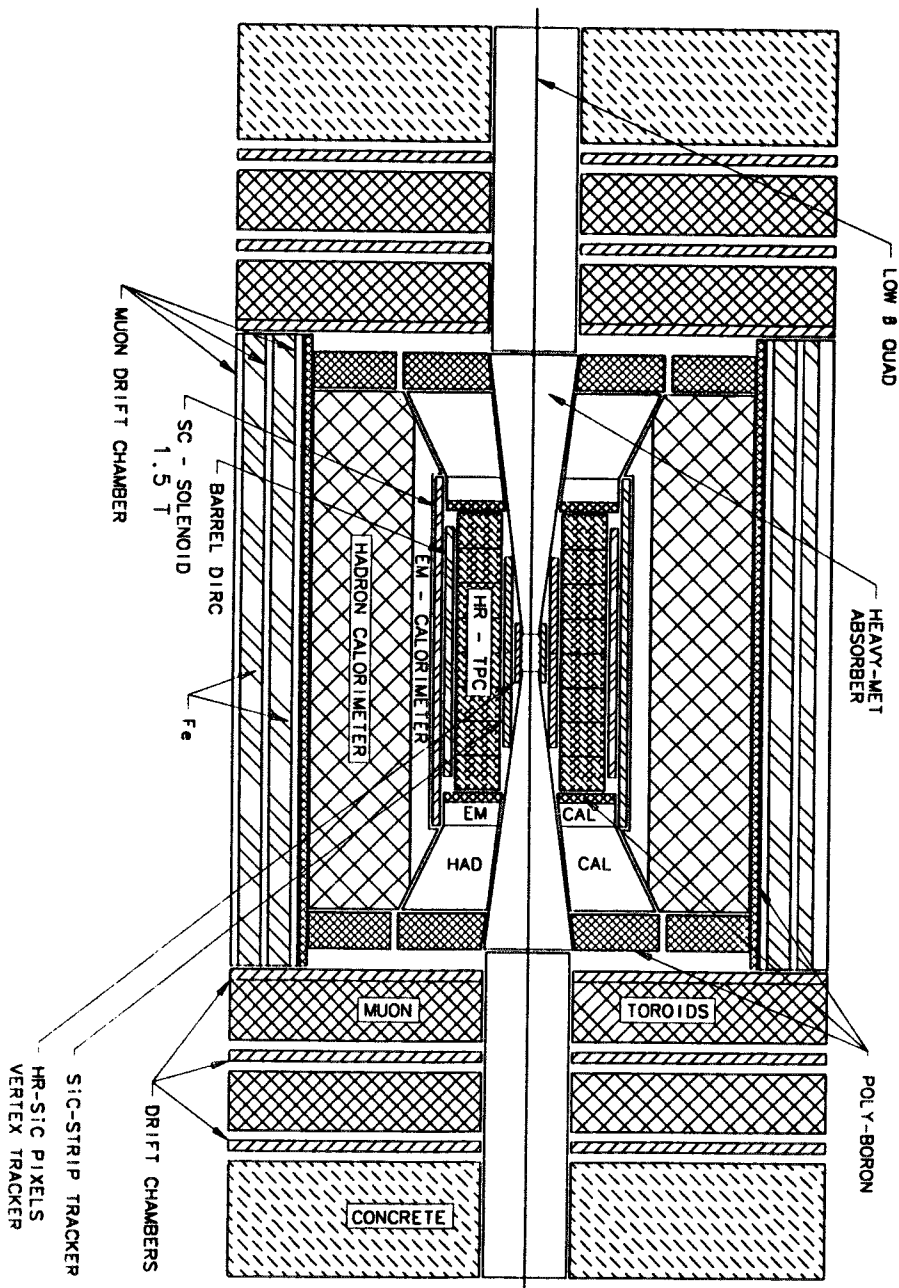
- Some GEANT work has been done to calculate backgrounds at a lower energy muon collider \rightarrow 250 x 250 GeV. This was before the recent improvements to the final focus which led to an order of magnitude reduction in backgrounds:

250 x 250 GeV \rightarrow 1.5×10^6 decays / m



- These background fluxes are comparable to those computed for a 2 x 2 TeV collider so we anticipate that the backgrounds at a lower energy machine will be similar to those at the 2 x 2 TeV machine EXCEPT the Bethe-Heitler muon background which is much better. A more detailed calculation is being done at BNL.





Hit Density in a Vertex Detector

- Consider a layer of Silicon at a radius of 10 cm. The GEANT results for the radial particle fluxes per crossing yield:

750 photons/cm ²	->	2.3 Hits/cm ²
110 neutrons/cm ²	->	0.1 Hits/cm ²
1.3 charged tracks/cm ²	->	1.3 Hits/cm ²
TOTAL		3.7 Hits/cm²

- -> 0.4% occupancy in 300 x 300 μm^2 pixels.
- The corresponding numbers at 5cm radius are 13.2 Hits/cm² -> 1.3% occupancy.
- This doesn't sound too bad. For comparison, SLD has about 40 Hits/cm² on the inner layer of their CCD detector.

Radiation Dose in Silicon Vertex Detector

- Consider a silicon layer at a radius of 10 cm. The dose due to non-ionizing energy loss can be calculated from the MARS or GEANT results (which give consistent results) taking into account particle type, energy spectra, and fluxes.

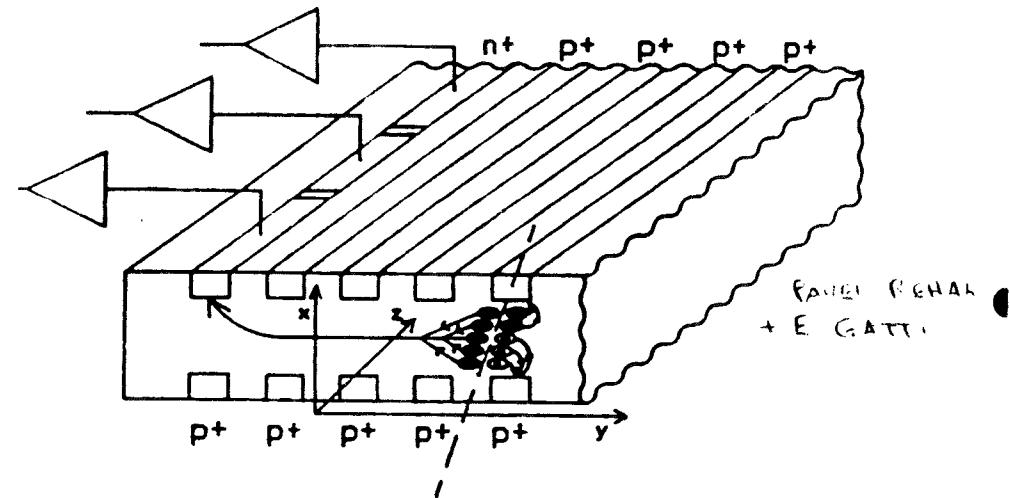
$$\begin{aligned} \phi_{\text{NIEL}} = & \phi_p + \phi_\pi + 0.5\phi_\mu + 0.1\phi_e + \\ & + \phi_{n > 0.1 \text{ MeV}} + 0.01\phi_\gamma \end{aligned}$$

- $\rightarrow \phi_{\text{NIEL}} = 240 \text{ per cm}^2 \text{ per crossing.}$

MARS predictions for 1 year ($= 10^7$ secs) of operation:

2 x 2 TeV muon collider	$7 \times 10^{13} \text{ cm}^2$
LHC at $10^{34} \text{ cm}^{-2} \text{ s}^{-1}$ (CMS)	$8 \times 10^{13} \text{ cm}^2$

Silicon Drift Detector (SDD)

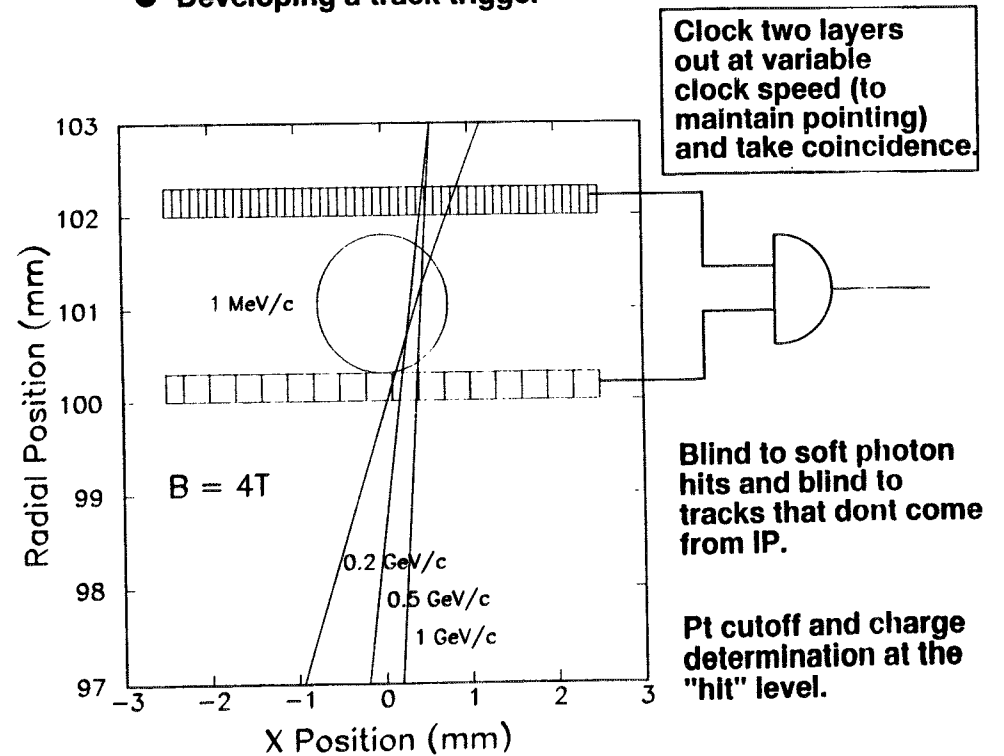


- EXPLOIT $10 \mu\text{s}$ BETWEEN BEAM CROSSINGS \Rightarrow FEW MICRON RESOLUTION IN DRIFT DIRECTION
- WITH $50 \mu\text{m} \times 300 \mu\text{m}$ DETECTORS & 6 LAYERS $\Rightarrow 2 \times 10^9$ CHANNELS
- EACH $20 \mu\text{s}$ CLEAR IF NO TRIGGER, ABORT BEAMS IF TRIGGER & TAKE 100 ms (?) TO READ OUT DEVICE.

Pixel Microtelescope

Type inversion in Si-microstrip detectors occur around a fluence of 10^{13} /cm². To collect the charge we need to increase the bias voltage from 30 V to 200-300 V for a 300 micron thick detector. This would make the Si drift chamber unusable in high fluences.

- Most of the background hits in a silicon vertex detector close to the muon collider IP arise from very low energy (~ 1 MeV) photon interactions.
- At Snowmass we thought of a possible way of screening out these background hits to facilitate:
 - Getting the first layer at the smallest viable radius
 - Developing a track trigger

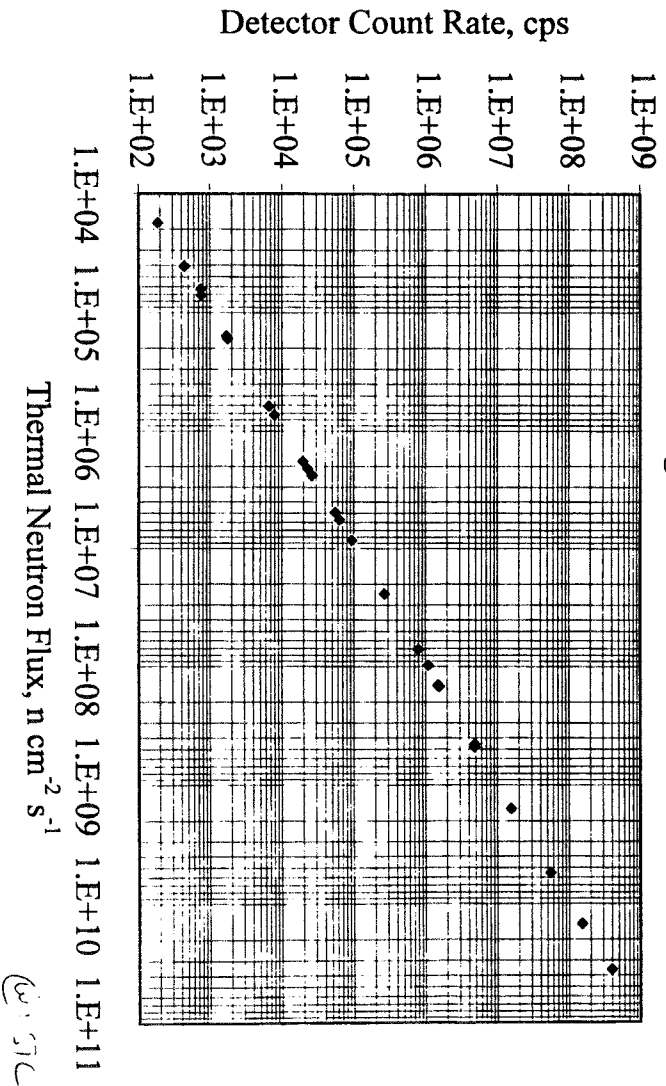


Material property	Silicon	GaAs	3C SiC	4H SiC	Diamond
Bandgap (eV)	1.1	1.43	2.3	3.2	5.5
Resistivity ($\Omega\text{-cm}$)	-10^5	-10^8	-	-10^7	$>10^{11}$
Breakdown field (V/cm)	-10^5	-10^5	1.5×10^6	3×10^6	1800
Electron mobility ($\text{cm}^2/\text{V}\cdot\text{s}$)	1350	6000	750	800	1200
Hole mobility ($\text{cm}^2/\text{V}\cdot\text{s}$)	~ 480	~ 400	40	115	1200
Saturation drift velocity (cm/s)	107	107	2.5×10^7	2×10^7	2.2×10^7
Dielectric constant	11.9	13.1	-	-	5.7
Cohesive energy (eV/atom)	4.63	-	-	-	7.37
Energy to create e-h pair (eV)	3.6	4.2	8.3 (est'd.)	8.3 (est'd.)	13
Ave. Ionized signal/100 μm ($\# e^-$)	9200	13000	6400 (est'd.)	6400 (est'd.)	3600

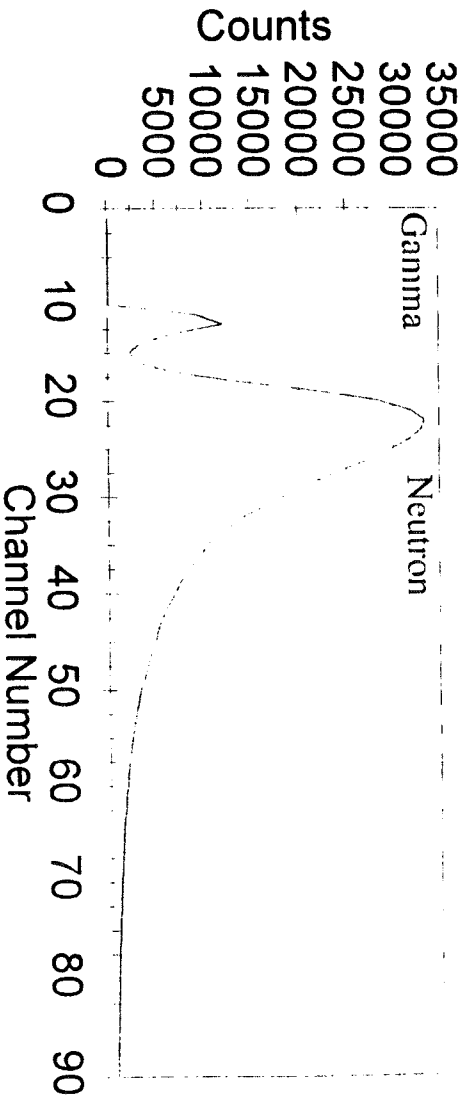
Table I. Comparison of potential particle detector material properties

Calibration Function of SiC Detector

Flux Range: $1\text{E}4 - 3\text{E}10 \text{ n cm}^{-2} \text{ s}^{-1}$

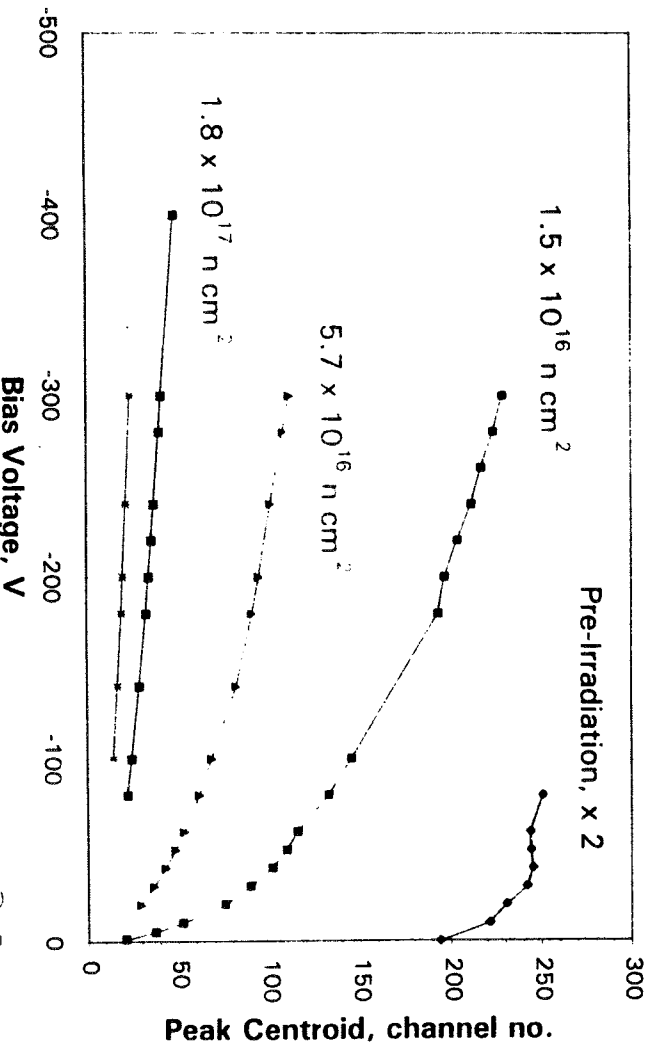


Separation of Neutron and Gamma Signals



Thermal neutron flux = $3.2E10$ n/sq. cm/s
 Gamma field = 50,000 R/h

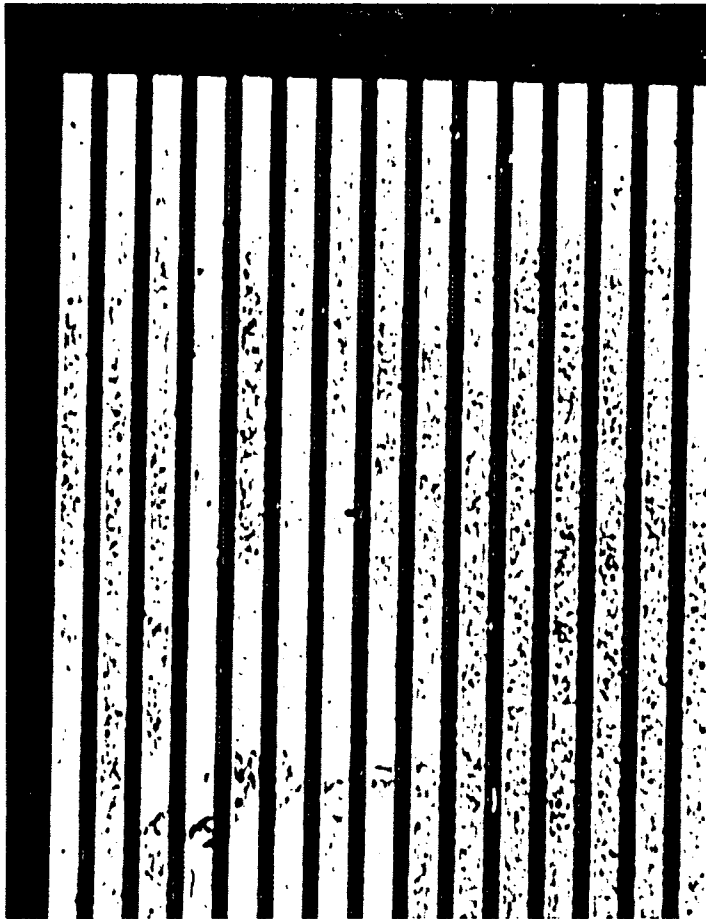
Peak Centroid versus Applied Voltage for PN-Junction Diode L12-4



QJL

Outer Tracker

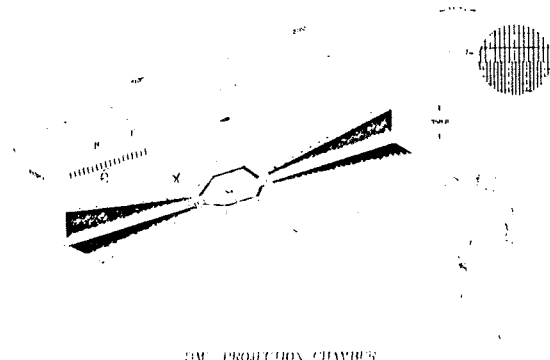
SiC



M. ATAC

Option 1: Silicon strips or large pixels

Option 2: TPC

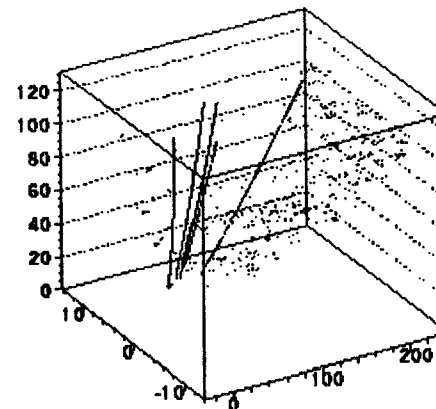


He + 10% CF₄

-> 6 cm/ μ s at
E = 1500 V/cm

(Note: time
between cross-
ings = 10 ns)

Ion buildup ->
 $\Delta E/E = 0.7\%$



Y VS X VS Z

The background occupancy
of O(1%) can be reduced by
rejecting large pulse heights
from photon and neutron
induced recoils.

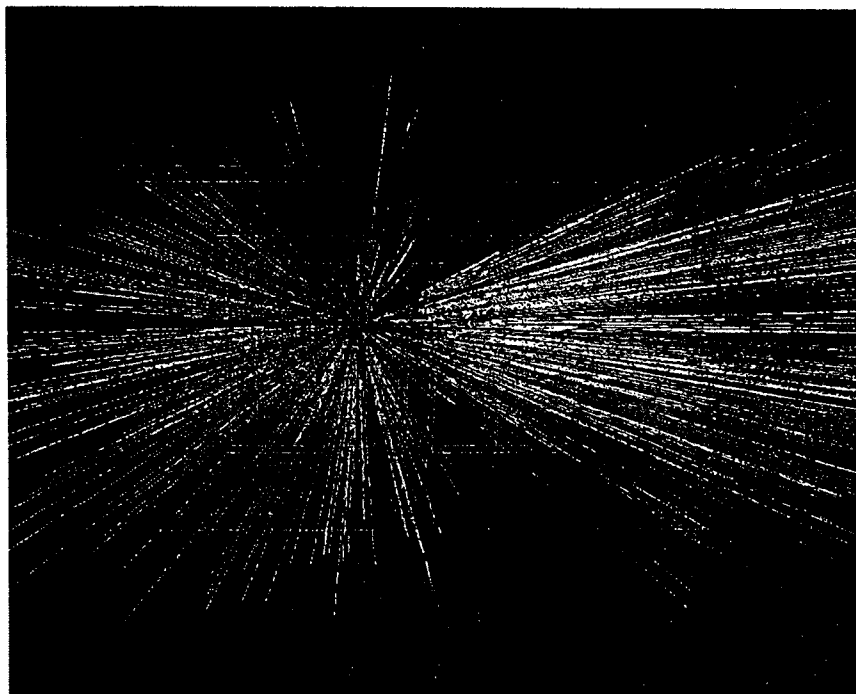
Performance of the Large Scale TPC System in the Heavy Ion Experiment NA49

S. Wenig

CERN

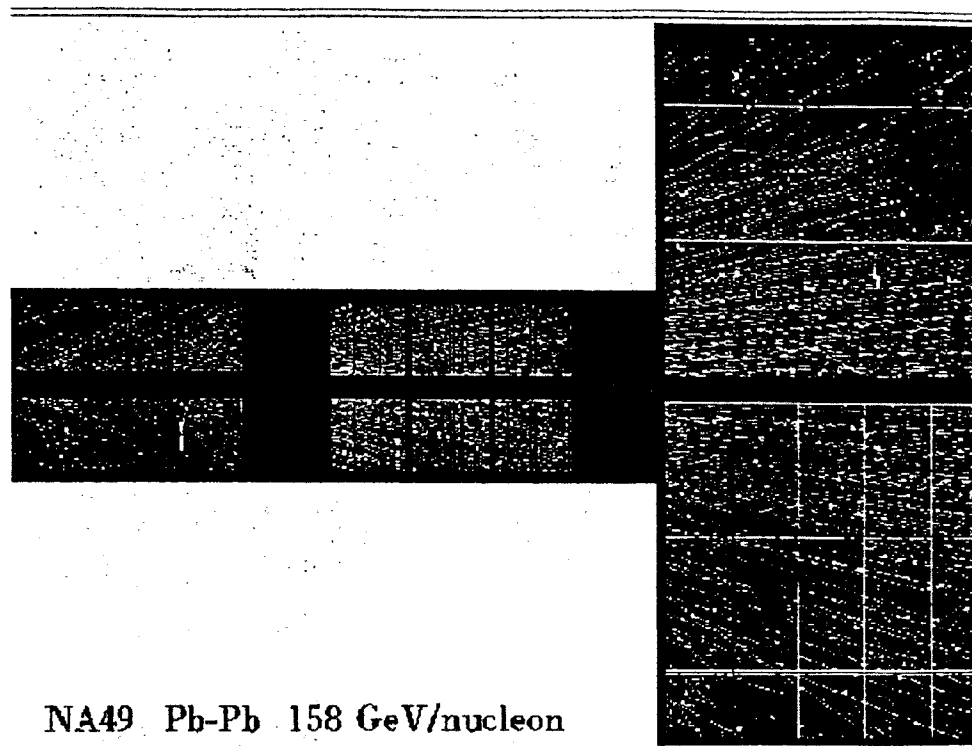
for the NA49 Collaboration

Athens - LBNL - Birmingham - Bratislava - Budapest - CERN -
GSI - UCD - Dubna - IKF - Krakow - UCLA - Marburg - MPI -
Yale - Seattle - Warsaw - Zagreb



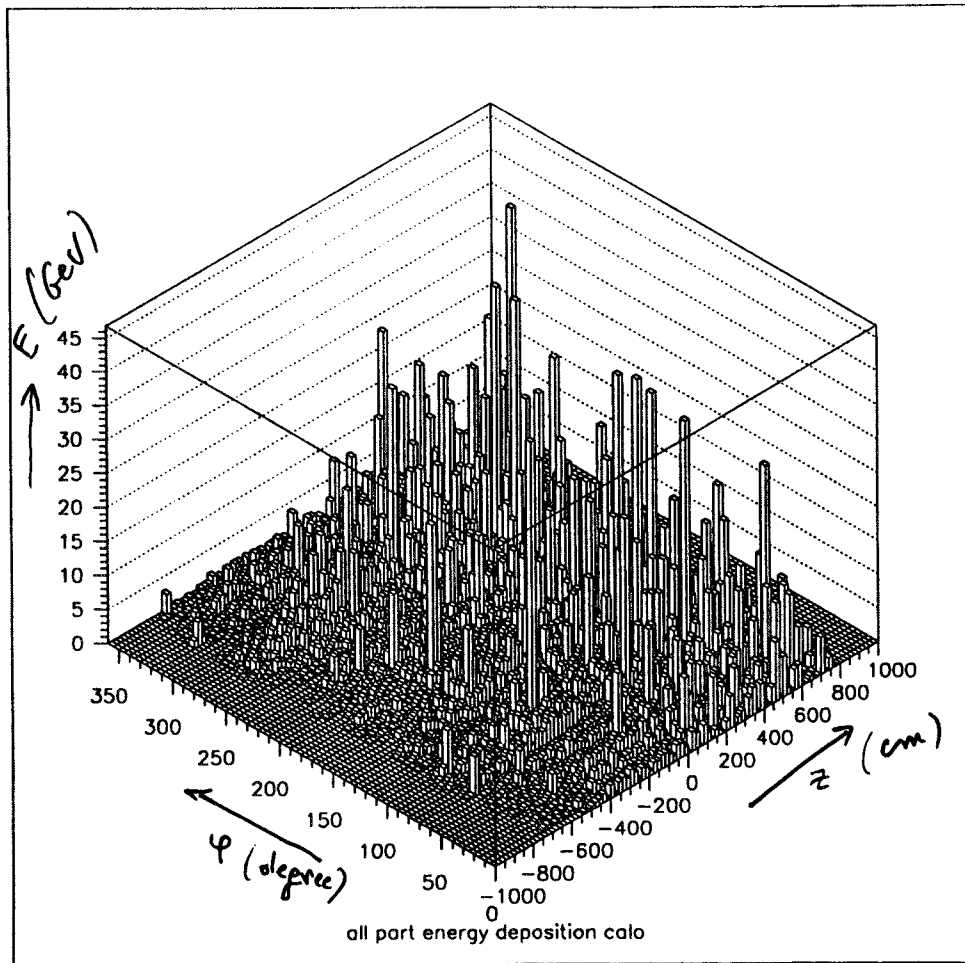
TOP VIEW

- 7 mm high slice around beam



- extremely high track density
 - ~ 1200 tracks in total
 - 400-600 tracks per TPC

FEBR - 97



BEAM TEST RESULTS FROM A FINE-SAMPLING QUARTZ FIBER CALORIMETER FOR ELECTRON, PHOTON AND HADRON DETECTION

N. Akchurin¹⁾, S. Ayan²⁾, G. Bencze³⁾, K. Chikin⁹⁾, H. Cohn⁴⁾,
 S. Doulas⁵⁾†, I. Dumanoglu⁶⁾, E. Eskut⁶⁾, A. Fenyvesi³⁾, A. Ferrando⁷⁾,
 M.C. Fouz⁷⁾, O. Ganel⁸⁾, V. Gavrilo⁹⁾, Y. Gershtein⁹⁾, C. Hajdu³⁾,
 J. Iosifidis¹¹⁾, M.I. Josa⁷⁾, A. Khan⁷⁾, S.B. Kim⁵⁾, V. Kolosov⁹⁾,
 S. Kuleshov⁹⁾, J. Langland¹⁾, D. Litvintsev⁹⁾, J.-P. Merlo⁵⁾‡, J. Molnar³⁾,
 A. Nikitin⁹⁾, Y. Onel¹⁾, G. Önengüt⁶⁾, D. Osborne⁵⁾, N. Özdeş-Koca⁶⁾,
 A. Penzo¹⁰⁾, E. Pesen²⁾, V. Podrasky¹¹⁾, A. Rosowsky^{3)*}, J.M. Salicio¹¹⁾,
 C. Sanzeni¹¹⁾, R. Sever²⁾, H. Silvestri¹¹⁾, V. Stolin⁹⁾, L. Sulak⁵⁾,
 J. Sullivan⁵⁾, A. Ulyanov⁹⁾, A. Umashev⁹⁾, S. Uzunian⁹⁾, G. Vesztergombi³⁾,
 R. Wigmans⁴⁾, D. Winn¹¹⁾, R. Winsor¹⁾, P. Zalan³⁾ and M. Zeyrek²⁾

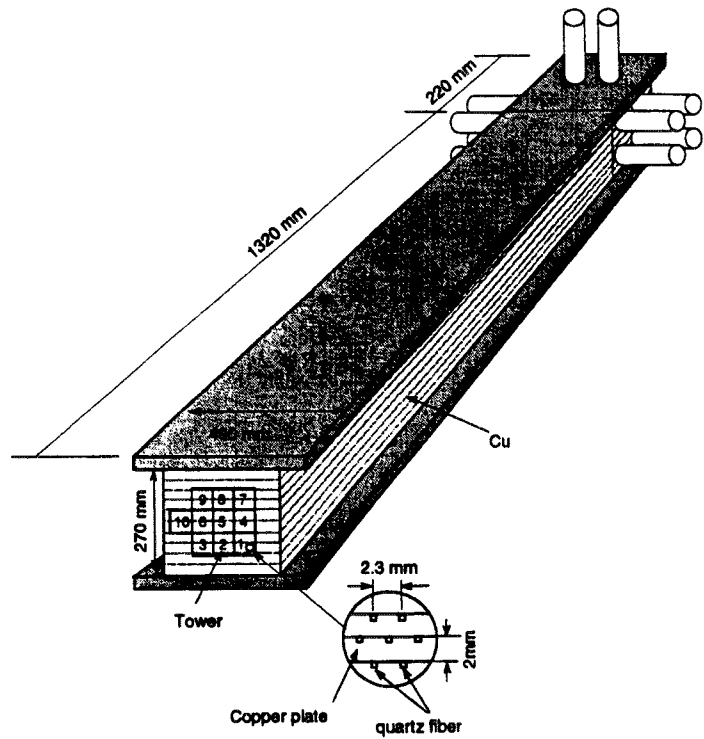
- 1) University of Iowa, Iowa City, U.S.A.
- 2) Middle East Technical University, Ankara, Turkey.
- 3) KFKI-RMKI, Budapest, Hungary.
- 4) Oak Ridge National Laboratory, Oak Ridge, U.S.A.
- 5) Boston University, Boston, U.S.A.
- 6) Çukurova University, Adana, Turkey.
- 7) CIEMAT, Madrid, Spain.
- 8) Texas Tech University, Lubbock, U.S.A.
- 9) ITEP, Moscow, Russia
- 10) Università di Trieste and INFN, Sez. Trieste, Trieste, Italy
- 11) Fairfield University, Fairfield, U.S.A.

† Now at Northeastern University, Boston, U.S.A.

‡ Now at University of Iowa

* Now at C.E.N. Saclay, Gif-sur-Yvette, France

Prototype of very forward hadronic calorimeter



Shower secondary particle produced in Copper by an incident particle.

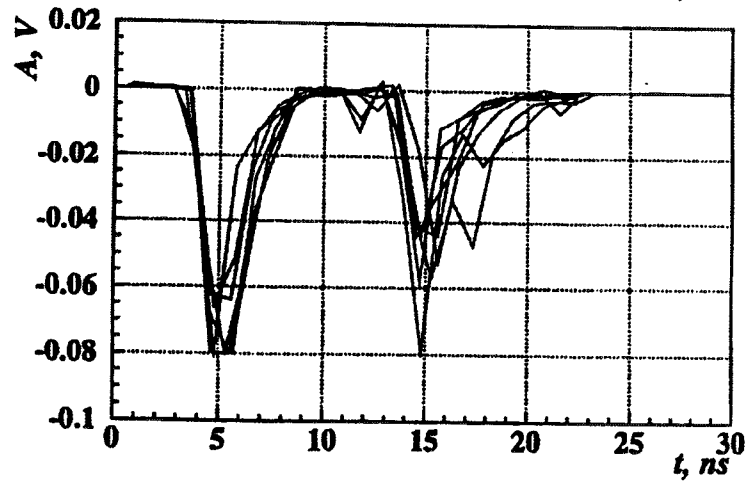
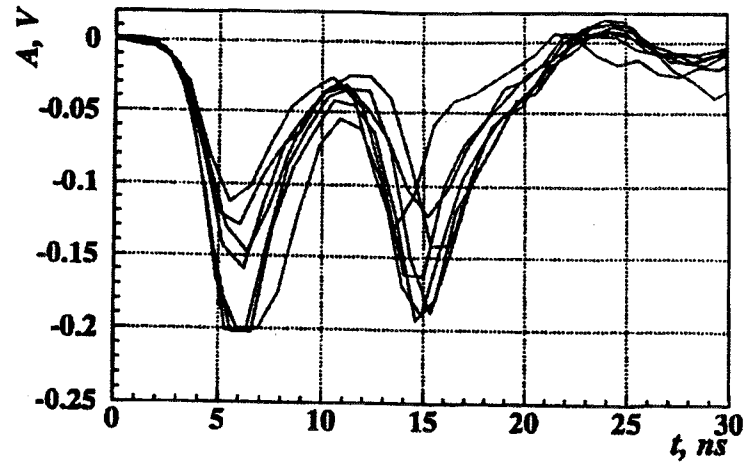
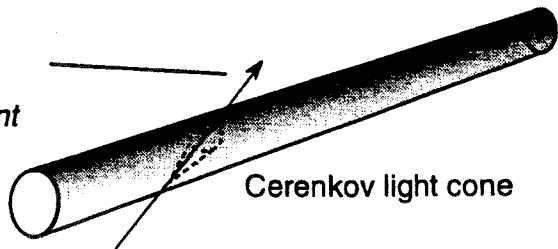


Figure 21

Quartz Fibre VF

Light is generated by Cerenkov effect
 fast and sensitive to relativistic charged particles
 insensitive to low energy n's, slow hadrons,
 induced radioactivity
 narrower and shorter hadronic showers
 predominantly sensitive to e.m. component

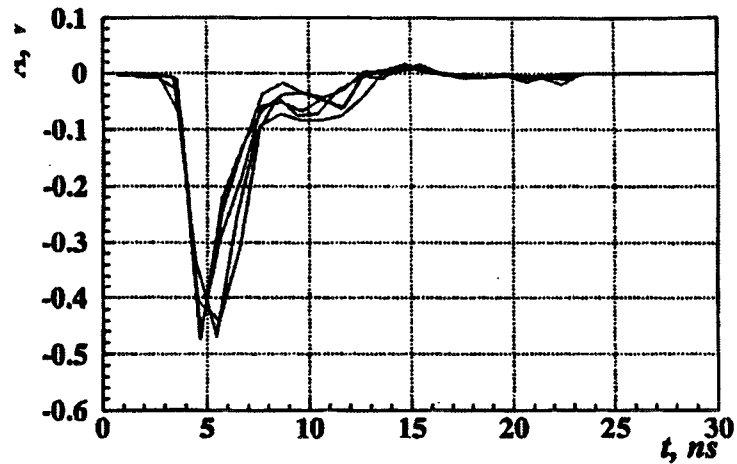
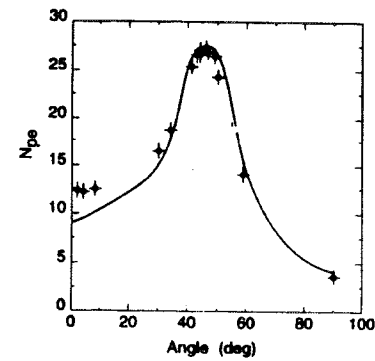
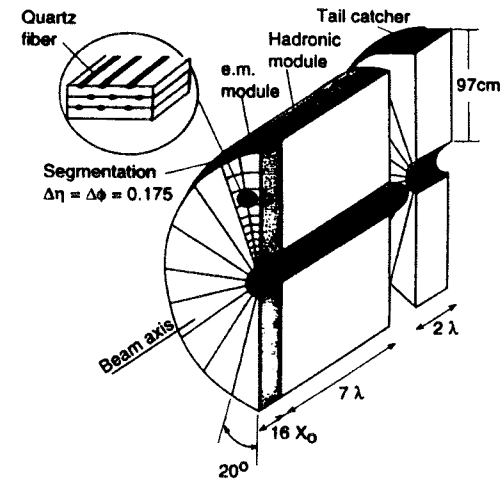
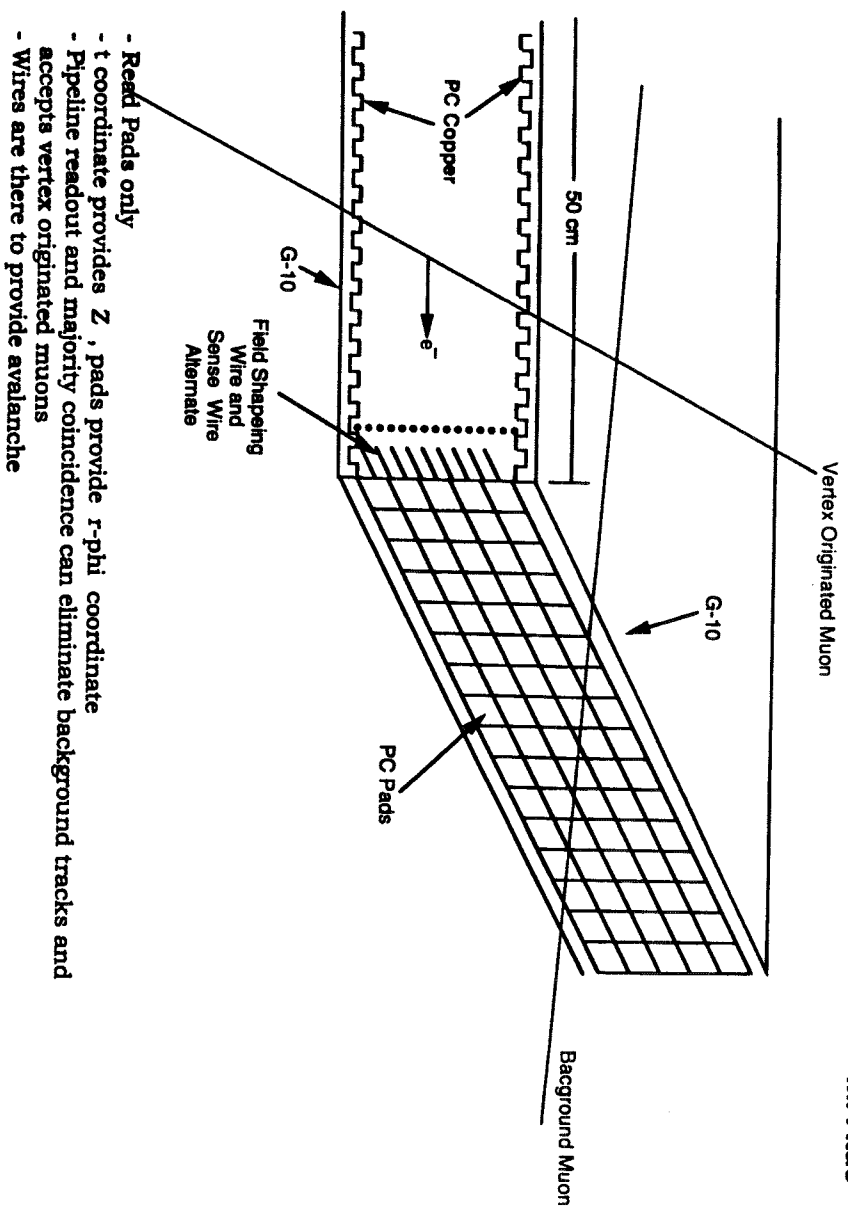


Figure 22



Choose configuration
 in which fibres run
 almost parallel to the
 incident particles





HAVE NO FEAR
DETECTOR
TECHNOLOGIES ARE NEAR